PPAR Research

Target PPARs to Cure Age-Related Diseases

Lead Guest Editor: Yu-En Gao
Guest Editors: Yongqiang Gao, Lexiang Yu, and Jincheng Wang

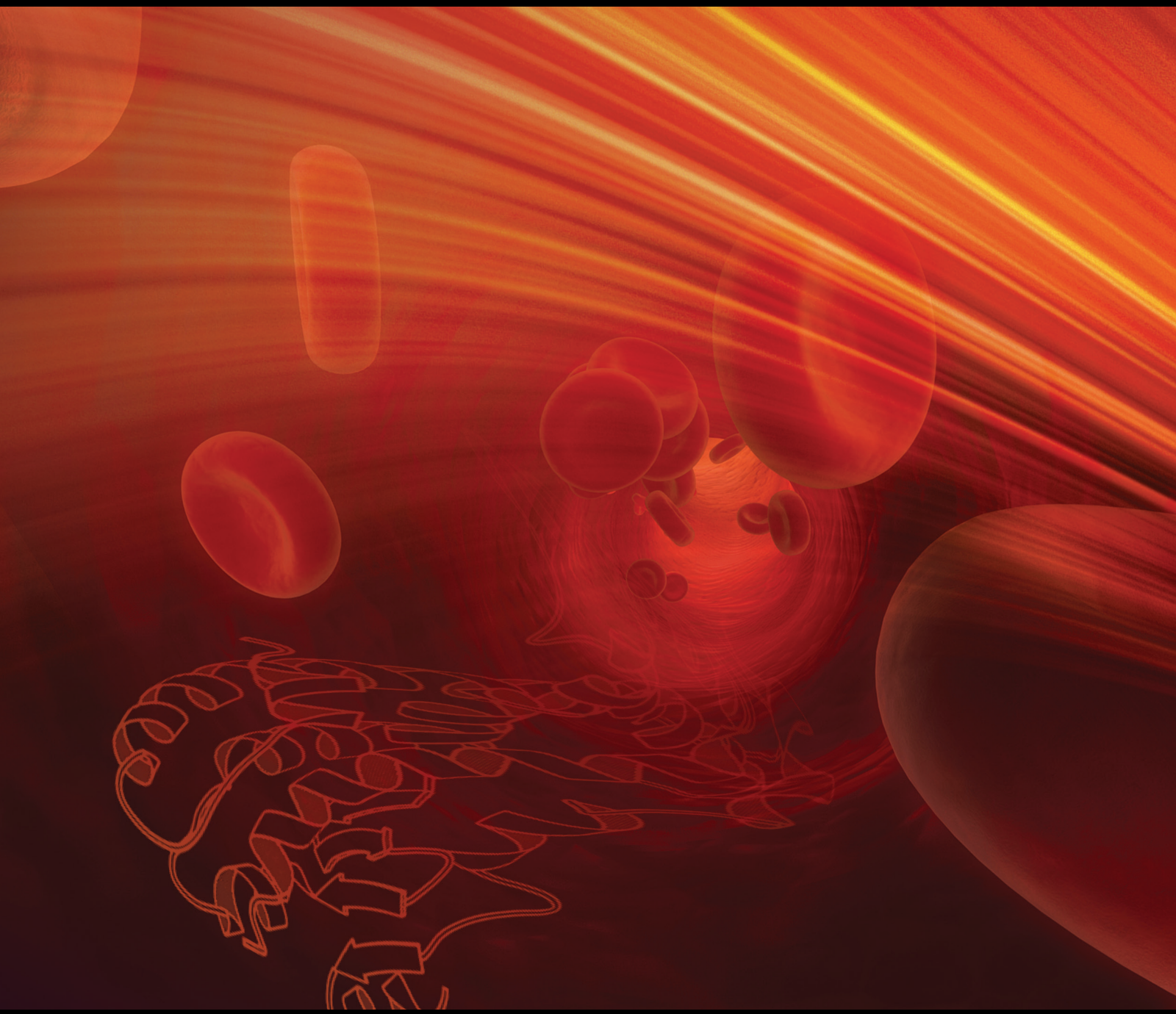

Target PPARs to Cure Age-Related Diseases

PPAR Research

Target PPARs to Cure Age-Related Diseases

Lead Guest Editor: Yu-En Gao
Guest Editors: Yongqiang Gao, Lexiang Yu, and Jincheng Wang

Contents

Hindawi
PPAR Research
Volume 2023, Article ID 4481354, 18 pages
https://doi.org/10.1155/2023/4481354

Research Article

PPARG: A Promising Therapeutic Target in Breast Cancer and Regulation by Natural Drugs

De-Hui Li,[1] **Xu-Kuo Liu**,[2] **Xiao-Tong Tian**,[2] **Fei Liu**,[3] **Xu-Jiong Yao**,[1] **and Jing-Fei Dong**[1]

[1]*The First Affiliated Hospital of Hebei University of Chinese Medicine, Hebei Province Hospital of Chinese Medicine, Shijiazhuang 050011, China*
[2]*Graduate School of Hebei University of Chinese Medicine, Shijiazhuang 050091, China*
[3]*Hebei University of Chinese Medicine, Shijiazhuang 050091, China*

Correspondence should be addressed to De-Hui Li; 258289951@qq.com and Jing-Fei Dong; 371005045@qq.com

Received 21 January 2023; Revised 2 April 2023; Accepted 11 May 2023; Published 8 June 2023

Academic Editor: Yongqiang Gao

Breast cancer (BC) is the most common type of cancer among females. Peroxisome proliferator-activated receptor gamma (PPARG) can regulate the production of adipocyte-related genes and has anti-inflammatory and anti-tumor effects. Our aim was to investigate PPARG expression, its possible prognostic value, and its effect on immune cell infiltration in BC, and explore the regulatory effects of natural drugs on PPARG to find new ways to treat BC. Using different bioinformatics tools, we extracted and comprehensively analyzed the data from the Cancer Genome Atlas, Genotype-Tissue Expression, and BenCaoZuJian databases to study the potential anti-BC mechanism of PPARG and potential natural drugs targeting it. First, we found that PPARG was downregulated in BC and its expression level correlates with pathological tumor stage (pT-stage) and pathological tumor-node-metastasis stage (pTNM-stage) in BC. PPARG expression was higher in estrogen receptor-positive (ER+) BC than in estrogen receptor-negative (ER−) BC, which tends to indicate a better prognosis. Meanwhile, PPARG exhibited a significant positive correlation with the infiltration of immune cells and correlated with better cumulative survival in BC patients. In addition, PPARG levels were shown to be positively associated with the expression of immune-related genes and immune checkpoints, and ER+ patients had better responses to immune checkpoint blocking. Correlation pathway research revealed that PPARG is strongly associated with pathways, such as angiogenesis, apoptosis, fatty acid biosynthesis, and degradation in ER+ BC. We also found that quercetin is the most promising natural anti-BC drug among natural medicines that upregulate PPARG. Our research showed that PPARG may reduce BC development by regulating the immune microenvironment. Quercetin as PPARG ligands/agonists is a potential natural drug for BC treatment.

1. Introduction

Breast cancer (BC) currently ranks first in incidence and second in mortality among cancers in females worldwide [1], representing a major health burden globally. Treatment methods for BC include surgery, radiotherapy, chemotherapy, endocrine therapy, and gene-targeted therapy, which depend on the underlying subtype and stage of BC. Despite significant progress in the field, the pathogenesis of BC remains unclear. Estrogen receptor positive (ER+) patients account for a higher proportion of all BC patients. The growth of ER+ tumor is driven by ER signal. Endocrine therapy is the main treatment. Representative drugs, such as tamoxifen, combined with radiotherapy and targeted therapy can effectively enhance the survival quality and prognosis of patients. Therefore, ER+ patients tend to have a better prognosis than estrogen receptor-negative (ER−) patients, but resistance inevitably develops over time, and drug resistance will gradually emerge. The therapeutic effect of second-line drugs is generally weaker than that of first-line drugs. Despite significant advances in diagnosis and treatment, some BC patients still have poor outcomes and prognosis. Finding new therapeutic targets and prognostic markers for BC is important to improve the efficiency and accuracy of BC treatment.

Peroxisome proliferator-activated receptor (PPAR) is a type of ligand-activated transcription factor that belongs to the nuclear receptor superfamily [2]. It participates in the control of lipid and carbohydrate turnover and their homeostasis and has important roles in cell differentiation and apoptosis, inflammation, vascular biology, and cancer [3]. Peroxisome proliferator-activated receptor gamma (PPARG) is the focus of research and a key factor in the regulation of lipid metabolism and energy homeostasis. It is an important treatment target for various metabolic diseases, inflammatory responses, cardiovascular diseases, and a variety of tumors [4, 5]. PPARG is also a key factor in immune regulation, since it has the ability to directly bind to DNA and activate transcription of target genes in immune cells [6–8]. PPARG is an important promoter of macrophage differentiation and M2 macrophage polarization [9, 10] and controls the lipid metabolism of various immune cells [9, 11–13]. The lipid microenvironment is associated with immune cell function in combination with classical transactivation. In an inflammatory response, PPARG can competitively inhibit the transduction of NF-κB, JAK-STAT, and other signaling pathways, and inhibit the transactivation activity of pro-inflammatory transcription factors induced by cytokines, regulating the function and activity of macrophages, B cells, T cells, DC cells, and other immune cells. Its ligand reduces the damage caused by inflammatory responses to the body by inhibiting macrophage activation and inflammatory cytokine production. For example, the combination of anti-inflammatory drugs for experimental inflammatory bowel disease (IBD) and PPARG may become a new method for the treatment of IBD [14]. However, the current study on whether overexpression of PPARG affects the immune microenvironment of BC is not sufficient, and the mechanism is not well understood. Using bioinformatics, we studied PPARG expression and prognostic value in BC, its effect on immune cell infiltration, and immune checkpoints to better investigate the biological role of PPARG in BC cells. Further research is needed to explore potential natural drugs targeting PPARG in the treatment of BC, providing new insights into the detection and treatment of BC.

2. Methods

2.1. Pan-Cancer PPARG Expression Analysis. We obtained tumor data and associated clinical information from the Cancer Genome Atlas (TCGA; https://portal.gdc.cancer.gov/) and Genotype-Tissue Expression (GTEx; https://www.gtexportal.org/) databases. In addition, we employed the Wilcoxon test to examine the differential expression of PPARG in cancer and normal tissues. Statistical analysis was performed using version 4.0.3 of the R software. To be considered statistically significant, the criterion for p-value was set at less than 0.05.

2.2. Association Analysis between PPARG Expression and Clinical Characteristics of BC. We retrieved BC RNAseq data along with relevant clinical information from the TCGA database. The BC samples were categorized into high and low expression groups based on the median level of PPARG gene expression. Clinicopathological characteristics were analyzed in relation to PPARG gene expression. Variables studied included survival status, age, gender, pathologic tumor stage (pT-stage), pathologic node stage (pN-stage), pathological metastasis stage (pM-stage), and pathological tumor-node-metastasis stage (pTNM-stage). The data were expressed as mean ± SD, and unpaired t-tests were used for statistical evaluation. The association between PPARG and clinical characteristic variables was investigated using chi-square or Fisher's exact tests.

2.3. Prognostic Value Analysis of PPARG Gene in BC. We utilized BC RNAseq data and corresponding clinical information acquired from TCGA. The survival curve was generated using the "survminer" and the "Survival" software packages in R v4.0.3 to study the relationship between PPARG expression level and BC prognosis. Statistical analysis was performed using log-rank testing and univariate Cox regression to derive the p-values, hazard ratios (HR), and 95% confidence intervals (CI). A p-value lower than 0.05 was used to define statistical significance. Subsequently, we further investigated the prognostic value of the PPARG gene in BC by utilizing the Kaplan–Meier plotter (https://kmplot.com/analysis/).

2.4. Analysis of the Correlation between PPARG and Immune Infiltration in BC. We first utilized Tumor Immune Estimation Resource (TIMER) (https://cistrome.shinyapps.io/timer/) to reveal the correlation between PPARG and the infiltrating levels of six different immune cell subtypes, as well as the relationship between immune cell infiltration levels and BC patients' cumulative survival rate. Then, we obtained RNAseq data and corresponding clinical information of estrogen receptor-positive BC from TCGA database, and verified the relationship among PPARG and six immune cell subtypes infiltration levels using Spearman's correlation analysis. The correlation plot was implemented using the R v4.0.3 software package "ggstatsplot", and A p-value below 0.05 indicates statistical significance.

2.5. Co-Expression Analysis of PPARG and Immune-Related Genes. Using BC RNAseq data and related clinical information from the TCGA database, the correlation between two genes was analyzed using "ggstatsplot" package in the R software with Spearman's correlation analysis for non-normally distributed quantitative variables. Additionally, the expression differences of immune checkpoint-related genes between ER+ and ER− BC were analyzed using "ggplot2" and "pheatmap" packages in the R software. Ultimately, the tumor immune dysfunction and exclusion (TIDE) algorithm was utilized to predict potential efficacy of immunotherapy [15]. Statistical significance is demonstrated when the p-value is equal to or less than 0.05.

2.6. Analysis of the Correlation between PPARG and Pathways. We utilized BC RNAseq data obtained from the TCGA database and corresponding clinical information. Gene sets containing relevant pathways were collected [16] and analyzed using the gene set variation analysis package in the R software version 4.0.3 with the parameter

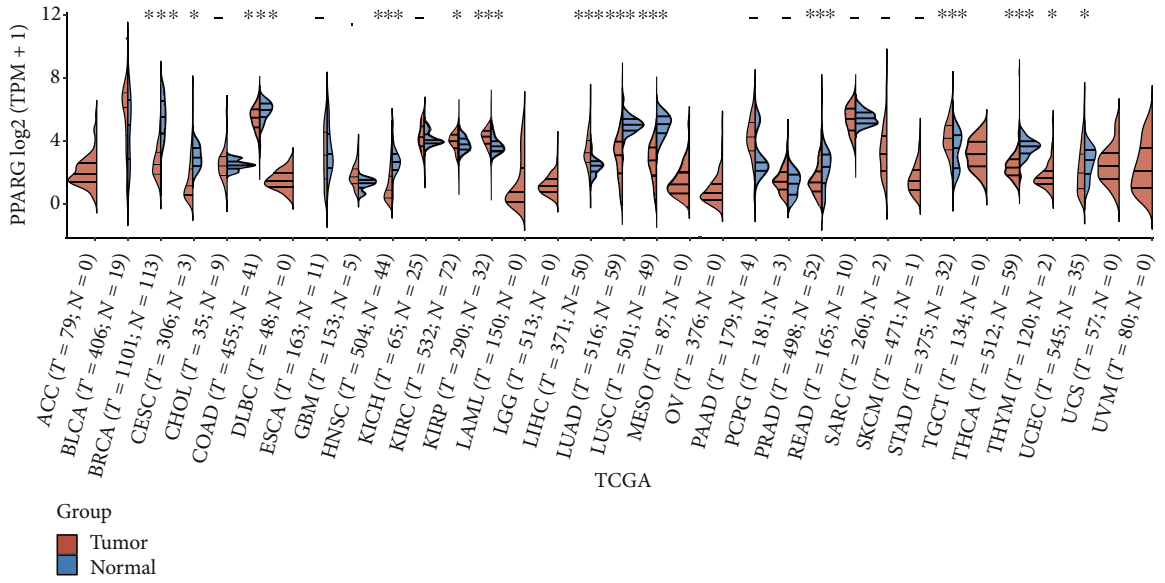

(a)

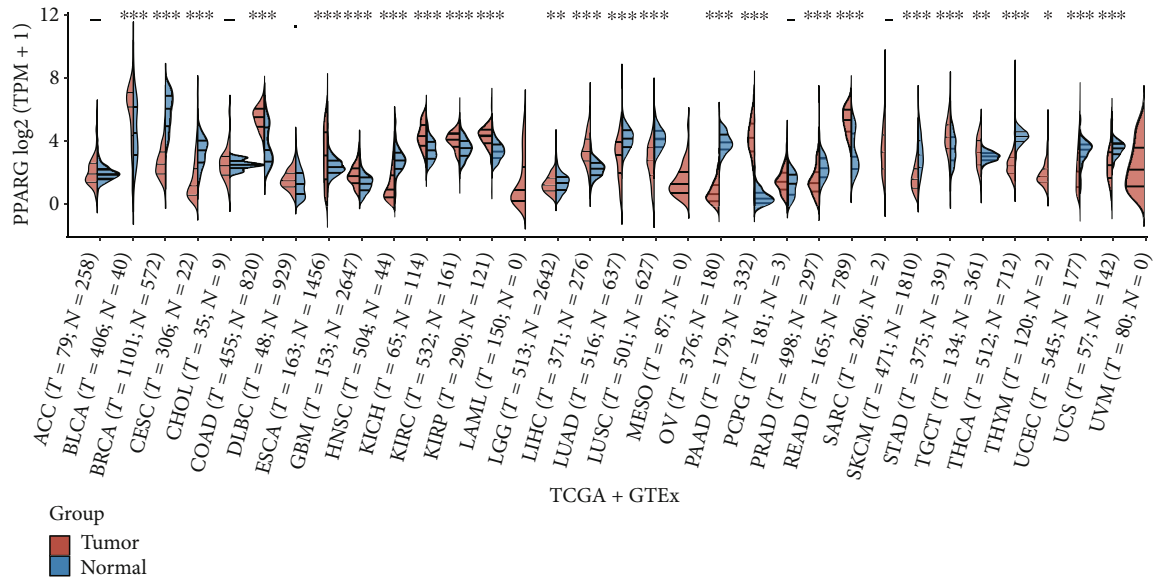

(b)

Figure 1: Continued.

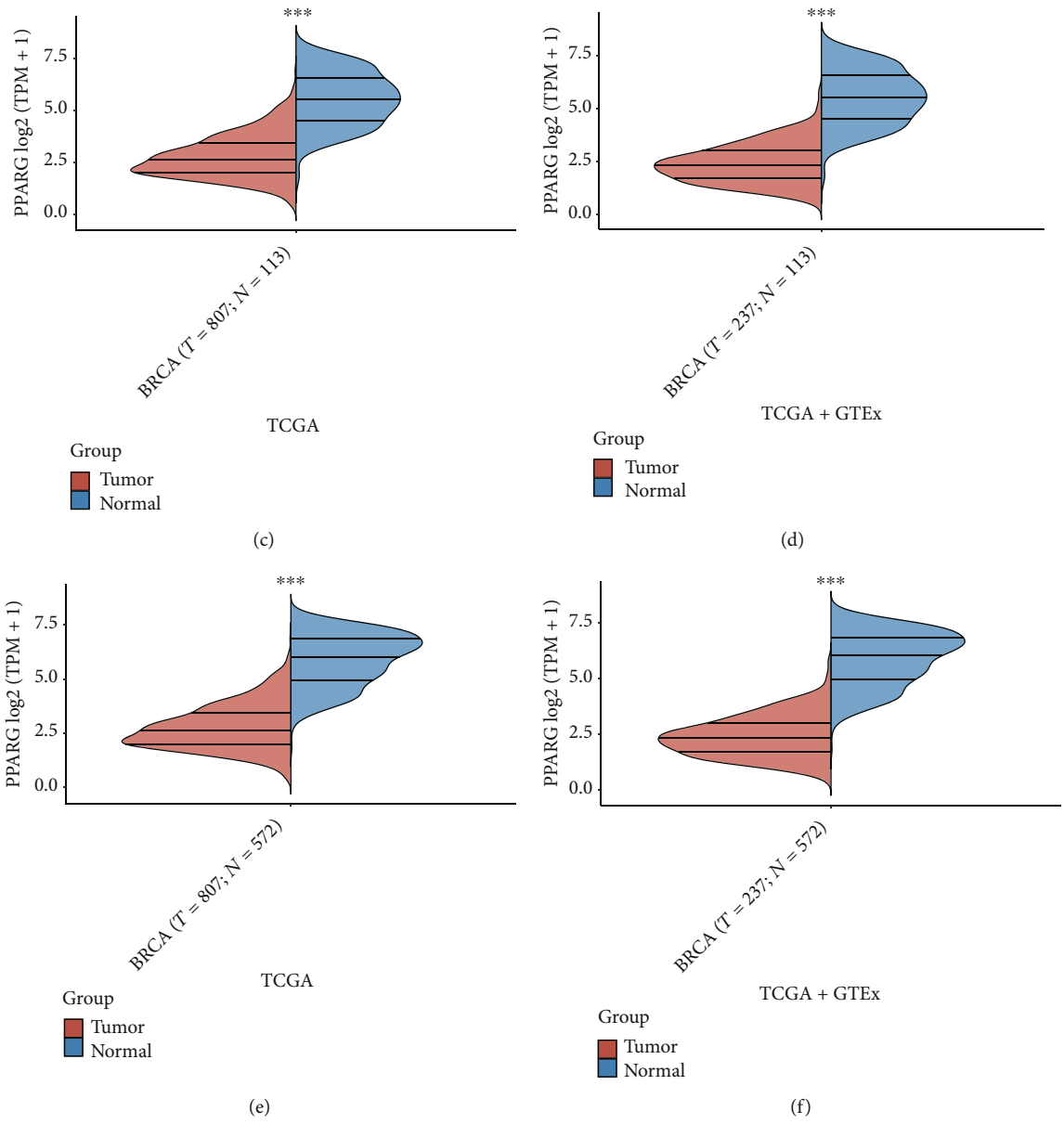

Figure 1: Continued.

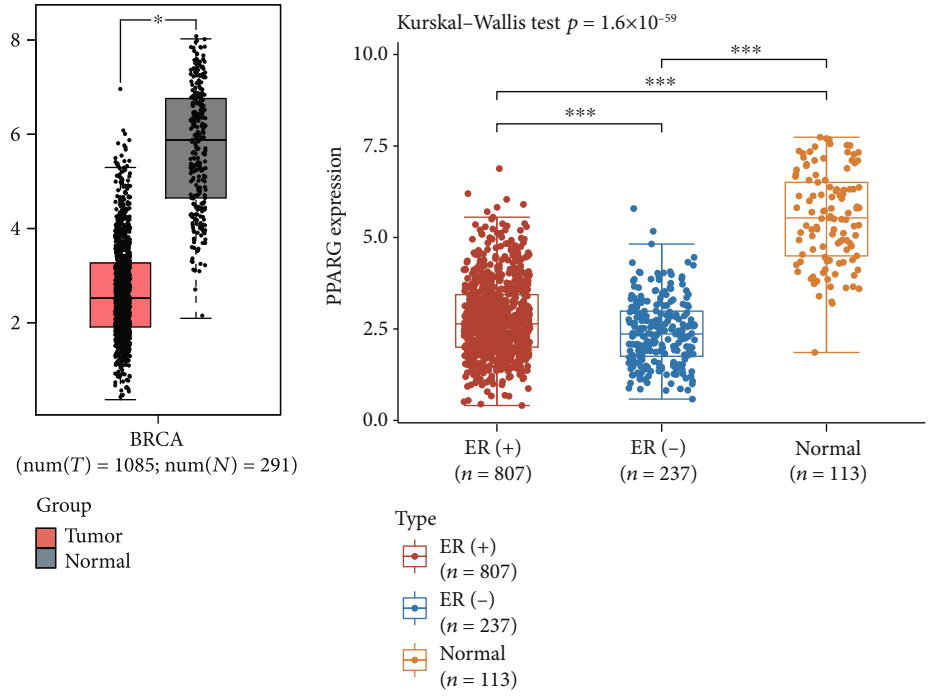

Figure 1: Pan-cancer and ER+/− BC analysis of PPARG expression. (a and b) PPARG expression in tumor and normal tissues in TCGA and TCGA + GTEx pancarcinoma data, the result shows that PPARG is downregulated in BC. (c and d) PPARG expression in ER+ BC and normal tissues in TCGA and TCGA + GTEx data, compared with normal tissues, PPARG is downregulated in ER+ BC. (e and f) PPARG expression in ER− BC and normal tissues in TCGA and TCGA + GTEx data, compared with normal tissues, PPARG is downregulated in ER− BC. (g) PPARG expression in BC and normal tissues in GEPIA data, the expression of PPARG is lower in BC than in normal tissue. (h) Differential expression of PPARG in ER+ and ER− BCs, the expression of PPARG is higher in ER+ BC than in ER− BC. $^{*}p < 0.05$, $^{**}p < 0.001$, and $^{***}p < 0.0001$.

method = "ssgsea." Finally, we used the Spearman's correlation analysis method to investigate the correlation between PPARG gene and pathway scores. A p-value below 0.05 was deemed to be statistically significant.

2.7. Mining of Potential Natural Compounds Regulating PPARG for BC Treatment. The BenCaoZuJian (HERB) database, a specialized high-throughput experimental and reference database for traditional Chinese medicine, was used to search for active compounds and herbal medicines targeting the PPARG receptor. Relevant data were extracted using reference mining, and searched the PubMed database to identify experimentally validated active compounds and natural drugs that regulate PPARG.

3. Results

3.1. Analysis of PPARG Expression in Pan-Cancer and ER+ BC. To research PPARG expression in pan-cancer and BC, we obtained RNAseq data and corresponding clinical information from 33 cancer types and 10,228 samples from TCGA and GTEx databases. First, we evaluated the PPARG expression in pan-cancer data from TCGA and GTEx. Results showed that PPARG was lowly expressed in 12 cancer types, including BC (BRCA), CESC, COAD, HNSC, LUAD, LUSC, OV, SKCM, PRAD, THCA, UCEC, UCS, KIRP, LIHC, STAD, KICH, KIRC, PAAD, and READ (see Figures 1(a) and 1(b)). Next, we evaluated the expression of PPARG in ER+, ER− BC, and normal tissue. We found that PPARG was lowly expressed in both ER+ and ER− BC compared with normal tissue (see Figures 1(c), 1(d), 1(e), and 1(f)). Furthermore, we further validated the low expression of PPARG in BC tissues using the Gene Expression Profile Interaction Analysis (GEPIA) online tool (http://gepia.cancer-pku.cn/; see Figure 1(g)). Furthermore, we analyzed the relationship between PPARG levels and ER status in BC and found that PPARG expression was higher in ER+ BC than in ER− BC (see Figure 1(h)). Taken together, these results suggest that PPARG is lowly expressed in BC.

3.2. PPARG Expression Levels in BC Patients in relation to Clinicopathological Characteristics. We obtained RNAseq data and associated clinical information of 1101 BC cases from the TCGA database. The cases were categorized into high-expression and low-expression groups according to the median level of PPARG gene expression. We examined the correlation between PPARG expression and clinicopathological features. The outcome indicated that PPARG expression level was related to pT-stage and pTNM-stage of BC (see Table 1 and Figure 2(a)). In ER+ BC, PPARG expression levels correlated with survival status, age, pT-stage, and pTNM-stage (see Table 2 and Figure 2(b)). This result suggests that PPARG may be implicated in the pathogenesis of BC, particularly in ER+ BC, and may hold promise as a prognostic indicator.

Table 1: PPARG expression levels in BC patients in relation to clinicopathological characteristics.

	Clinicopathological characteristics	High expression group	Low expression group	p -Value
Status	Alive	480	467	0.333
	Dead	71	83	
Age	Mean (SD)	57.6 (13)	59.1 (13.4)	0.069
	Median [Min, Max]	58 [26, 90]	59 [26, 90]	
Gender	Female	546	543	0.769
	Male	5	7	
pT-stage	TX	0	3	0.007
	T1	161	120	
	T2	292	347	
	T3	83	55	
	T4	15	25	
	NX	7	13	
pN-stage	N0	252	264	0.173
	N1	187	179	
	N2	56	64	
	N3	49	30	
pM-stage	MX	86	77	0.182
	M0	455	455	
	M1	7	15	
pTNM-stage	X	5	8	0.041
	I	102	80	
	II	296	328	
	III	136	115	
	IV	6	14	

3.3. Prognostic Value of PPARG in BC. To evaluate the value of PPARG in predicting the prognosis of BC patients, we obtained RNAseq data and relevant clinical information from the TCGA database for 807 ER+ BC patients and 237 ER− BC patients. We applied survival correlation analysis to research the correlation among PPARG expression and BC prognosis. The results of the KM survival analysis showed that PPARG was a protective factor in ER+ BC ($p = 0.0057$), with higher expression associated with better prognosis (see Figure 3(a)). The corresponding survival times at 50% for the high expression and low expression groups were 11.4 and 9.5 years, respectively. However, there was no correlation between PPARG expression level and survival in ER− BC patients (see Figure 3(b)). We further validated these results using the online Kaplan–Meier plotter (http://kmplot.com/analysis/; see Figures 3(c) and 3(d)). Overall, these findings highlight the potential of PPARG as a therapeutic target and prognostic biomarker for ER+ BC.

3.4. PPARG Expression Is Associated with BC Immune Microenvironment. To investigate the mechanisms behind the better prognosis associated with high PPARG expression, we utilized the TIMER tool to discover a link between PPARG and the degree of infiltration of six immune cell subtypes. The results showed that BC patients with higher levels of immune cell infiltration had better cumulative survival rates compared with those with lower levels of infiltration (see Figure 4(a)). Additionally, PPARG expression was shown to be positively related to the level of infiltration of CD8+ T cells (Cor = 0.279, $p = 5.96 \times 10^{-19}$), $CD4^+$ T cells (Cor = 0.25, $p = 3.18 \times 10^{-15}$), macrophages (Cor = 0.266, $p = 2.1 \times 10^{-17}$), neutrophils (Cor = 0.176, $p = 4.75 \times 10^{-8}$), and dendritic cells (Cor =0.186, $p = 8.11 \times 10^{-9}$), with $CD8^+$ T cells having the highest correlation (see Figure 4(b)). Based on the presented data, it can be concluded that patients with high expression of PPARG in BC exhibit better cumulative survival rates. This finding is corroborated by the results displayed in Figure 3. Furthermore, we obtained RNAseq data and related clinical data of ER+ BC from the TCGA database, and Spearman's correlation analysis confirmed the relationship between PPARG and the degree of infiltration of six immune cell subtypes (see Figure 4(c)). The results indicate that high PPARG expression is intimately linked to the immunological microenvironment of BC. This suggests that PPARG potentially exerts a crucial function in regulating the immune microenvironment of BC, which could have significant clinical implications for the development of novel therapeutic techniques for BC therapy.

3.5. Gene Co-Expression Analysis. To evaluate the mechanism by which PPARG is associated with immune cells in ER+ BC, we performed gene co-expression analysis. MHC genes, immune activation genes, immunosuppressive genes,

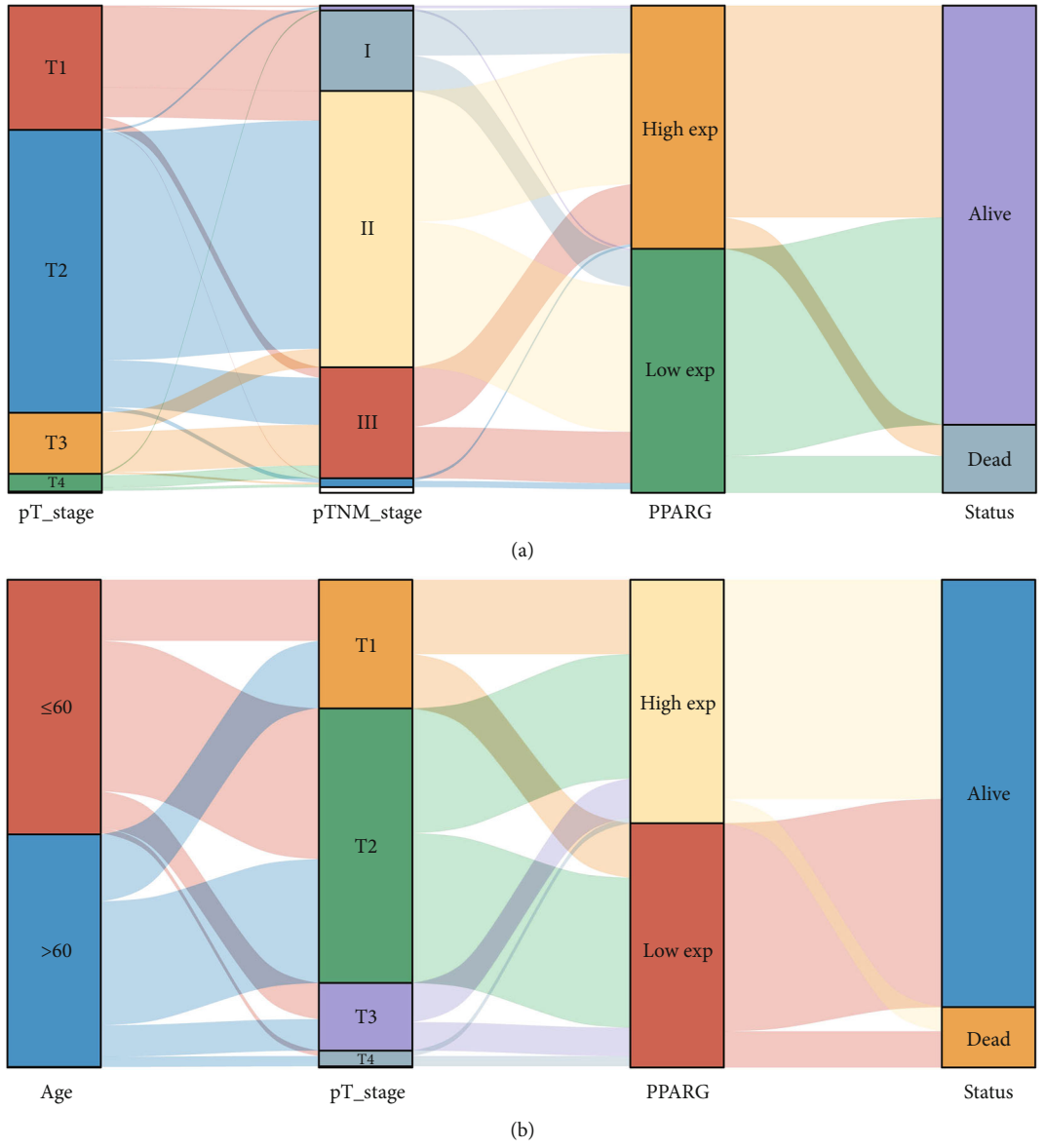

Figure 2: PPARG expression levels in BC patients in relation to clinicopathological characteristics. Each column represents a feature variable, with varying colors denoting different subtypes or stages, and the lines depicting the distribution of the same sample across the distinct feature variables. (a) PPARG expression level was related to pT-stage and pTNM-stage BC. (b) PPARG expression levels correlated with survival status, age, and pT-stage of ER+ BC.

and chemokine (receptor) related genes were studied. PPARG is co-expressed with all chemokine receptors listed, and its expression level is positively correlated with most chemokines. Meanwhile, PPARG expression was shown to be positively linked with the majority of MHC genes, such as HLA-DOA, HLA-DPB1, HLA-DRA, and HLA-E genes. It is noteworthy that the expression of PPARG is positively correlated with almost all immune suppressor genes (see Figure 5(a)).

We further compared the expression of immune checkpoints, which are molecules expressed on immune cells that inhibit immune cell function, leading to ineffective anti-tumor immune responses and tumor immune evasion, between ER+ and ER− BC. The results showed that immune checkpoints SIGLEC15 ($p = 1.17 \times 10^{-27}$), LAG3 ($p = 7.38 \times 10^{-16}$), PDCD1 ($p = 2.19 \times 10^{-10}$), CTLA4 ($p = 1.33 \times 10^{-17}$), TIGIT ($p = 4.76 \times 10^{-13}$), CD274 ($p = 1.10 \times 10^{-5}$), and PDCD1LG2 ($p = 7.19 \times 10^{-11}$) were expressed at lower levels in ER+ BC than in ER− BC (see Figure 5(b)). We found that ER+ patients exhibit stronger responses to immune checkpoint blockade (ICB) compared with ER− patients (see Figure 5(c)). A higher TIDE score is associated with reduced effectiveness of ICB therapy and shorter survival following such treatment [16]. Furthermore, the results showed that PPARG was co-expressed with these immune checkpoints (Table 3), indicating the potential of PPARG as an immunotherapy target.

3.6. Correlation Analysis between PPARG and Pathway. We obtained RNAseq data and associated clinical information for ER+ BC from TCGA database. The statistical analysis

Table 2: PPARG expression levels in ER+ and ER− BC patients in relation to clinicopathological characteristics.

		Clinicopathological characteristics	High expression group	Low expression group	p -Value
Status	ER+	Alive	364	343	0.041
		Dead	40	60	
	ER−	Alive	97	99	0.754
		Dead	22	19	
Age	ER+	Mean (SD)	58.2 (13)	60.5 (13.5)	0.015
		Median [Min, Max]	58 [26, 90]	61 [29, 90]	
	ER−	Mean (SD)	56.1 (11.8)	55.7 (12.9)	0.789
		Median [Min, Max]	55 [29, 85]	54.5 [26, 90]	
Gender	ER+	Female	399	396	0.768
		Male	5	7	
	ER−	Female	119	118	≤0.001
		Male	0	0	
pT-stage	ER+	TX	0	2	0.025
		T1	123	90	
		T2	207	247	
		T3	65	47	
		T4	9	17	
	ER−	TX	0	1	0.982
		T1	29	25	
		T2	72	77	
		T3	13	10	
		T4	5	5	
pN-stage	ER+	NX	6	10	0.182
		N0	181	175	
		N1	139	146	
		N2	39	51	
		N3	39	21	
	ER−	NX	1	1	0.375
		N0	61	75	
		N1	32	30	
		N2	15	7	
		N3	10	5	
pM-stage	ER+	MX	67	70	0.553
		M0	329	320	
		M1	6	10	
	ER−	MX	15	10	0.571
		M0	101	106	
		M1	2	2	
pTNM-stage	ER+	X	4	7	0.013
		I	81	60	
		II	211	231	
		III	100	92	
		IV	6	9	
	ER−	X	0	1	0.292
		I	19	16	
		II	65	82	
		III	31	15	
		IV	1	2	

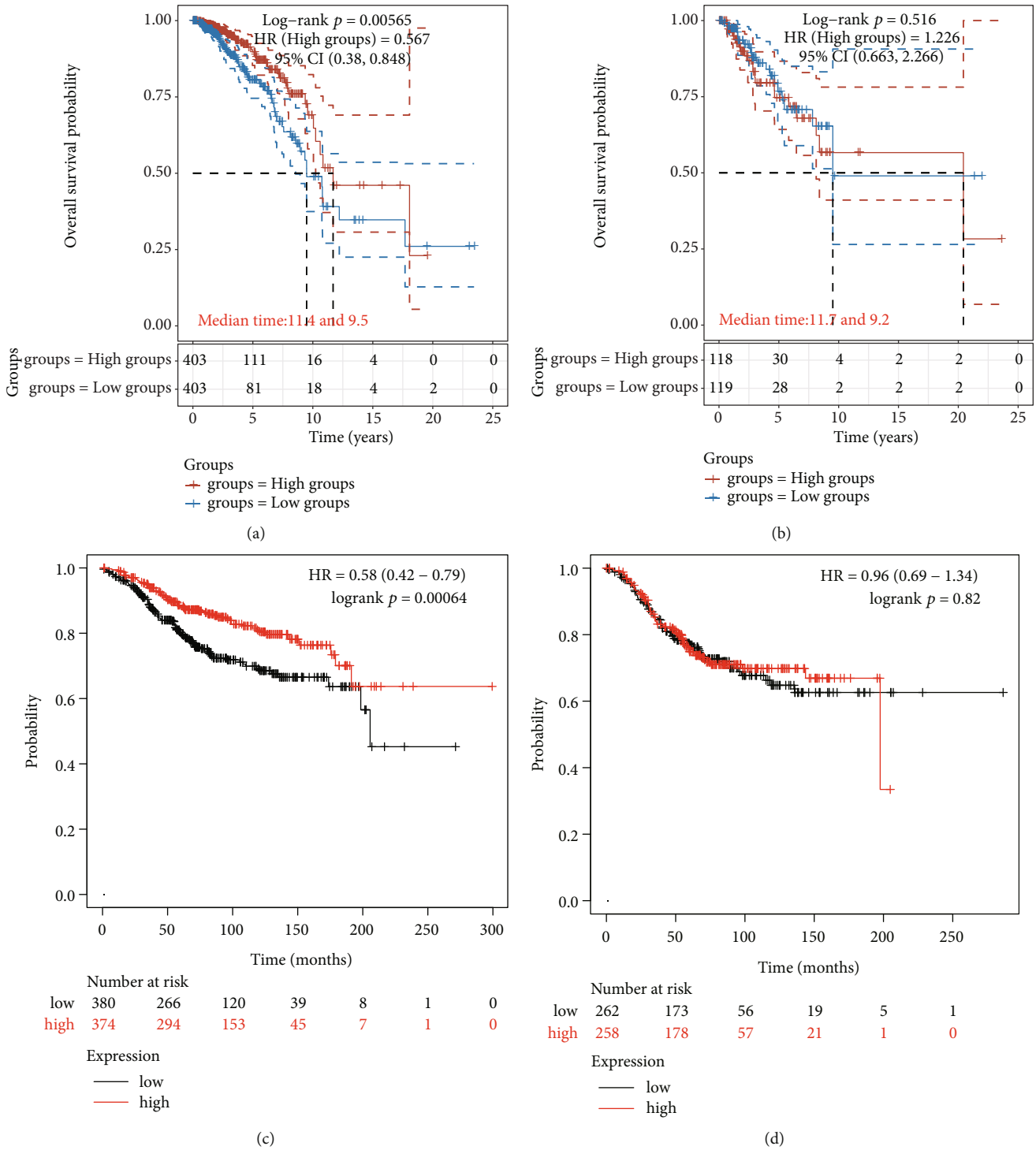

Figure 3: PPARG expression and the prognosis of BC. The KM survival curve of the PPARG gene in TCGA data is shown, wherein diverse groups were analyzed utilizing the log-rank test. HR (High exp.) represents the HR between the high and low expression groups. An HR > 1 indicates that the gene is a risk factor (higher expression is associated with poorer prognosis), whereas an HR < 1 indicates that the gene is a protective factor (higher expression is associated with better prognosis). The 95% CI represents the range of HR values with a certain level of certainty. Median time represents the time at which the survival rates of the high expression and low expression groups intersect at 50% (i.e., the median survival time). (a) Kaplan–Meier analysis of overall survival for ER+ BC in TCGA, PPARG gene is a protective factor in ER+ BC. (b) Kaplan–Meier analysis of overall survival for ER– BC in TCGA, survival of patients with ER– BC is not associated with the expression level of PPARG. (c) Kaplan–Meier analysis of overall survival for ER+ BC in Kaplan–Meier plotter, PPARG gene is a protective factor in ER + BC. (d) Kaplan–Meier analysis of overall survival for ER– BC in in Kaplan–Meier plotter, survival of patients with ER– BC is not associated with the expression level of PPARG.

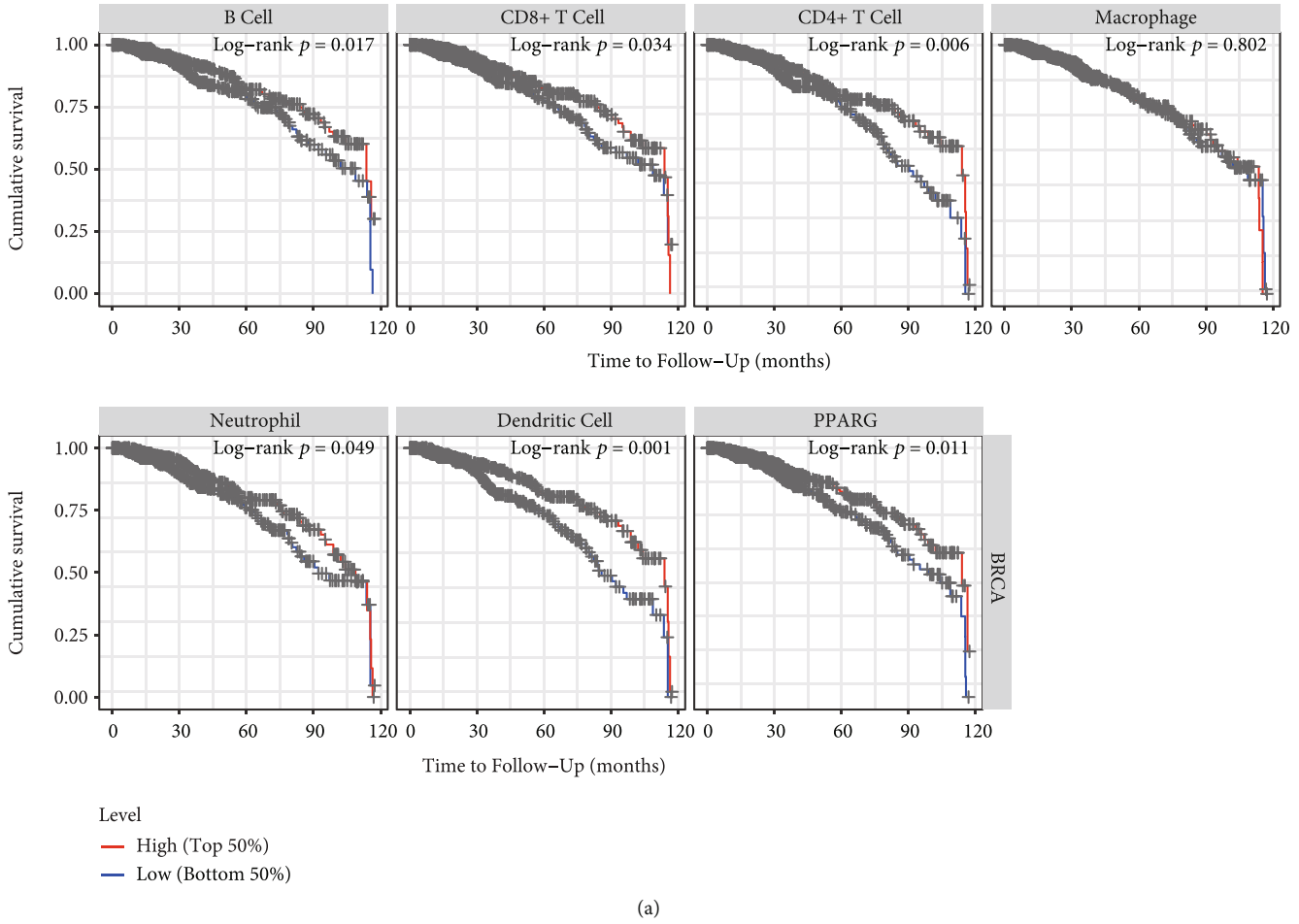

(a)

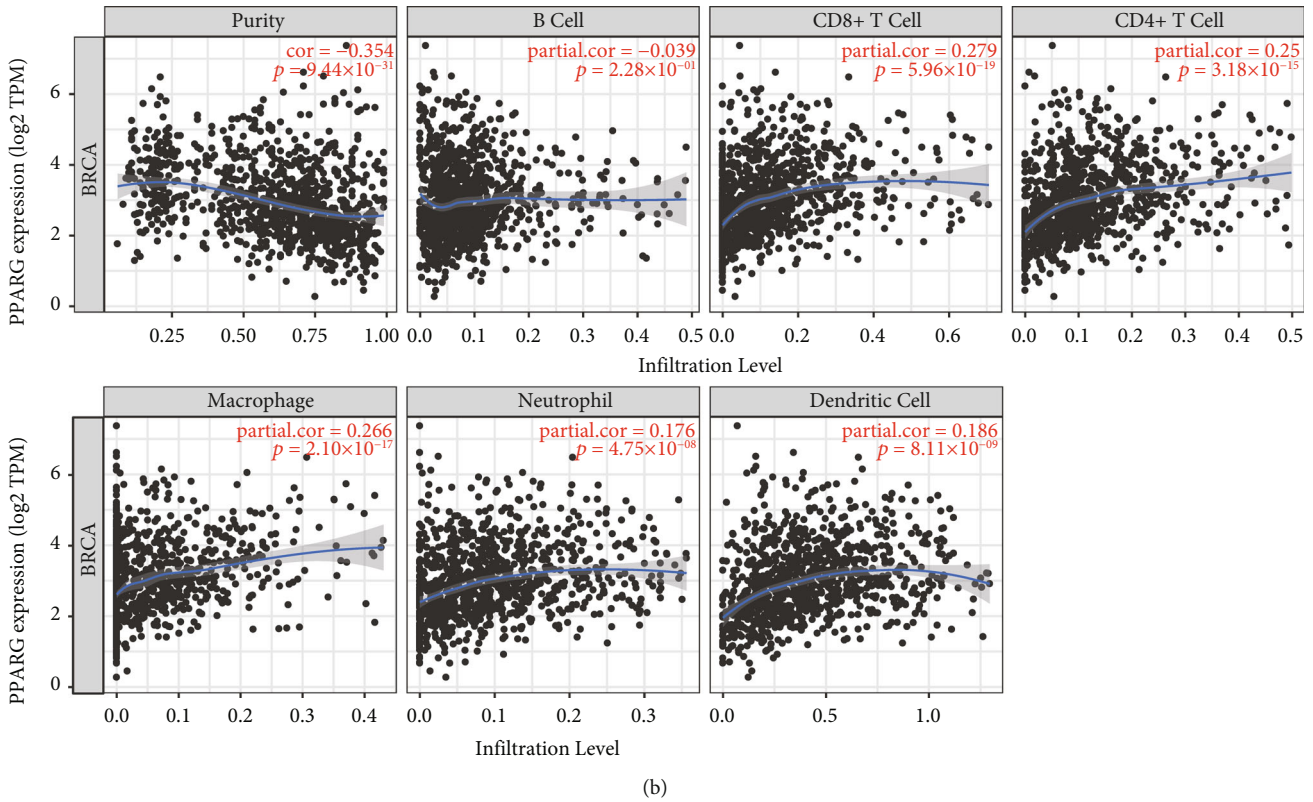

(b)

Figure 4: Continued.

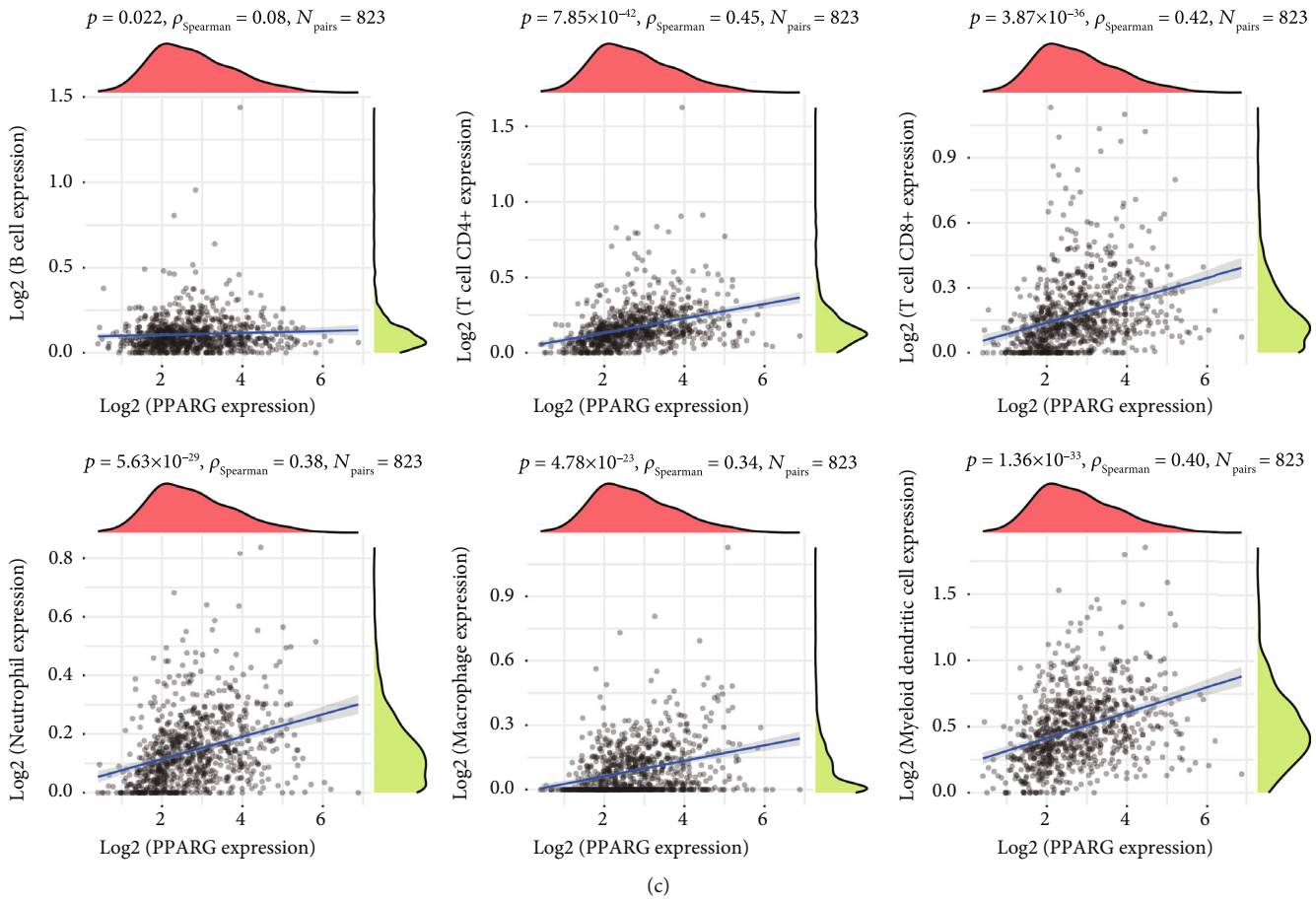

(c)

Figure 4: PPARG expression correlates with the immune microenvironment of BC. (a) Correlation between immune cell infiltration level and BC cumulative survival rate. (b) Correlation between PPARG expression levels and BC immune cell infiltration degree. (c) Correlation between PPARG expression and immune score in ER+ BC. The horizontal axis in the figure represents the distribution of the expression level of the first gene, whereas the vertical axis represents the distribution of the immune score. The right density curve shows the trend of immune score distribution, whereas the top density curve shows the trend of gene distribution. The correlation *p*-value and coefficient, as well as the method used to calculate the correlation, are indicated at the top.

revealed that PPARG is closely associated with various pathways, including angiogenesis, apoptosis, epithelial–mesenchymal transition (EMT) markers, fatty acid biosynthesis, fatty acid degradation, and glycolysis–gluconeogenesis, in estrogen receptor-positive BC (see Figure 6). Given its involvement in several critical pathways that contribute significantly to tumor growth, progression, and metastasis, these findings provide additional evidence to support the potential targeting of PPARG for the treatment of ER+ BC. Therefore, by modulating the expression or activity of PPARG, it may be possible to interfere with these pathways and inhibit tumor growth and metastasis. These discoveries offer a foundation for the development of novel PPARG-related BC treatment approaches.

3.7. Regulation of PPARG by Natural Drugs. We utilized the HERB database to search for active compounds and Chinese herbal medicines targeting the PPARG receptor, and identified experimentally verified active compounds and natural drugs. Natural drugs that up-regulate PPARG include apigenin [17], betaine [18], morusin [19], madecassoside [20], oridonin [21], curcumin [22], cannabidiol [23], piperine [24], prostaglandin A1 [25], 6-shogaol [26], epigallocatechin 3-gallate [27], rosmarinic acid [28], salvianolic acid b [29], madecassic acid [30], chrysin (5,7-di-OH-flavone) [31], and quercetin [32]. Natural drugs that down-regulated PPARG included resveratrol [33], celastrol [34], cordycepin [35], ginkgetin [36], tangeretin [37], tauroursodeoxycholic acid [38], vanillic acid [39], honokiol [40], and tannic acid [41] (see Figure 7). As discussed earlier, these results suggest that natural drugs that up-regulate PPARG may have therapeutic potential in treating ER+ BC, whereas those that down-regulate PPARG may have a negative impact on the treatment outcome. This provides a basis for the development of new natural drugs or drug combinations for further investigation of their potential in treating ER+ BC.

4. Discussion

ER+ BC is the most common subtype of BC. While endocrine therapy reduces BC recurrence and mortality, acquired resistance developed during treatment remains a significant

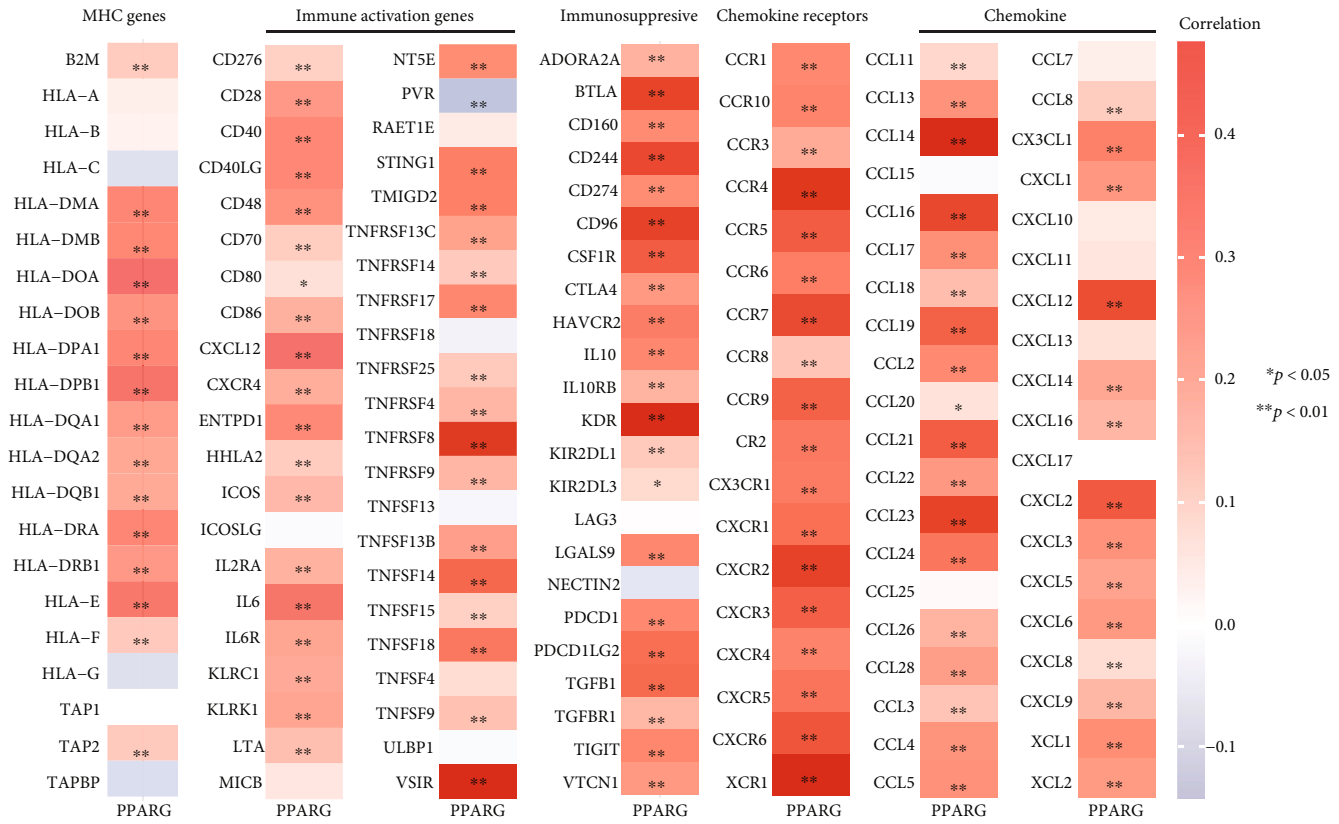

(a)

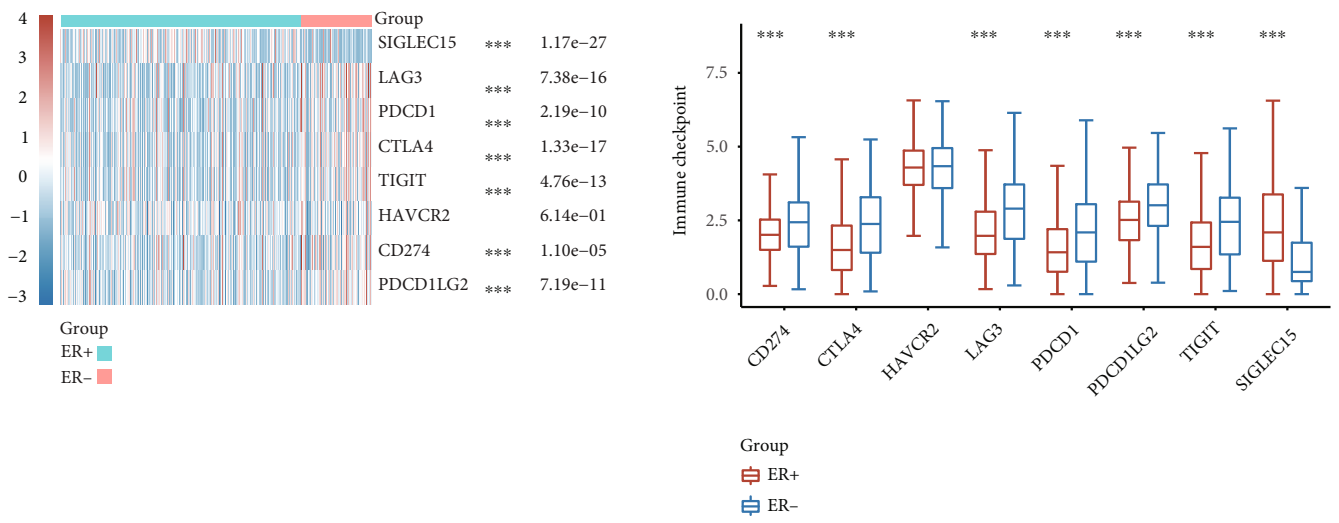

(b)

Figure 5: Continued.

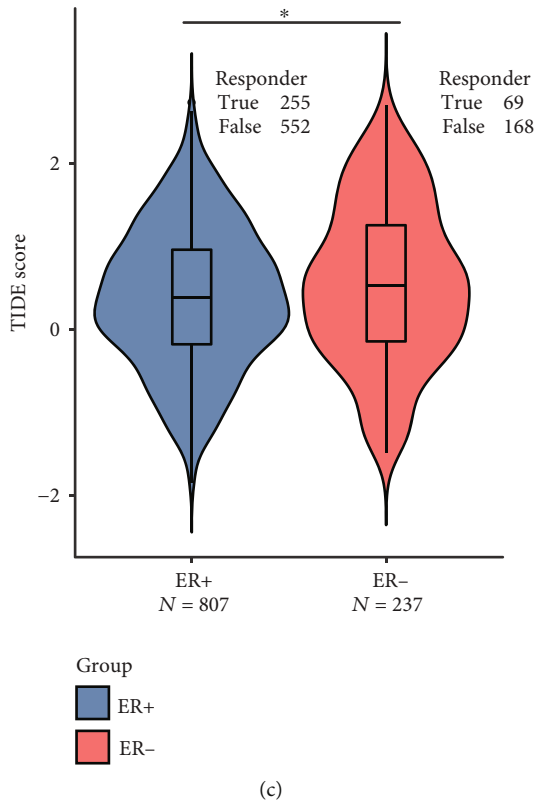

(c)

Figure 5: Co-expression analysis of PPARG, immune-related genes, and immune checkpoint molecules in BC. (a) Co-expression of PPARG with MHC genes, immunoactivation genes, immunosuppressive genes, chemokine receptor-related genes, and chemokine-related genes. (b) Different expression of immune checkpoints between ER+ and ER− BCs, $^{***}p < 0.001$. (c) Different responses of ER+ and ER− BCs to immune checkpoint blocking therapy, $^{*}p < 0.05$.

Table 3: Correlation between PPARG and immune checkpoints in estrogen receptor-positive BC.

Genes	Cor	p-Value
CD274	0.235364	$1.28 \times 10^{-11**}$
CTLA4	0.212676	$1.05 \times 10^{-9**}$
HAVCR2	0.268371	$8.86 \times 10^{-15**}$
LAG3	0.003241	0.926766
PDCD1	0.243537	$2.32 \times 10^{-12**}$
PDCD1LG2	0.294025	$1.48 \times 10^{-17**}$
TIGIT	0.248973	$7.23 \times 10^{-13**}$
SIGLEC15	0.194715	$2.46 \times 10^{-8**}$

$^{**}p < 0.001$.

challenge [42]. Drug resistance mechanisms involve various factors, such as the tumor immune microenvironment, gene regulation, estrogen and comodulated cofactors, growth factor signaling pathways, autophagy and apoptosis mechanisms, non-coding RNA regulation, and immune surveillance [43]. Currently, tumor immunity and immunotherapy have become the forefront of tumor research and are recognized as important anti-tumor pathways. The prognosis and treatment of BC are strongly associated with the stage and subtype of BC. Therefore, it is crucial to explore immune-related prognostic factors that are more generally applicable to immunotherapy of BC. These findings provide a basis for developing new natural drugs or drug combinations for further investigating their potential in the treatment of ER+ BC.

The tumor microenvironment (TME) is crucial in the progression of tumors [44], and the responsiveness of BC patients to immunotherapy depends on the dynamic response among tumor cells as well as immune infiltrating cells in TME. PPARG belongs to the ligand-activated transcription factor family and it is expressed in a variety of immune cells. It plays a critical role in various immunological processes, such as energy metabolism, cell division, inflammatory response, and cancer development and progression. Therefore, targeting PPARG may hold promise as an immunotherapy approach for BC and be associated with drug resistance and prognosis based on TME infiltration characterization of cancer tissue. Clinical studies have demonstrated the key role of PPARG in tumorigenesis and development in various types of tumors, including BC, liver cancer, lung cancer, and neurological tumors, through the inhibition of cancer cell proliferation or the promotion of cancer cell apoptosis and autophagy. However, our understanding of PPARG in BC remains incomplete, and there are few studies on its differential expression in different types of BC and its relevance with BC prognosis, which requires further in-depth study.

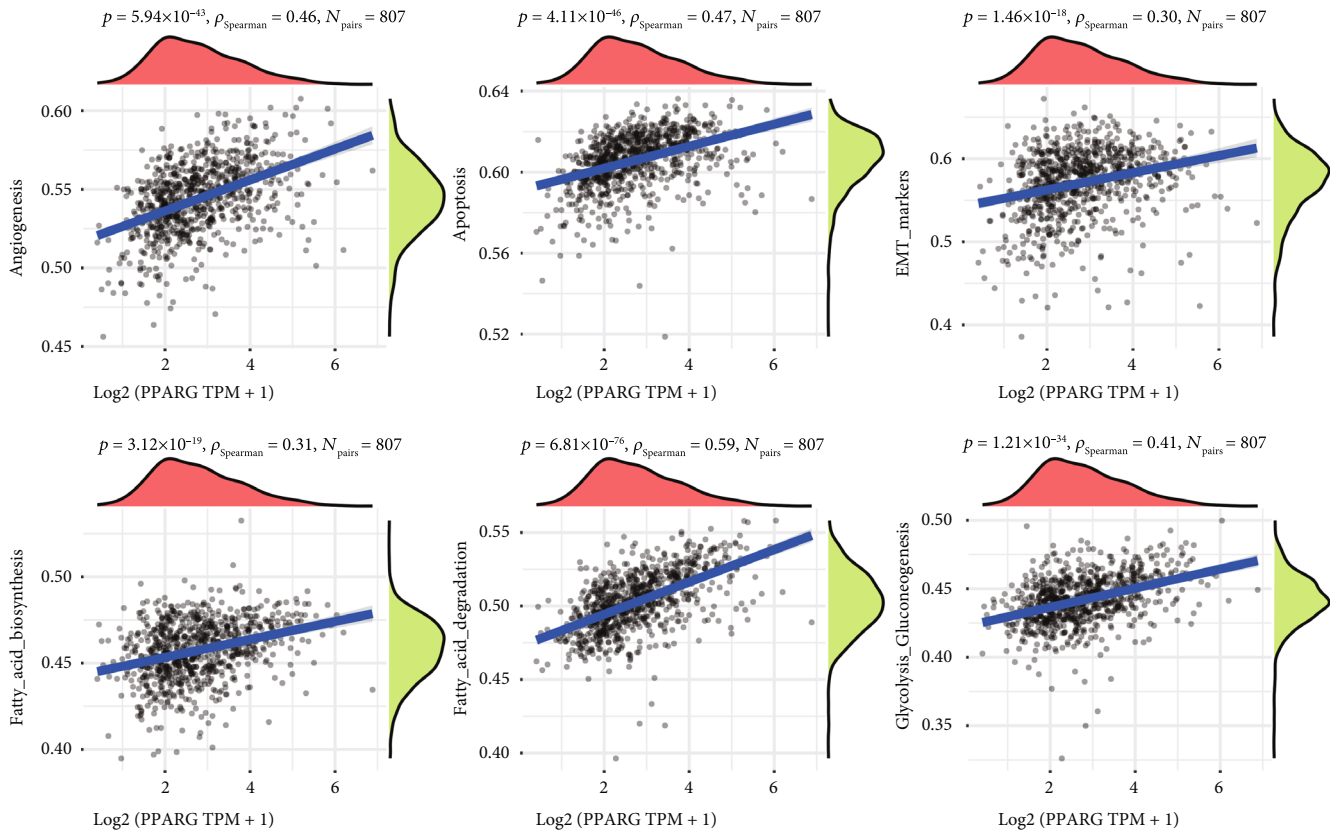

Figure 6: Spearman's correlation analysis between PPARG and path score. The *x*-axis in the picture shows gene expression, whereas the *y*-axis reflects pathway score. The right density curve depicts the trend of the pathway score distribution, whereas the topmost curve portrays the trend of distribution in gene expression level. The top numerical value (shown by the blue curve within the coordinate axis) indicates the correlation *p*-value, correlation coefficient, and method used to calculate the correlation between a single gene and pathway score.

From this study, we first found that PPARG was poorly expressed in BC. (Figures 1(a) and 1(b)). We then analyzed different types of BC and found that PPARG was underexpressed in both ER+ and ER− BC (Figures 1(c), 1(d), 1(e), and 1(f)), whereas PPARG expression is higher in ER + BC compared with ER− BC (Figure 1(h)). These results demonstrate that PPARG is expressed differently in different types of BC. Next, we evaluated the relationship between PPARG expression levels and clinicopathological variables from a clinical perspective. We discovered that the level of PPARG expression was associated with BC pT-stage and pTNM-stage (Table 1 and Figure 2(a)), and correlated with the survival status and pT-stage of ER+ BC (Table 2 and Figure 2(b)). To analyze the prognostic value of PPARG gene in BC, we used Kaplan–Meier and verified the previous results (Figure 3(c) and 3(d)). This is consistent with the findings of Jiang et al. [45]. With larger BC tumor size, the occurrence of axillary lymph node metastasis, and the increase of BC histological grade and TNM stage, PPARG expression level decreased significantly. High expression of PPARG often represents a higher overall survival rate.

There are many kinds of immune cells infiltration in TME. Studying the regulation of PPARG on immune cell infiltration levels in the TME is important to clarify its effects on BC development, metastasis, treatment, and drug resistance. PPARG not only regulates macrophage differentiation and polarization [46], but also regulates lipid metabolism of immune cells [47, 48], inhibits the production of various cytokines, such as TNF*α*, IL-1B, and IL-6 [49, 50], downregulates chemokines and receptors (IL-12, CD80, CXCL10, and RANTES), and recruits Th1 lymphocytes. PPARG can alter gene expression independently of DNA binding, and this type of transrepression may be the main molecular mechanism driving the function of macrophages, dendritic cells, and T cells in terms of their phenotype and secretory output [4], making PPARG associated with the dynamic regulation of TME. When exploring the correlation between PPARG expression and the immune microenvironment in BC, we selected the six cells mentioned above as study cells. We found that the cumulative survival rate of BC patients with high immune cell infiltration levels was better (see Figure 4(a)). Spearman's correlation analysis results also verified the correlation of PPARG with the level of infiltration of six immune cell subtypes (see Figure 4(c)), confirming that PPARG expression was positively correlated with these cells (see Figure 4(b)). The aforementioned findings indicate that BC patients with high expression of PPARG exhibit relatively better overall survival prognosis, which is consistent with the results depicted in Figure 3.

The results of our co-expression analysis showed that PPARG was positive for co-expression with all listed chemokine receptors and positively correlated with most MHC

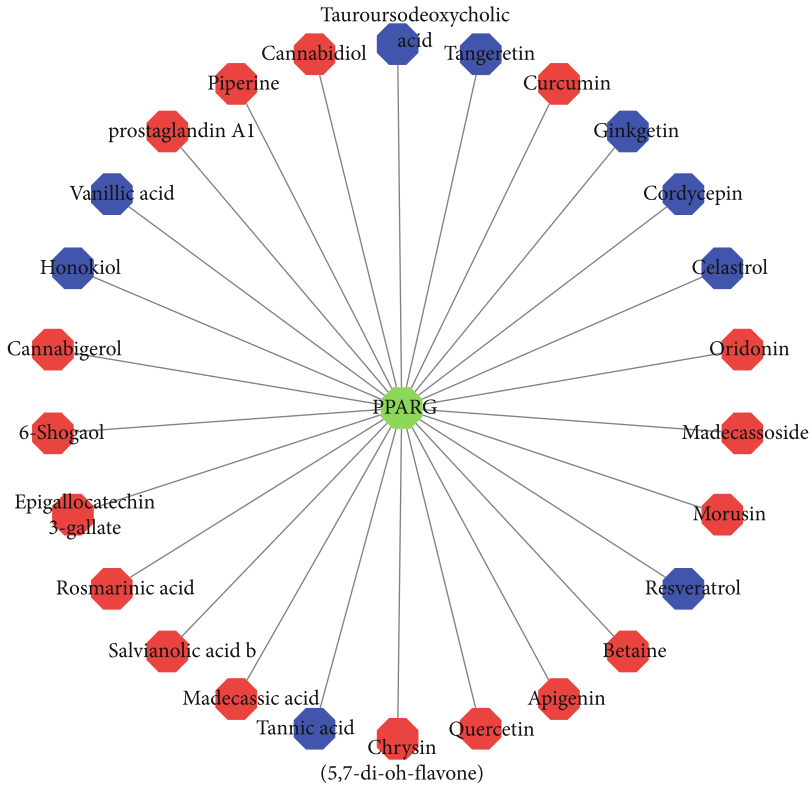

Figure 7: Regulation of PPARG by natural drugs (red represents up-regulated natural drugs, whereas blue represents down-regulated natural drugs).

genes. We found that CCR7 and CXCR2 of neutrophils, as well as CSF1R and CCL16 of macrophages were significantly correlated with PPARG expression in BC. These results suggest that PPARG may regulate macrophage polarization in BC. The expression of dendritic cell markers HLA-DPB1, HLA-DRA, and HLA-DPA1 were significantly correlated with the expression of PPARG, suggesting a close relationship between PPARG expression and the infiltration level of dendritic cells. Since dendritic cells can promote tumor progression by cross-presenting tumor antigens to activate the cross-initiating process of $CD8^+$ T cells [15], this finding is significant. Notably, almost all immunosuppressive genes were co-expressed with PPARG. The mechanism may be related to PPARG's regulation of the balance between immune cell infiltration and immunosuppression. On the one hand, it can enhance the chemotaxis and retention of immune cells and promote the beneficial immune response to kill tumor cells. On the other hand, the expression of immunosuppressive genes can be regulated by inhibiting the activity of immune cells to avoid the excessive immune response leading to normal tissue damage. In addition, PPARG may suppress the immune response by participating in the regulation of polarization of M2-type macrophages. More possible regulatory mechanisms need to be further explored.

Recent findings suggest that PPARG can affect a variety of biological functions by regulating and expressing different signaling pathways, such as β2-adrenaline promoting of BC growth and angiogenesis through the downregulation of PPARG [51], and as a PPARγ agonist, VSP-17 is capable of inhibiting the process of EMT, thereby suppressing the migration and invasion of triple-negative BC cells, through the PPARG/AMPK signaling pathway [52]. Correlation analysis of PPARG with pathways reveals that PPARG is highly correlated with angiogenesis, apoptosis, EMT markers, fatty acid biosynthesis, fatty acid degradation, glycolysis–gluconeogenesis, and other pathways. These findings illustrate that PPARG might be a viable therapeutic target, BC patients with relatively high PPARG expression may have a better prognosis, and ligands/agonists of PPARG are a new way to treat advanced BC.

By searching the HERB database, we have discovered that some natural drugs are capable of regulating the expression of PPARG. Among these drugs, those that upregulate the expression of PPARG may have potential for use in treating and preventing BC, which could lead to improved prognosis and better outcomes for BC patients. Quercetin and curcumin are two natural drugs that have received a lot of attention due to their promising research findings. According to recent research, quercetin has been shown to increase adiponectin secretion and prevent atherosclerosis by regulating factors, such as PPARG [53]. Additionally, it has been demonstrated to inhibit the development and progression of BC and other tumors [54]. Specifically, quercetin has a potent anti-tumor effect by inducing reactive oxygen species (ROS)-dependent apoptosis in MCF-7 BC cells, and it also induces apoptosis in human BC cells by activating PTEN to inhibit the PI3K/AKT and JNK signaling pathways

[55, 56]. Moreover, quercetin nanoparticles have been found to exhibit in vitro efficacy and in vivo safety, making them a promising potential anti-BC agent [57].

Curcumin interferes with the EMT process and inhibits BC cell migration, inducing BC apoptosis and cell death [58, 59]. Other natural drugs that upregulate PPARG include apigenin, betaine, morusin, madecassoside, oridonin, piperine, prostaglandin A1, cannabigerol, and others. Several flavonoids, such as apigenin, have been studied for the treatment of experimental colitis [14, 60], Apigenin inhibits p65 translocation to the nucleus by activating PPARG, reduces the expression of NF-κB, and contributes to the polarization of M2 macrophages. It also alleviates hepatic and muscle steatosis [17]. Cannabinol can regulate human metabolism, reduce β-amyloid toxicity and inflammation in rats through PPARG antagonism, and induce apoptosis through PPARG, which has therapeutic effects on liver, cervical, and lung cancers [61]. These natural compounds and active ingredients have been shown to be novel PPARG ligands in clinical trials, and their therapeutic effects and clinical value for other diseases, including BC, warrant further exploration.

5. Conclusion

Our study concludes that downregulation of PPARG is linked with poor prognosis in BC. PPARG may regulate tumor-infiltrating cells in the TME through different pathways, thereby affecting tumor development. PPARG could be a promising target for BC treatment, and natural products and compounds from traditional Chinese medicine can modulate its expression, offering a new therapeutic approach for BC treatment.

Data Availability

Data supporting this research article are available from the corresponding author or first author on reasonable request.

Conflicts of Interest

The author(s) declare(s) that they have no conflicts of interest.

Acknowledgments

This research was supported by the National Natural Science Foundation of China (Grant no. 81603412); Health Commission of Hebei Province (Grant no. 20220962); Scientific Research Project of Hebei Administration of Traditional Chinese Medicine (Grant no. 2023045); General Projects for Improving Scientific Research Capacity of Hebei College of Traditional Chinese Medicine (Grant no. KTY2019009); Hebei Province "Three Three Three Talent Project" funded project (Grant no. A202002008); and Hebei Graduate Innovation Funding Project (Grant nos. XCXZZSS2023017 and XCXZZSS2023027).

References

[1] H. Sung, J. Ferlay, R. L. Siegel et al., "Global cancer statistics 2020: GLOBOCAN estimates of incidence and mortality worldwide for 36 cancers in 185 countries," *CA: A Cancer Journal for Clinicians*, vol. 71, no. 3, pp. 209–249, 2021.

[2] D. J. Mangelsdorf, C. Thummel, M. Beato et al., "The nuclear receptor superfamily: the second decade," *Cell*, vol. 83, no. 6, pp. 835–839, 1995.

[3] B. Zhao, Z. Xin, P. Ren, and H. Wu, "The role of PPARs in breast cancer," *Cell*, vol. 12, no. 1, p. 130, 2023.

[4] M. Hernandez-Quiles, M. F. Broekema, and E. Kalkhoven, "PPARgamma in metabolism, immunity, and cancer: unified and diverse mechanisms of action," *Frontiers in Endocrinology*, vol. 12, 2021.

[5] J. Porcuna, J. Mínguez-Martínez, and M. Ricote, "The PPARα and PPARγ epigenetic landscape in cancer and immune and metabolic disorders," *International Journal of Molecular Sciences*, vol. 22, no. 19, p. 10573, 2021.

[6] Y. M. Oh, M. Mahar, E. E. Ewan, K. M. Leahy, G. Zhao, and V. Cavalli, "Epigenetic regulator UHRF1 inactivates REST and growth suppressor gene expression via DNA methylation to promote axon regeneration," *Proceedings of the National Academy of Sciences of the United States of America*, vol. 115, no. 52, pp. E12417–E12426, 2018.

[7] Y. Yang, Y. Zhou, Y. Wei, and T. Zhang, "Research progress of the role of PPARγ in autoimmune diseases," *Acta Pharmaceutica Sinica*, vol. 57, no. 10, pp. 3124–3132, 2022.

[8] A. Banno, A. T. Reddy, S. P. Lakshmi, and R. C. Reddy, "PPARs: key regulators of airway inflammation and potential therapeutic targets in asthma," *Nuclear Receptor Research*, vol. 5, p. 101306, 2018.

[9] T. Roszer, M. P. Menendez-Gutierrez, M. I. Lefterova et al., "Autoimmune kidney disease and impaired engulfment of apoptotic cells in mice with macrophage peroxisome proliferator-activated receptor γ or retinoid X receptor α deficiency," *Journal of Immunology*, vol. 186, no. 1, pp. 621–631, 2011.

[10] K. Wakabayashi, M. Okamura, S. Tsutsumi et al., "The peroxisome proliferator-activated receptor γ/retinoid X receptor α heterodimer targets the histone modification enzyme PR-Set7/Setd8 gene and regulates adipogenesis through a positive feedback loop," *Molecular and Cellular Biology*, vol. 29, no. 13, pp. 3544–3555, 2009.

[11] C. Wongtrakool, J. Ko, A. J. Jang et al., "MicroRNA-98 reduces nerve growth factor expression in nicotine-induced airway remodeling," *Journal of Biological Chemistry*, vol. 295, no. 52, pp. 18051–18064, 2020.

[12] J. Wei, A. K. Ghosh, J. L. Sargent et al., "PPARγ downregulation by TGFß in fibroblast and impaired expression and function in systemic sclerosis: a novel mechanism for progressive fibrogenesis," *PLoS One*, vol. 5, no. 11, p. e13778, 2010.

[13] S. Kohno, H. Endo, A. Hashimoto et al., "Inhibition of skin sclerosis by 15deoxy delta12,14-prostaglandin J2 and retrovirally transfected prostaglandin D synthase in a mouse model of bleomycin-induced scleroderma," *Biomedicine and Pharmacotherapy*, vol. 60, no. 1, pp. 18–25, 2006.

[14] J. Decara, P. Rivera, A. J. López-Gambero et al., "Peroxisome proliferator-activated receptors: experimental targeting for the treatment of inflammatory bowel diseases," *Frontiers in Pharmacology*, vol. 11, 2020.

[15] P. Jiang, S. Gu, D. Pan et al., "Signatures of T cell dysfunction and exclusion predict cancer immunotherapy response," *Nature Medicine*, vol. 24, no. 10, pp. 1550–1558, 2018.

[16] J. Wei, K. Huang, Z. Chen et al., "Characterization of glycolysis-associated molecules in the tumor microenvironment revealed by pan-cancer tissues and lung cancer single cell data," *Cancers*, vol. 12, no. 7, p. 1788, 2020.

[17] X. Feng, D. Weng, F. Zhou et al., "Activation of PPARγ by a natural flavonoid modulator, apigenin ameliorates obesity-related inflammation via regulation of macrophage polarization," *eBioMedicine*, vol. 9, pp. 61–76, 2016.

[18] M. R. Lakshman, K. Reyes-Gordillo, R. Varatharajalu et al., "Novel modulators of hepatosteatosis, inflammation and fibrogenesis," *Hepatology International*, vol. 8, no. S2, pp. 413–420, 2014.

[19] H. Li, Q. Wang, L. Dong et al., "Morusin suppresses breast cancer cell growth in vitro and in vivo through C/EBPβ and PPARγ mediated lipoapoptosis," *Journal of Experimental and Clinical Cancer Research*, vol. 34, no. 1, p. 137, 2015.

[20] X. Xu, Y. Wang, Z. Wei et al., "Madecassic acid, the contributor to the anti-colitis effect of madecassoside, enhances the shift of Th17 toward Treg cells via the PPARγ/AMPK/ACC1 pathway," *Cell Death and Disease*, vol. 8, no. 3, p. e2723, 2017.

[21] Y. Lu, Y. Sun, J. Zhu et al., "Oridonin exerts anticancer effect on osteosarcoma by activating PPAR-γ and inhibiting Nrf2 pathway," *Cell Death and Disease*, vol. 9, no. 1, p. 15, 2018.

[22] B. Stefanska, "Curcumin ameliorates hepatic fibrosis in type 2 diabetes mellitus – insights into its mechanisms of action," *British Journal of Pharmacology*, vol. 166, no. 8, pp. 2209–2211, 2012.

[23] W. H. Hind, T. J. England, and S. E. O'Sullivan, "Cannabidiol protects an in vitro model of the blood–brain barrier from oxygen-glucose deprivation via PPARγ and 5-HT1A receptors," *British Journal of Pharmacology*, vol. 173, no. 5, pp. 815–825, 2016.

[24] Z. G. Ma, Y. P. Yuan, X. Zhang, S. C. Xu, S. S. Wang, and Q. Z. Tang, "Piperine attenuates pathological cardiac fibrosis via PPAR-γ/AKT pathways," *eBioMedicine*, vol. 18, pp. 179–187, 2017.

[25] G. B. Xu, L. Q. Yang, P. P. Guan, Z. Y. Wang, and P. Wang, "Prostaglandin A1 inhibits the cognitive decline of APP/PS1 transgenic mice via PPARγ/ABCA1-dependent cholesterol efflux mechanisms," *Neurotherapeutics*, vol. 16, no. 2, pp. 505–522, 2019.

[26] B. S. Tan, O. Kang, C. W. Mai et al., "6-Shogaol inhibits breast and colon cancer cell proliferation through activation of peroxisomal proliferator activated receptor γ (PPARγ)," *Cancer Letters*, vol. 336, no. 1, pp. 127–139, 2013.

[27] A. Peng, T. Ye, D. Rakheja et al., "The green tea polyphenol (−)-epigallocatechin-3-gallate ameliorates experimental immune-mediated glomerulonephritis," *Kidney International*, vol. 80, no. 6, pp. 601–611, 2011.

[28] X. Zhang, Z. G. Ma, Y. P. Yuan et al., "Rosmarinic acid attenuates cardiac fibrosis following long-term pressure overload via AMPKα/Smad3 signaling," *Cell Death and Disease*, vol. 9, no. 2, p. 102, 2018.

[29] A. Sun, H. Liu, S. Wang et al., "Salvianolic acid B suppresses maturation of human monocyte-derived dendritic cells by activating PPARγ," *British Journal of Pharmacology*, vol. 164, no. 8, pp. 2042–2053, 2011.

[30] X. Yun, Y. Fang, C. Lv et al., "Inhibition of the activation of γδT17 cells through PPARγ-PTEN/Akt/GSK3β/NFAT pathway contributes to the anti-colitis effect of madecassic acid," *Cell Death and Disease*, vol. 11, no. 9, p. 752, 2020.

[31] N. Rani, S. Bharti, J. Bhatia, T. C. Nag, R. Ray, and D. S. Arya, "Chrysin, a PPAR-γ agonist improves myocardial injury in diabetic rats through inhibiting AGE-RAGE mediated oxidative stress and inflammation," *Chemico-Biological Interactions*, vol. 250, pp. 59–67, 2016.

[32] J. Q. Ma, Z. Li, W. R. Xie, C. M. Liu, and S. S. Liu, "Quercetin protects mouse liver against CCl_4-induced inflammation by the TLR2/4 and MAPK/NF-κB pathway," *International Immunopharmacology*, vol. 28, no. 1, pp. 531–539, 2015.

[33] H. D. Wang, Y. M. Shi, L. Li, J. D. Guo, Y. P. Zhang, and S. X. Hou, "Treatment with resveratrol attenuates sublesional bone loss in spinal cord-injured rats," *British Journal of Pharmacology*, vol. 170, no. 4, pp. 796–806, 2013.

[34] S. K. Choi, S. Park, S. Jang et al., "Cascade regulation of PPARγ(2) and C/EBPα signaling pathways by celastrol impairs adipocyte differentiation and stimulates lipolysis in 3T3-L1 adipocytes," *Metabolism*, vol. 65, no. 5, pp. 646–654, 2016.

[35] S. Takahashi, M. Tamai, S. Nakajima et al., "Blockade of adipocyte differentiation by cordycepin," *British Journal of Pharmacology*, vol. 167, no. 3, pp. 561–575, 2012.

[36] Y. L. Cho, J. G. Park, H. J. Kang et al., "Ginkgetin, a biflavone from *Ginkgo biloba* leaves, prevents adipogenesis through STAT5-mediated PPAR γ and C/EBPα regulation," *Pharmacological Research*, vol. 139, pp. 325–336, 2019.

[37] R. Suguro, X. C. Pang, Z. W. Yuan, S. Y. Chen, Y. Z. Zhu, and Y. Xie, "Combinational applicaton of silybin and tangeretin attenuates the progression of non-alcoholic steatohepatitis (NASH) in mice via modulating lipid metabolism," *Pharmacological Research*, vol. 151, p. 104519, 2020.

[38] M. B. Jiménez-Castro, M. Elias-Miro, M. Mendes-Braz et al., "Tauroursodeoxycholic acid affects PPARγ and TLR4 in steatotic liver transplantation," *American Journal of Transplantation*, vol. 12, no. 12, pp. 3257–3271, 2012.

[39] Y. Jung, J. Park, H. L. Kim et al., "Vanillic acid attenuates obesity via activation of the AMPK pathway and thermogenic factors in vivo and in vitro," *FASEB Journal*, vol. 32, no. 3, pp. 1388–1402, 2018.

[40] S. H. Liu, W. J. Lee, D. W. Lai et al., "Honokiol confers immunogenicity by dictating calreticulin exposure, activating ER stress and inhibiting epithelial-to-mesenchymal transition," *Molecular Oncology*, vol. 9, no. 4, pp. 834–849, 2015.

[41] F. Nie, Y. Liang, H. Xun, J. Sun, F. He, and X. Ma, "Inhibitory effects of tannic acid in the early stage of 3T3-L1 preadipocytes differentiation by down-regulating PPARγ expression," *Food and Function*, vol. 6, no. 3, pp. 894–901, 2015.

[42] A. B. Hanker, D. R. Sudhan, and C. L. Arteaga, "Overcoming endocrine resistance in breast cancer," *Cancer Cell*, vol. 37, no. 4, pp. 496–513, 2020.

[43] J. Cui and X. M. You, "Research progress in depression and tumor immune microenvironment," *Medical Recapitulate*, vol. 28, no. 14, pp. 2784–2789, 2022.

[44] T. F. Gajewski, H. Schreiber, and Y. X. Fu, "Innate and adaptive immune cells in the tumor microenvironment," *Nature Immunology*, vol. 14, no. 10, pp. 1014–1022, 2013.

[45] Y. Jiang, W. S. Liu, Y. Q. Huang et al., "Expression and clinical significance of PPARγ in different molecular subtypes of breast cancer," *Chinese Journal of Clinical Medicine*, vol. 20, no. 2, pp. 114–117, 2013.

[46] K. J. Moore, E. D. Rosen, M. L. Fitzgerald et al., "The role of PPAR-γ in macrophage differentiation and cholesterol uptake," *Nature Medicine*, vol. 7, no. 1, pp. 41–47, 2001.

[47] A. Chawla, W. A. Boisvert, C. H. Lee et al., "A PPARγ-LXR-ABCA1 pathway in macrophages is involved in cholesterol efflux and atherogenesis," *Molecular Cell*, vol. 7, no. 1, pp. 161–171, 2001.

[48] J. I. Odegaard, R. R. Ricardo-Gonzalez, M. H. Goforth et al., "Macrophage-specific PPARγ controls alternative activation and improves insulin resistance," *Nature*, vol. 447, no. 7148, pp. 1116–1120, 2007.

[49] J. S. Welch, M. Ricote, T. E. Akiyama, F. J. Gonzalez, and C. K. Glass, "PPARgamma and PPARdelta negatively regulate specific subsets of lipopolysaccharide and IFN-gamma target genes in macrophages," *Proceedings of the National Academy of Sciences of the United States of America*, vol. 100, no. 11, pp. 6712–6717, 2003.

[50] M. Ricote and C. K. Glass, "PPARs and molecular mechanisms of transrepression," *Biochimica et Biophysica Acta*, vol. 1771, no. 8, pp. 926–935, 2007.

[51] J. Zhou, Z. Liu, L. Zhang et al., "Activation of β2-adrenergic receptor promotes growth and angiogenesis in breast cancer by down-regulating PPARγ," *Cancer Research and Treatment*, vol. 52, no. 3, pp. 830–847, 2020.

[52] X. Xu, M. Liu, Y. Yang et al., "VSP17 suppresses the migration and invasion of triplenegative breast cancer cells through inhibition of the EMT process via the PPARγ/AMPK signaling pathway," *Oncology Reports*, vol. 45, no. 3, pp. 975–986, 2021.

[53] Q. Jia, H. Cao, D. Shen et al., "Quercetin protects against atherosclerosis by regulating the expression of PCSK9, CD36, PPARγ, LXRα and ABCA1," *International Journal of Molecular Medicine*, vol. 44, no. 3, pp. 893–902, 2019.

[54] M. Reyes-Farias and C. Carrasco-Pozo, "The anti-cancer effect of quercetin: molecular implications in cancer metabolism," *International Journal of Molecular Sciences*, vol. 20, no. 13, p. 3177, 2019.

[55] Q. Wu, P. W. Needs, Y. Lu, P. A. Kroon, D. Ren, and X. Yang, "Correction: different antitumor effects of quercetin, quercetin-3′-sulfate and quercetin-3-glucuronide in human breast cancer MCF-7 cells," *Food and Function*, vol. 10, no. 7, pp. 4452–4453, 2019.

[56] S. Zhu, W. Yu, L. Bi et al., "Quercetin induces apoptosis of human breast cancer cells by activating PTEN and inhibiting PI3K/AKT and JNK signaling pathways," *Xi Bao Yu Fen Zi Mian Yi Xue Za Zhi*, vol. 38, no. 8, pp. 714–720, 2022.

[57] H. A. Mohammed, G. M. Sulaiman, S. S. Anwar et al., "Quercetin against MCF7 and CAL51 breast cancer cell lines: apoptosis, gene expression and cytotoxicity of nano-quercetin," *Nanomedicine*, vol. 16, no. 22, pp. 1937–1961, 2021.

[58] B. B. Aggarwal and K. B. Harikumar, "Potential therapeutic effects of curcumin, the anti-inflammatory agent, against neurodegenerative, cardiovascular, pulmonary, metabolic, autoimmune and neoplastic diseases," *The International Journal of Biochemistry and Cell Biology*, vol. 41, no. 1, pp. 40–59, 2009.

[59] K. I. Priyadarsini, "The chemistry of curcumin: from extraction to therapeutic agent," *Molecules*, vol. 19, no. 12, pp. 20091–20112, 2014.

[60] R. Shukla, V. Pandey, G. P. Vadnere, and S. Lodhi, "Role of flavonoids in management of inflammatory disorders," in *Bioactive Food as Dietary Interventions for Arthritis and Related Inflammatory Diseases*, pp. 293–322, Academic Press, San Diego, 2019.

[61] S. E. O'Sullivan, "An update on PPAR activation by cannabinoids," *British Journal of Pharmacology*, vol. 173, no. 12, pp. 1899–1910, 2016.

Hindawi
PPAR Research
Volume 2023, Article ID 4962460, 36 pages
https://doi.org/10.1155/2023/4962460

Research Article

Development and Validation of the Promising PPAR Signaling Pathway-Based Prognostic Prediction Model in Uterine Cervical Cancer

Yan Zhang, Xing Li, Jun Zhang, Lin Mao, Zou Wen, Mingliang Cao, and Xuefeng Mu

Department of Obstetrics and Gynecology, Renmin Hospital of Wuhan University, Wuhan, China

Correspondence should be addressed to Yan Zhang; rm002125@whu.edu.cn

Received 22 December 2022; Revised 10 February 2023; Accepted 7 April 2023; Published 31 May 2023

Academic Editor: Jincheng Wang

A ligand-activated transcription factor, peroxisome proliferator-activated receptor (PPAR) regulates fatty acid uptake and transport. In several studies, upregulation of PPAR expression/activity by cancer cells has been associated with cancer progression. Worldwide, cancer of the cervix ranks fourth among women's cancers. Angiogenesis inhibitors have improved treatment for recurrent and advanced cervical cancer since their introduction 5 years ago. In spite of that, the median overall survival rate for advanced cervical cancer is 16.8 months, indicating that treatment effectiveness is still lacking. Thus, it is imperative that new therapeutic methods be developed. In this work, we first downloaded the PPAR signaling pathway-related genes from the previous study. In addition, the single-sample gene set enrichment analysis (ssGSEA) algorithm was applied to calculate the PPAR score of patients with cervical cancer. Furthermore, cervical cancer patients with different PPAR scores show different sensitivity to immune checkpoint therapy. In order to screen the genes to serve as the best biomarker for cervical cancer patients, we then construct the PPAR-based prognostic prediction model. The results revealed that PCK1, MT1A, AL096855.1, AC096711.2, FAR2P2, and AC099568.2 not only play a key role in the PPAR signaling pathway but also show good predictive value in cervical cancer patients. The gene set variation analysis (GSVA) enrichment analysis also proved that the PPAR signaling pathway is one of the most enriched pathways in the prognostic prediction model. Finally, further analysis revealed that AC099568.2 may be the most promising biomarker for the diagnosis, treatment, and prognosis in cervical cancer patients. Both the survival analysis and Receiver Operating Characteristic curve demonstrated that AC099568.2 plays a key role in cervical cancer patients. However, to our knowledge, this is the first time a study focused on the role of AC099568.2 in cervical cancer patients. Our work successfully revealed a new biomarker for cervical cancer patients, which also provides a new direction for future research.

1. Introduction

Each year, approximately 500,000 women are diagnosed with invasive uterine cervical cancer (UCC) worldwide, resulting in 273,000 deaths [1]. It is estimated that over 70% of cancer patients have reached a very advanced stage of their illness [2]. It is reported that 604,127 women worldwide will be diagnosed with cervical cancer by 2020 [3]. There could be approximately 7 million fewer cases of human papillomavirus (HPV) over the next half-century with screening campaigns and broad-spectrum vaccinations for HPV [4]. According to recent guidelines released by the International Federation of Gynecological Ecology and Obstetrics (FIGO), a variety of imaging tools, surgery, and pathology can be used to stage cervical cancer [5]. Given the high costs of additional tests, a clinical approach is still considered acceptable in low- and middle-income countries [6]. Although HPV infection is ubiquitous and a major etiological factor in the carcinogenesis process, it is not always detectable in all patients with UCCs [7]. Approximately 75% of cervical cancer patients develop polypoidal exophytic masses inside the ectocervix caused by squamous cell carcinoma [8]. There are also instances where the endocervix may become dilated due to ulcerations, barrel adenocarcinomas, or

adenosquamous cell carcinomas, which originate from the columnar epithelium [9]. There are several routes of spread, including the direct extension to the vaginal mucosa, the adjacent parametrial tissues, the bladder, or the rectum [10]. A growing body of knowledge is available about the oncology, tumor biology, and tumor morphology of cervical cancer at present. This field is also currently interested in identifying genetic, molecular, and immunohistochemical markers as early detection tools for precancerous lesions and neoplastic processes. As part of oncology, a biomarker is often a gene, DNA, RNA, protein, enzyme, antigen, or other cellular and biological product [11]. There is evidence that these lesions may occur at various stages of carcinogenesis under the influence of therapy. Many modern reviews and articles have discussed these lesions [12].

Since 1990, Issemann and Green have been discovering ligand-activated transcription factors called peroxisome proliferator-activated receptors (PPARs) [13]. There are three different subtypes of PPAR, PPAR α, and PPAR β/δ, which are located on different chromosomes and encoded by specific genes [14]. In spite of their significant homology, these three proteins differ in their tissue distribution, an affinity for ligands, and biological function [15]. Many modern reviews and articles on carcinogenesis describe how these lesions can be detected at various stages of carcinogenesis, as well as how therapy can influence their development [16]. However, few studies focused on the correlations between PPAR signaling pathways and UCC. Therefore, we aim to explore the potential association between UCC and PPAR signaling pathways by bioinformatics analysis.

The Cancer Genome Atlas (TCGA) database was used to obtain expression data for this study to investigate the role of PPAR signaling pathways in UCC. In addition, the single-sample gene set enrichment analysis (ssGSEA) algorithm was applied to explore the score of PPAR signaling in patients with UCC. A Gene Ontology (GO) enrichment analysis and a Kyoto Encyclopedia of Genes and Genomes (KEGG) enrichment analysis were also conducted in order to identify potential pathways closely related to the key genes. Finally, we decided to explore the potential biomarkers for better prognosis prediction of patients with UCC.

2. Methods

2.1. Dataset Downloaded. Data on mRNA expression and clinical information were downloaded from the Cancer Genome Atlas database for UCC patients. In addition, the genes that are closely associated with the PPAR were also obtained from the previous studies.

2.2. Tumor Immune Estimation Resource Analysis. The Tumor Immune Estimation Resource (TIMER) software program (https://cistrome.shinyapps.io/Timer/) provides a comprehensive approach to analyze immune infiltration in different cancer types. An analysis of TIMER was performed to determine whether immune cell infiltration was related to the level of expression of the immune-related cells.

2.3. Single-Sample Gene Set Enrichment Analysis. For each tumor case, an individual score was calculated using ssGSEA. In ssGSEA, ranking-based GSEA methods are used to compute overexpression measures for genes of interest relative to other genes in the genome. Based on log-transformed data from RNA-Seq or microarray experiments, ssGSEA scores were calculated. In the next step, we classified UCCs according to related pathways (ssGSEA scores) and analyzed both tumor purity and immune scores for each patient.

2.4. The Enrichment Pathway Analysis Based on the Key Genes. Using functional enrichment, the data were further analyzed to confirm the potential functions of the potential targets. GO is widely used to annotate genes with their functions, especially molecular functions (MF), biological pathways (BP), and cellular components (CC). Analyzing gene function and related high-level genome function information using KEGG enrichment analysis is practical and useful. An analysis of the GO function of potential mRNAs and enrichment of KEGG pathways was performed using the ClusterProfiler package in R to better understand the oncogenic functions of target genes.

2.5. Construction of the Prognostic Prediction Model of the PPAR Signaling Pathways. Module members (MM) represent gene expression profiles that are correlated with genes that belong to the module. We then performed univariate analyses of each gene in the module to identify genes associated with the prognosis that were significantly associated. We used COX regression based on the least absolute shrinkage and selection operator (LASSO) to further narrow down the candidate biomarkers for immunization prognosis using the "glmnet" R package. Using the "survminer" R package, samples were divided into low-risk and high-risk groups based on a bivariate model with nonzero coefficients. R was also used to perform the survival analysis.

2.6. Immune Cell Infiltration Analysis. An analysis of RNA-seq data from UCC patients in different subgroups was conducted to determine the relative proportions of 22 immune infiltrating cells. To determine whether immune cell infiltration and gene expression are related, Spearman correlation analysis was conducted.

2.7. Gene Set Variation Analysis. Gene set variation analysis (GSVA), an unsupervised, non-parametric method, was used to evaluate gene set enrichment. As a result of scoring the genes of interest, followed by determining the biological function of the sample, changes at the gene level were transformed into changes at the pathway level in this study. In the present study, gene sets were retrieved using the molecular signatures database (version 7.0). The GSVA algorithm was used to evaluate a wide range of samples for potential biological function changes.

2.8. Gene Set Enrichment Analysis. Gene sets were retrieved from MSigDB (http://www.gsea-msigdb.org/gsea/downloads.jsp). In order to identify enriched GO terms from the gene sets, GSEA was performed using the 50 best terms selected from each subtype.

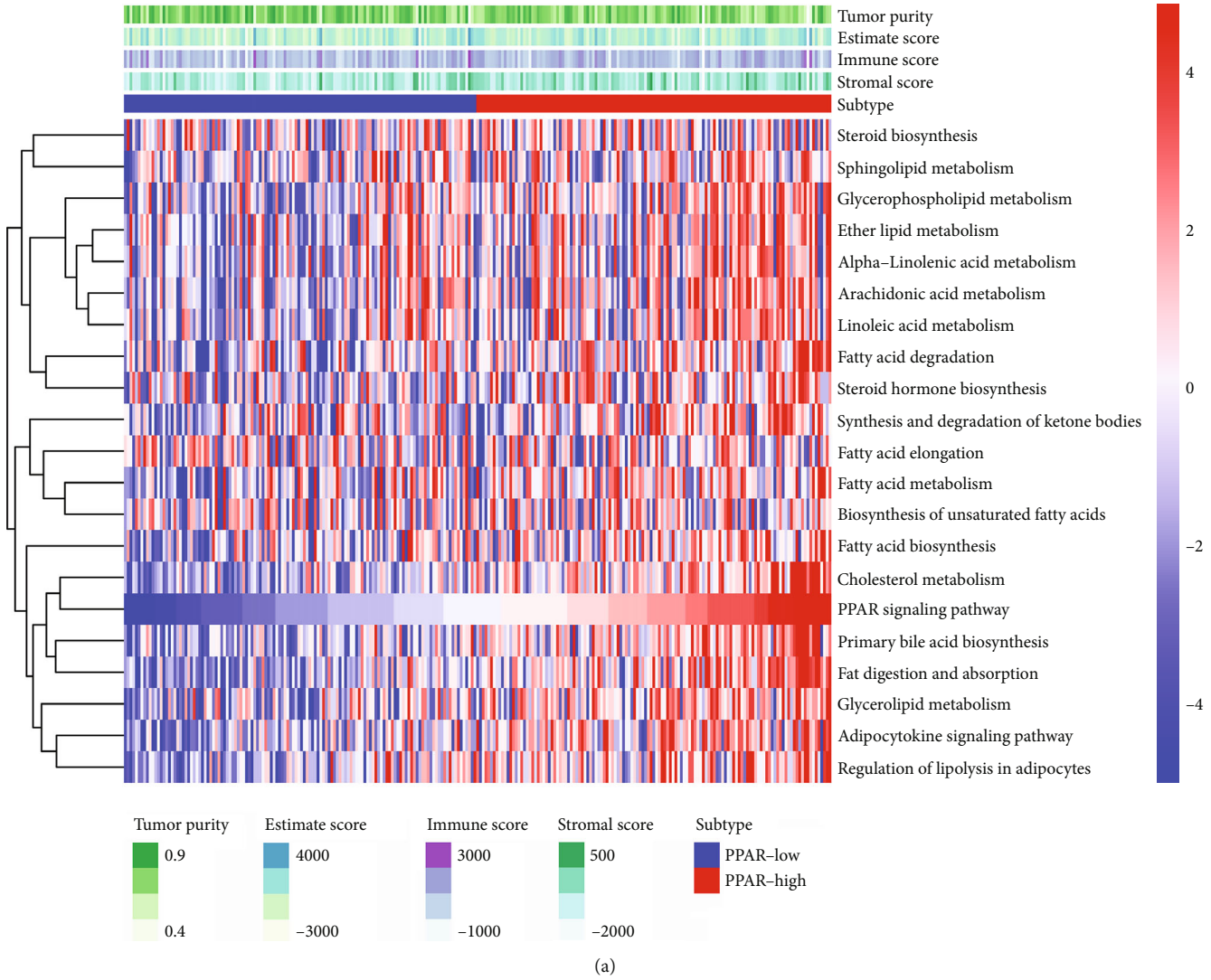

(a)

Figure 1: Continued.

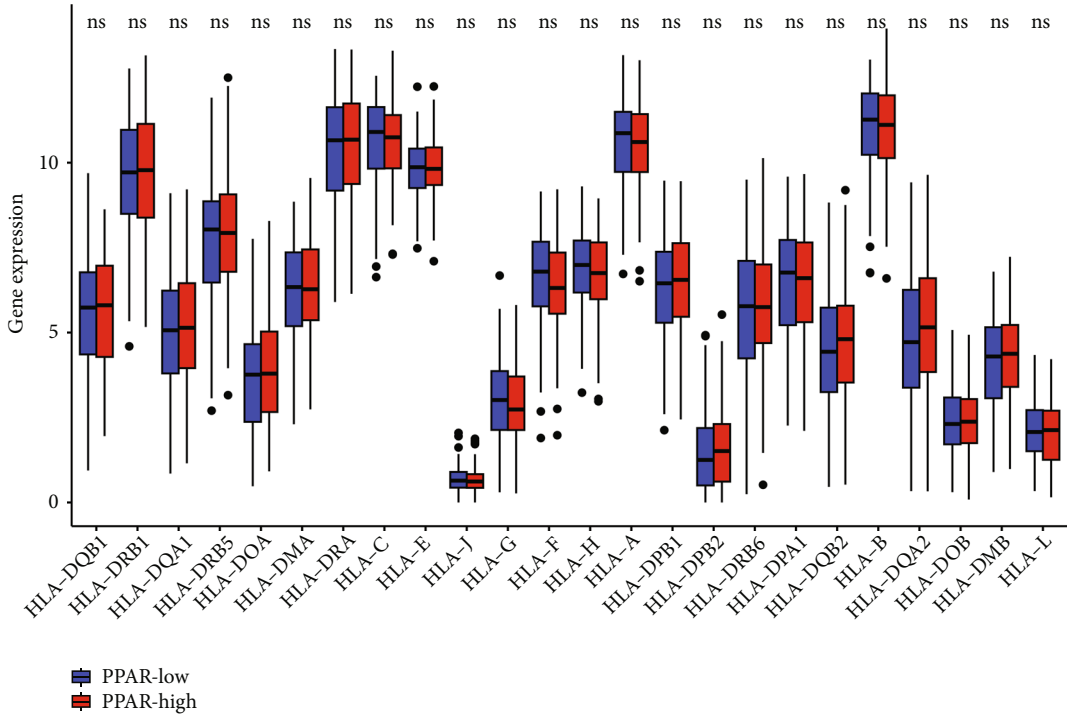

(b)

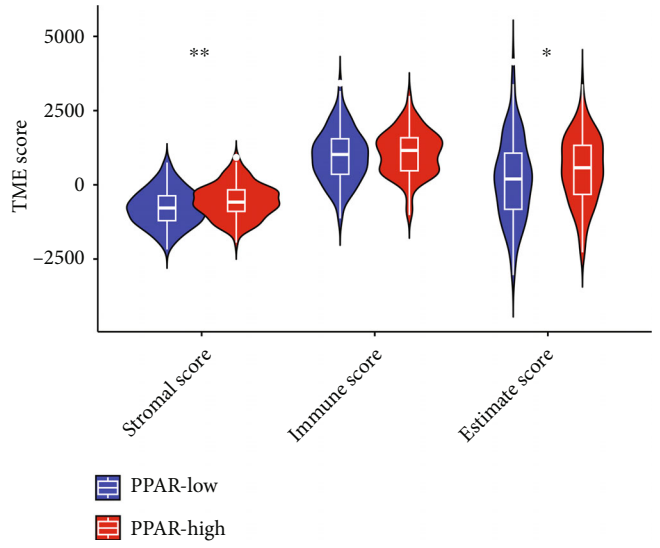

(c)

Figure 1: Continued.

(d)

Figure 1: Continued.

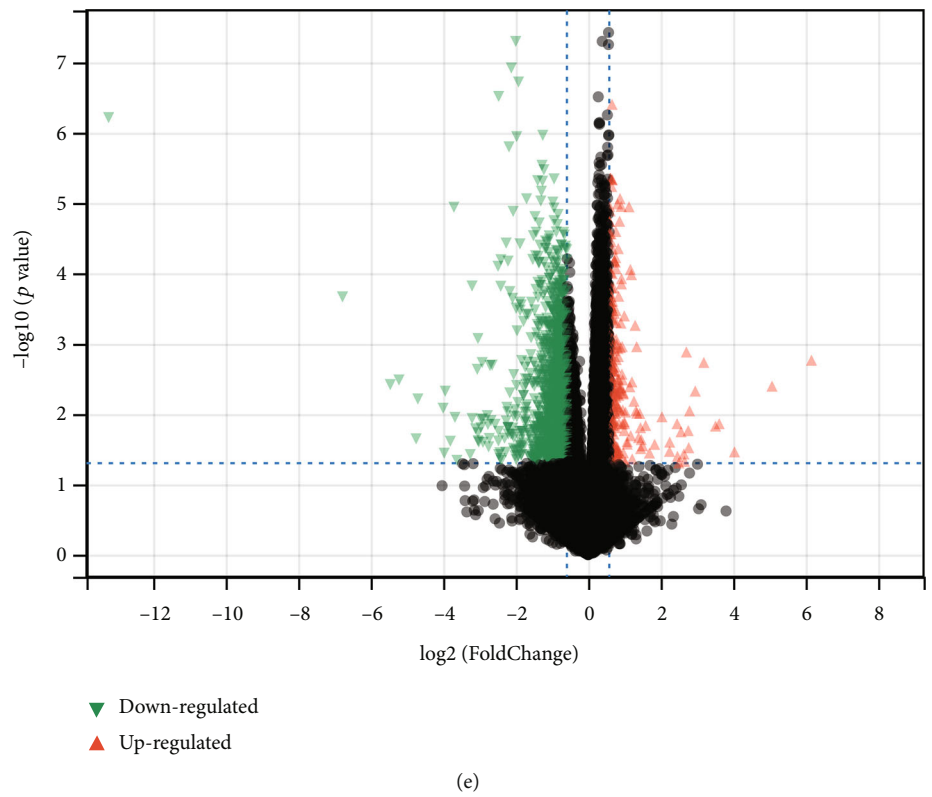

(e)

Figure 1: (a) The heat map reveals the results of the ssGSEA algorithm; (b) the different expression levels of HLA-related genes between low- and high-PPAR groups; (c) the different immune-related score between low- and high-PPAR groups; (d) the heat map demonstrated the differentially expressed genes between low- and high-PPAR groups; (e) the volcano map demonstrated the differentially expressed genes between low- and high-PPAR groups.

3. Results

3.1. The ssGSEA Algorithm Was Used to Obtain the PPAR Signaling Score for UCC Patients. On the basis of the former study, we successfully obtained the genes that play a key role in the PPAR signaling pathways. Finally, a total of 72 genes were regarded as the genes that are closely associated with the PPAR signaling pathways. Subsequently, by using the ssGSEA algorithm, the patients with UCC were successfully divided into low- and high-PPAR signaling pathways groups. In addition, we also evaluate other pathways, such as cholesterol metabolism, primary bile acid biosynthesis, fat digestion and absorption, glycerolipid metabolism, and regulation of lipolysis in adipocytes. The results demonstrated that the PPAR-high group is associated with the high pathways of cholesterol metabolism, primary bile acid biosynthesis, fat digestion and absorption, glycerolipid metabolism, and regulation of lipolysis in adipocytes (Figure 1(a)). Furthermore, we then explore the correlation between Human Leukocyte Antigen (HLA)-related genes and PPAR score (Figure 1(b)). The results did not show potential associations. In addition, we also discovered that high score of PPAR signaling pathway is associated with a higher stromal score and estimate score (Figure 1(c)). According to the differentially expressed analysis, 290 genes were found to be differentially expressed, including 57 genes that were up-regulated and 233 genes that were down-regulated (Figures 1(d) and 1(e)).

3.2. The Potential Pathways That Are Closely Associated with the Differentially Expressed Genes. Next, we performed the enrichment pathways analysis based on the 290 different expression genes. The results revealed that complement and coagulation cascades, PPAR signaling pathway, cholesterol metabolism, bile secretion, insulin resistance, fat digestion and absorption, and glycolysis are the most enriched pathways of KEGG terms (Figures 2(a) and 2(b)). Additionally, for Hallmark terms, the most enriched pathways involve coagulation, xenobiotic metabolism, bile acid metabolism, KRAS signaling dn, myogenesis, and angiogenesis (Figures 2(c) and 2(d)).

3.3. Evaluation of the Association between PPAR Score and Immune-Related Cells and Immune Checkpoint-Related Genes. Subsequently, we aim to explore the potential correlation between PPAR score and immune-related cells. A total of 22 types of immune-related cells were identified. The results finally revealed that the lower PPAR score is associated with more infiltration of CD4-activated T cells, while the higher PPAR score is associated with more infiltration of M2 macrophages (Figure 3(a)). In terms of the immune checkpoint genes, the PPAR score is positively associated with HAVCR2, while the PPAR score is negatively associated with CD274, PDCD1, CTLA4, LAG3, and PDCD1LG2 (Figures 3(b), 3(c), 3(d), 3(e), 3(f), and 3(g)).

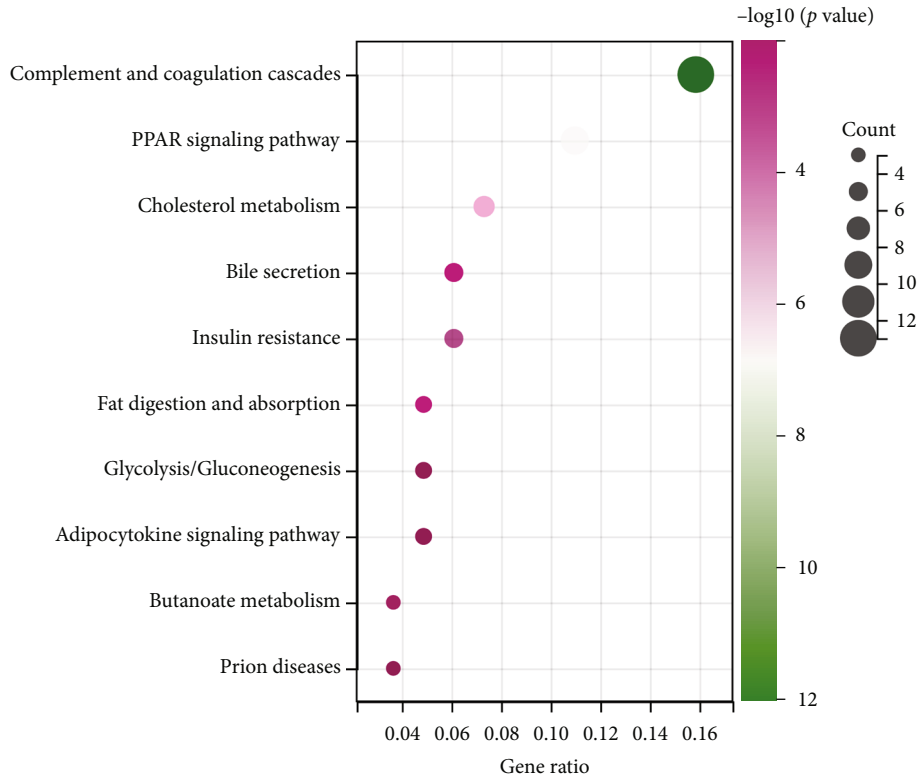

(a)

Figure 2: Continued.

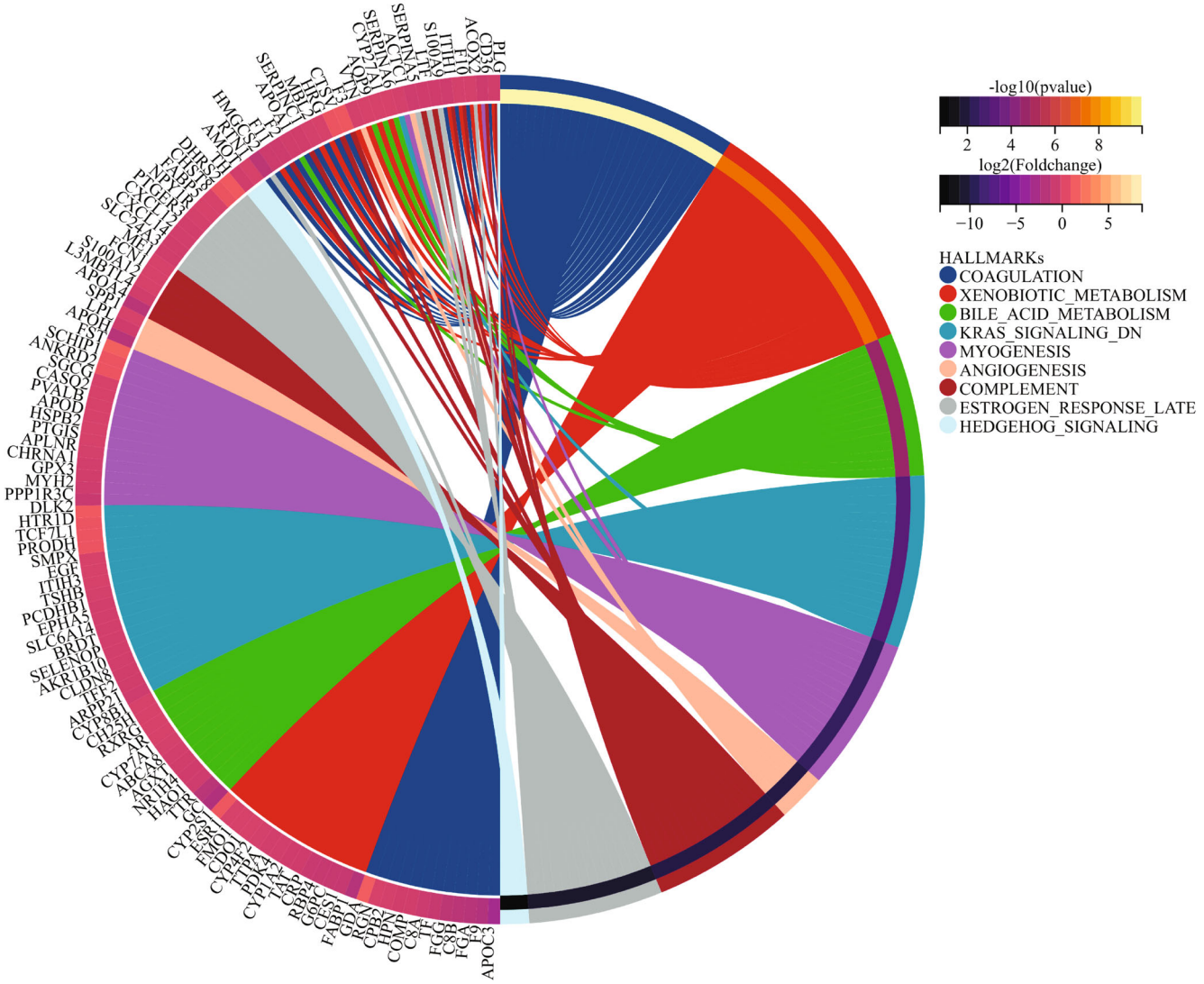

(b)

Figure 2: Continued.

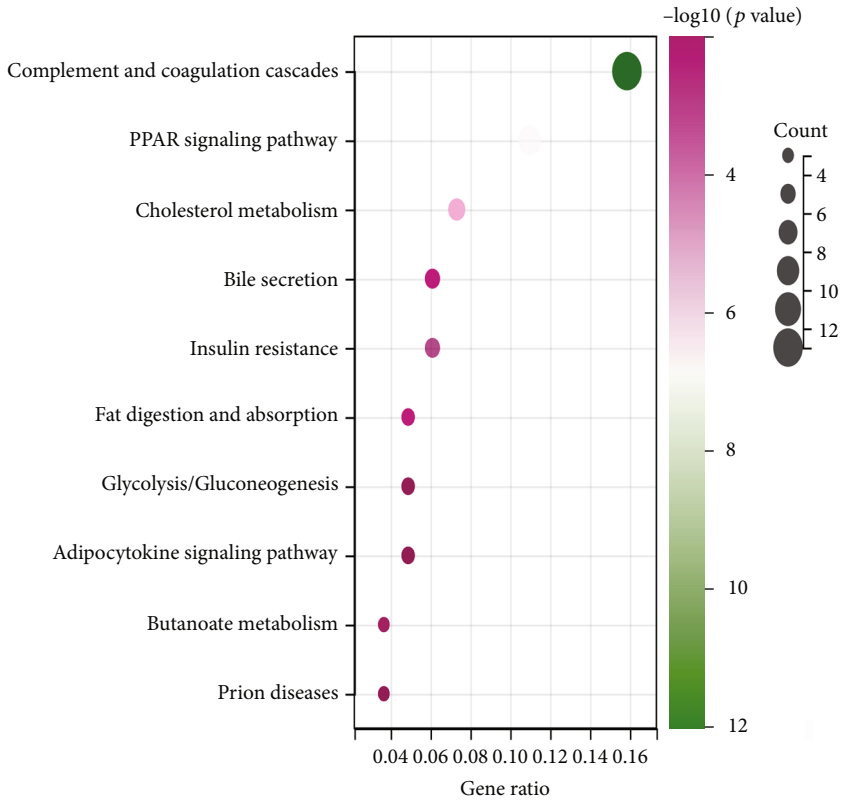

(c)

Figure 2: Continued.

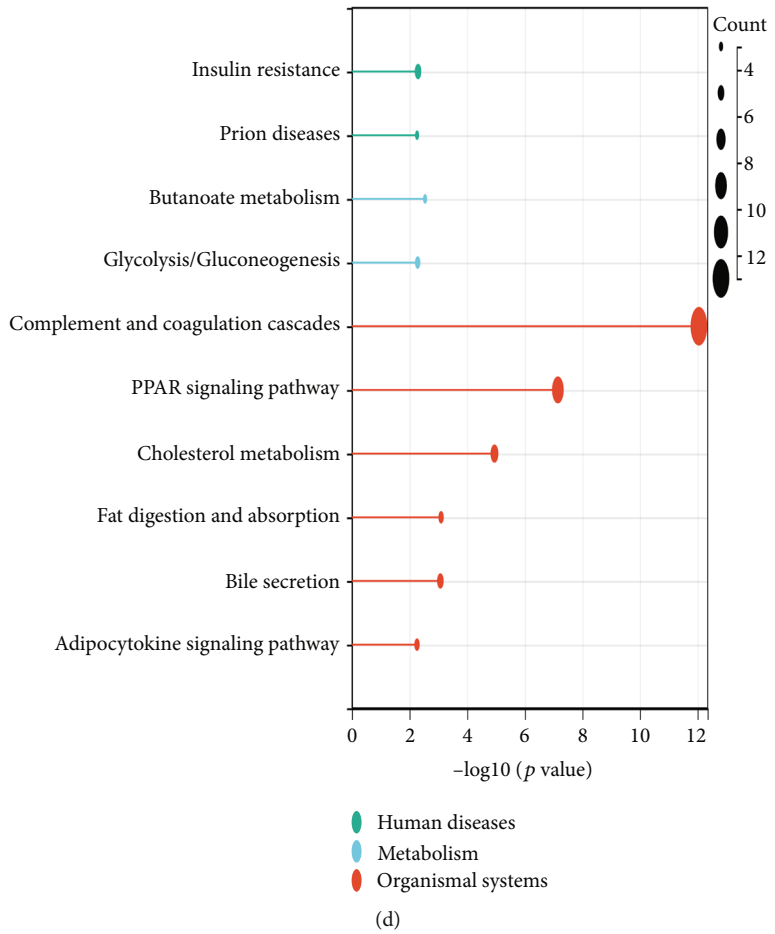

(d)

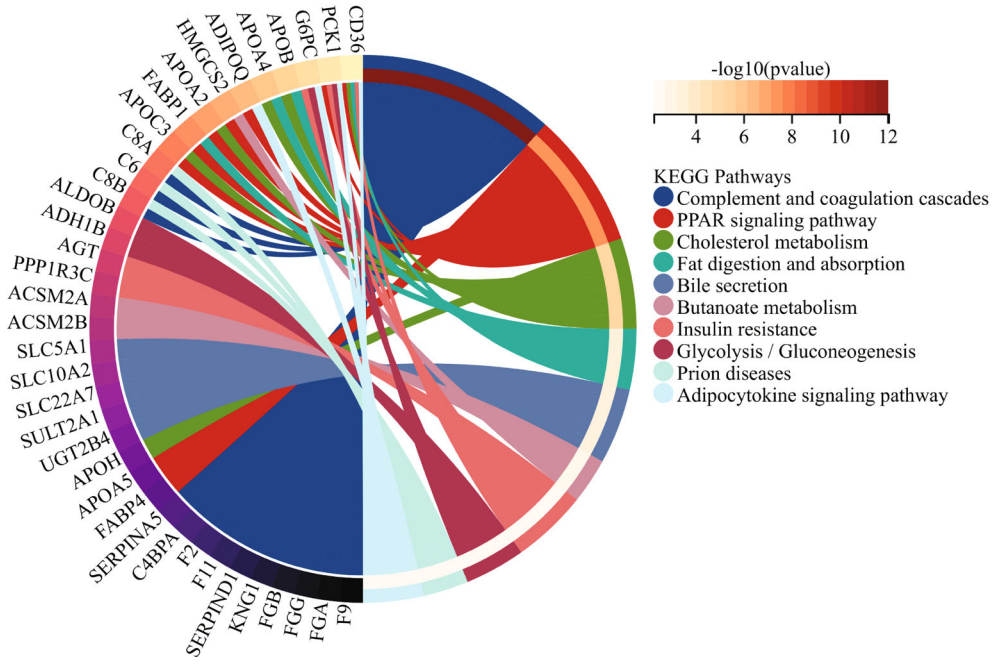

(e)

Figure 2: (a, c, and e) The results of KEGG enrichment analysis; (b and d) the enrichment analysis based on the Hallmark terms.

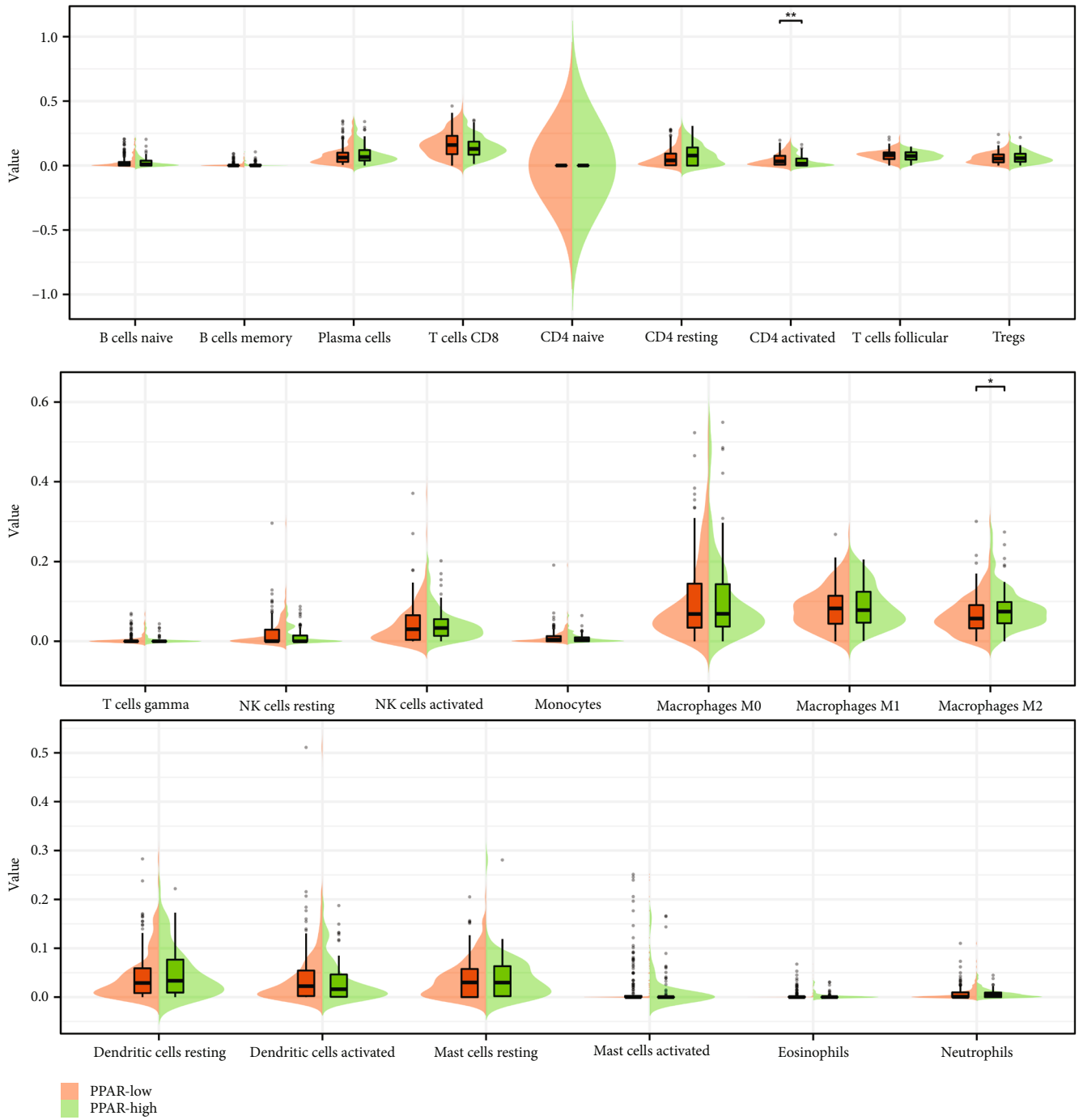

(a)

Figure 3: Continued.

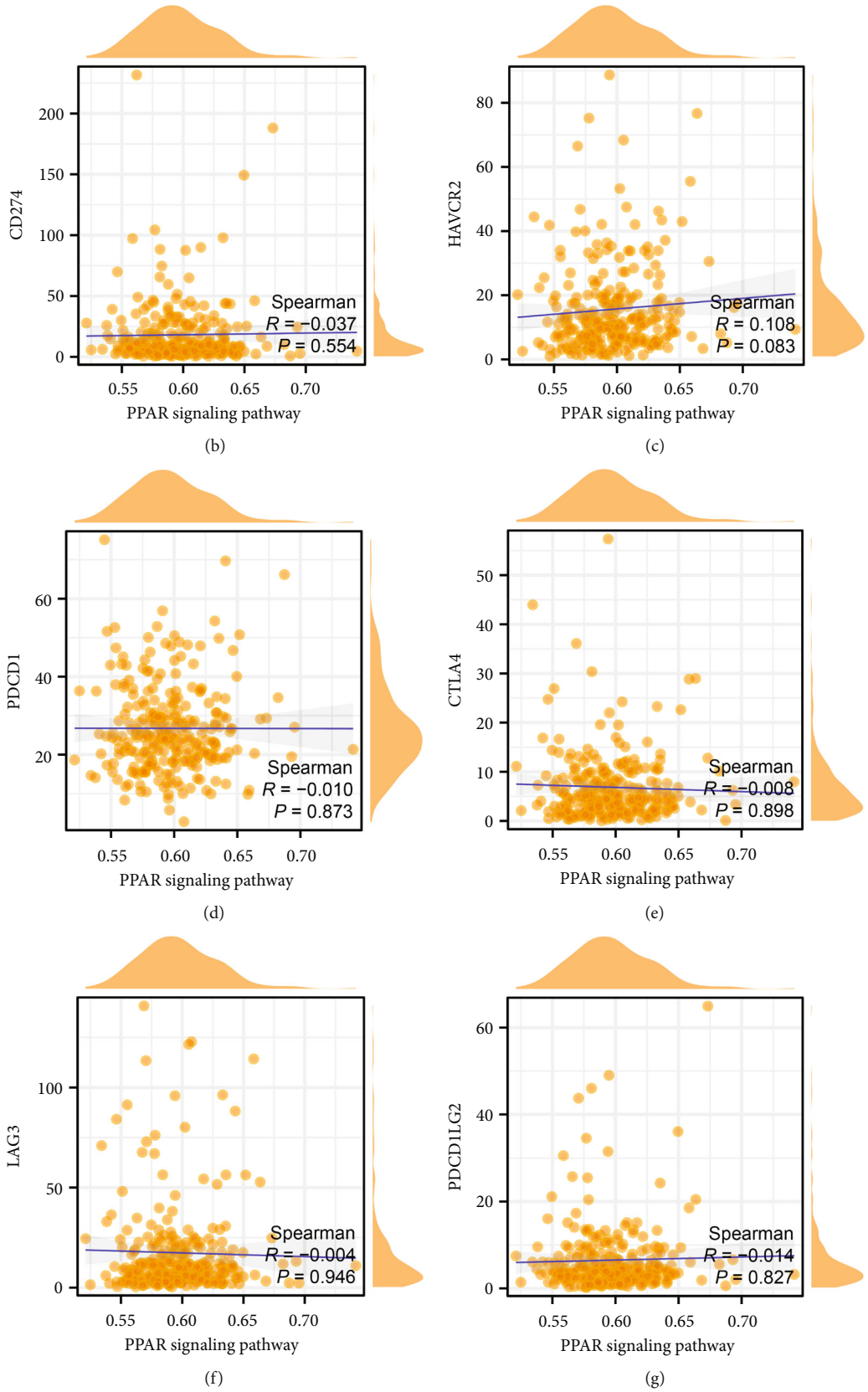

Figure 3: (a) The immune infiltration analysis between low- and high-PPAR groups; the correlation between PPAR score and CD274 (b); HAVCR2 (c); PDCD1 (d); CTLA4 (e); LAG3 (f); PDCD1LG2 (g).

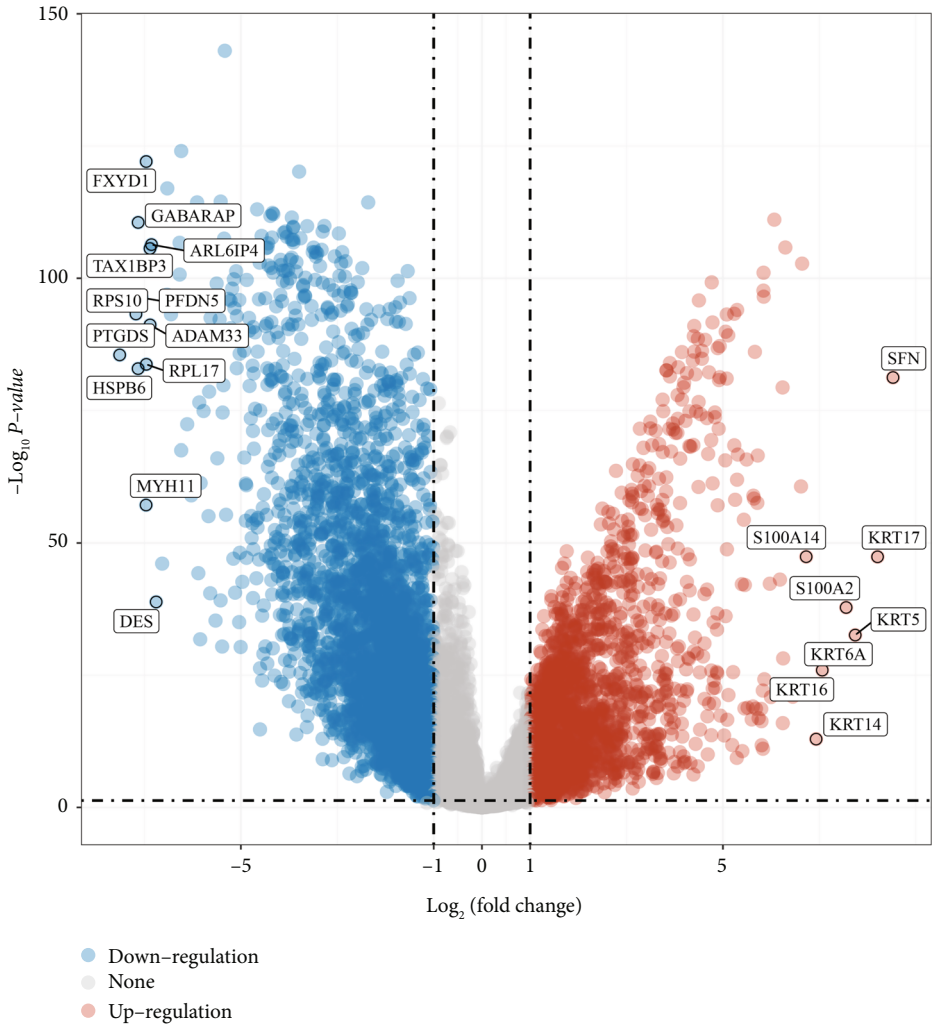

(a)

Figure 4: Continued.

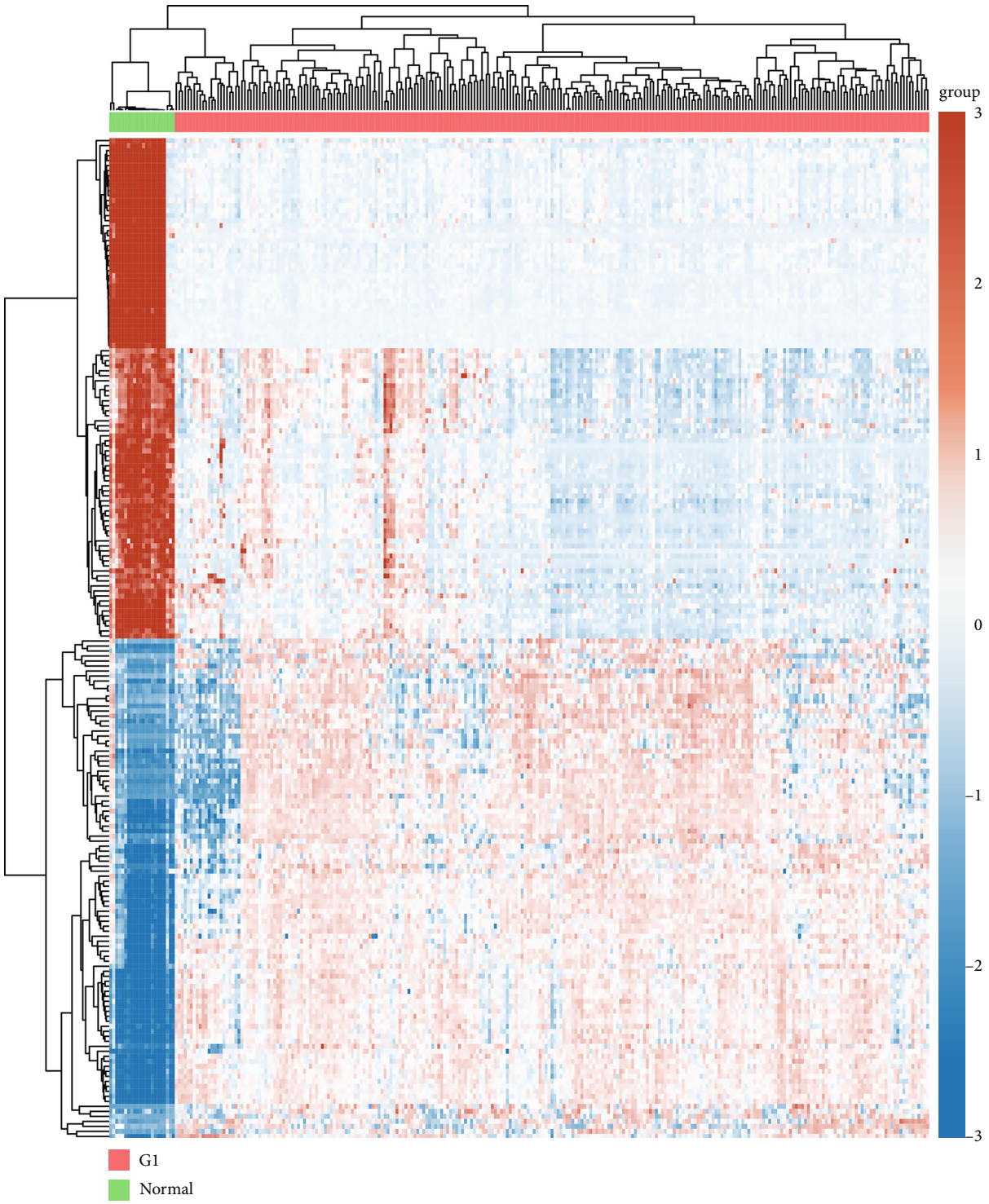

(b)

Figure 4: Continued.

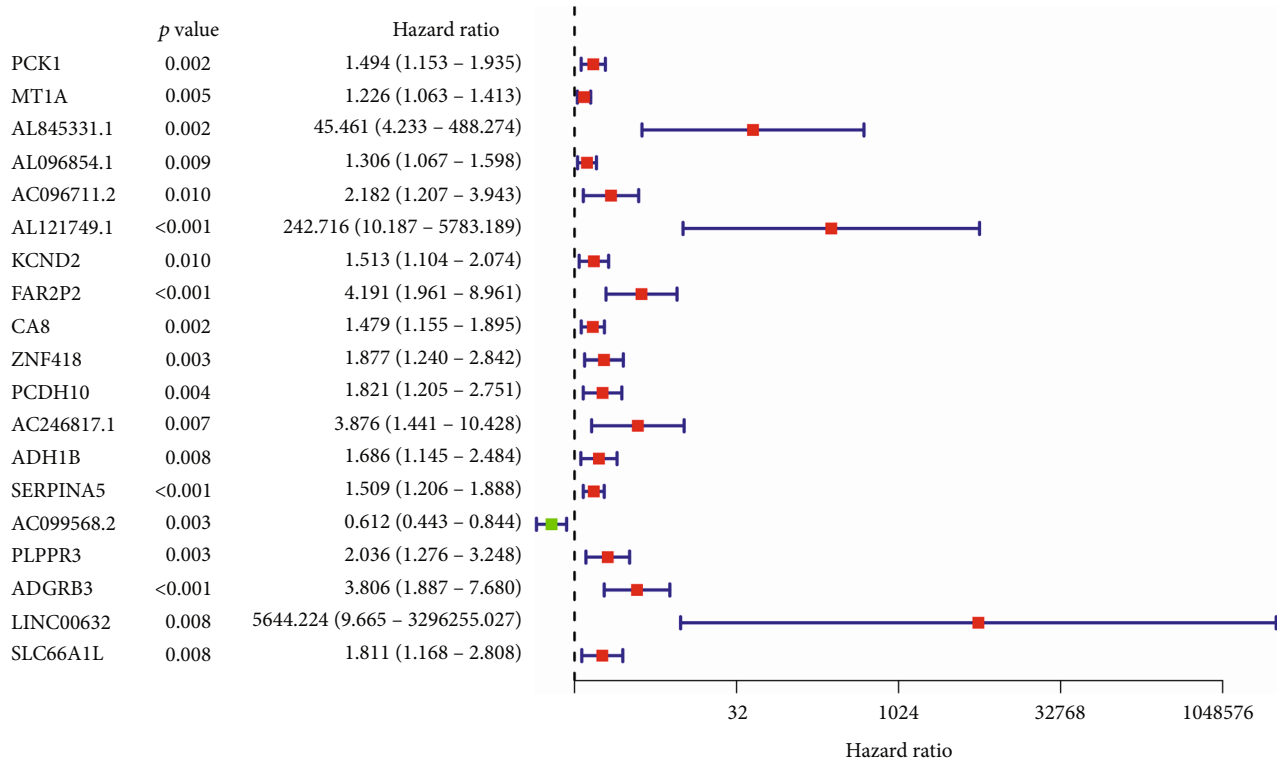

(c)

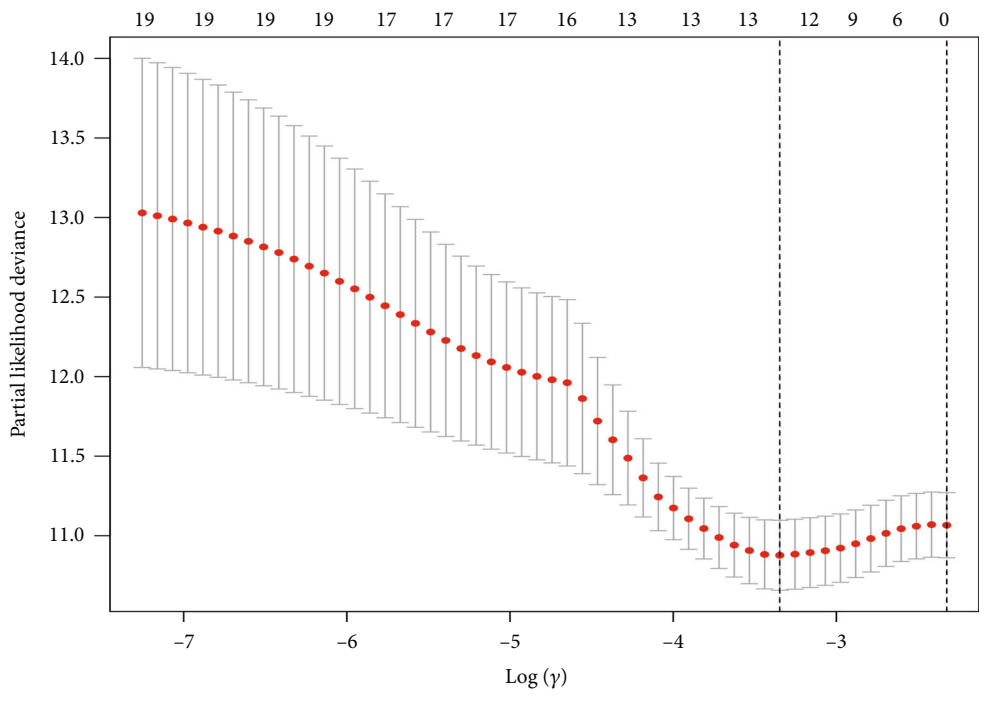

(d)

Figure 4: Continued.

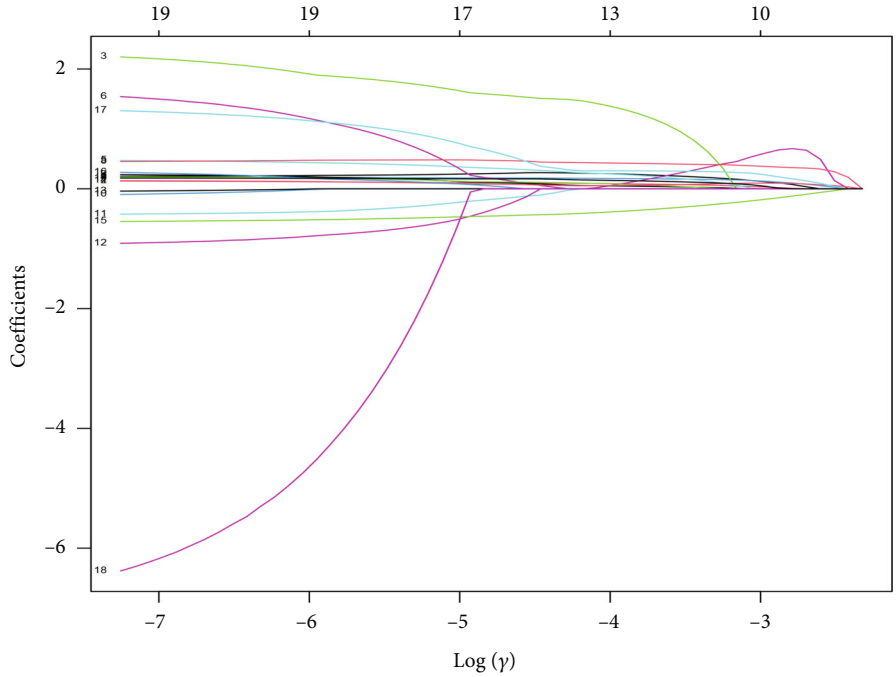

(e)

Figure 4: Continued.

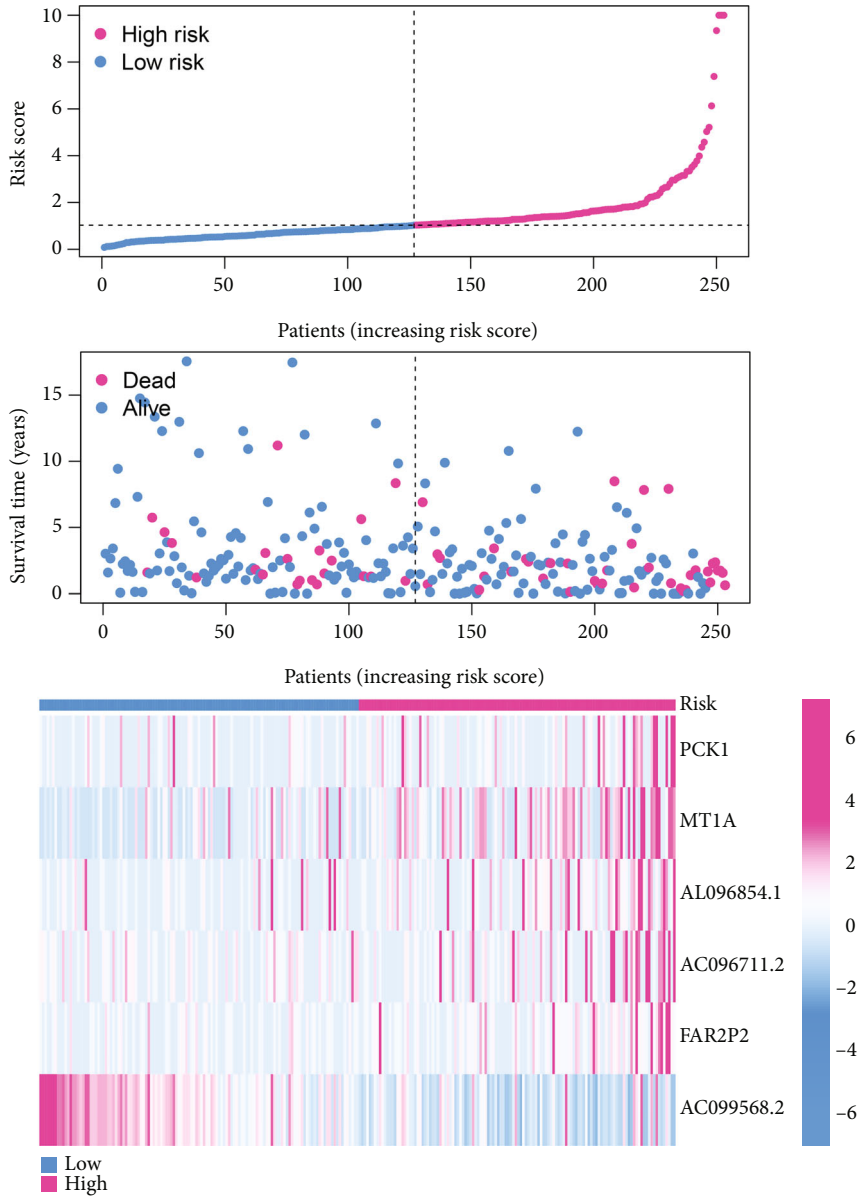

(f)

Figure 4: Continued.

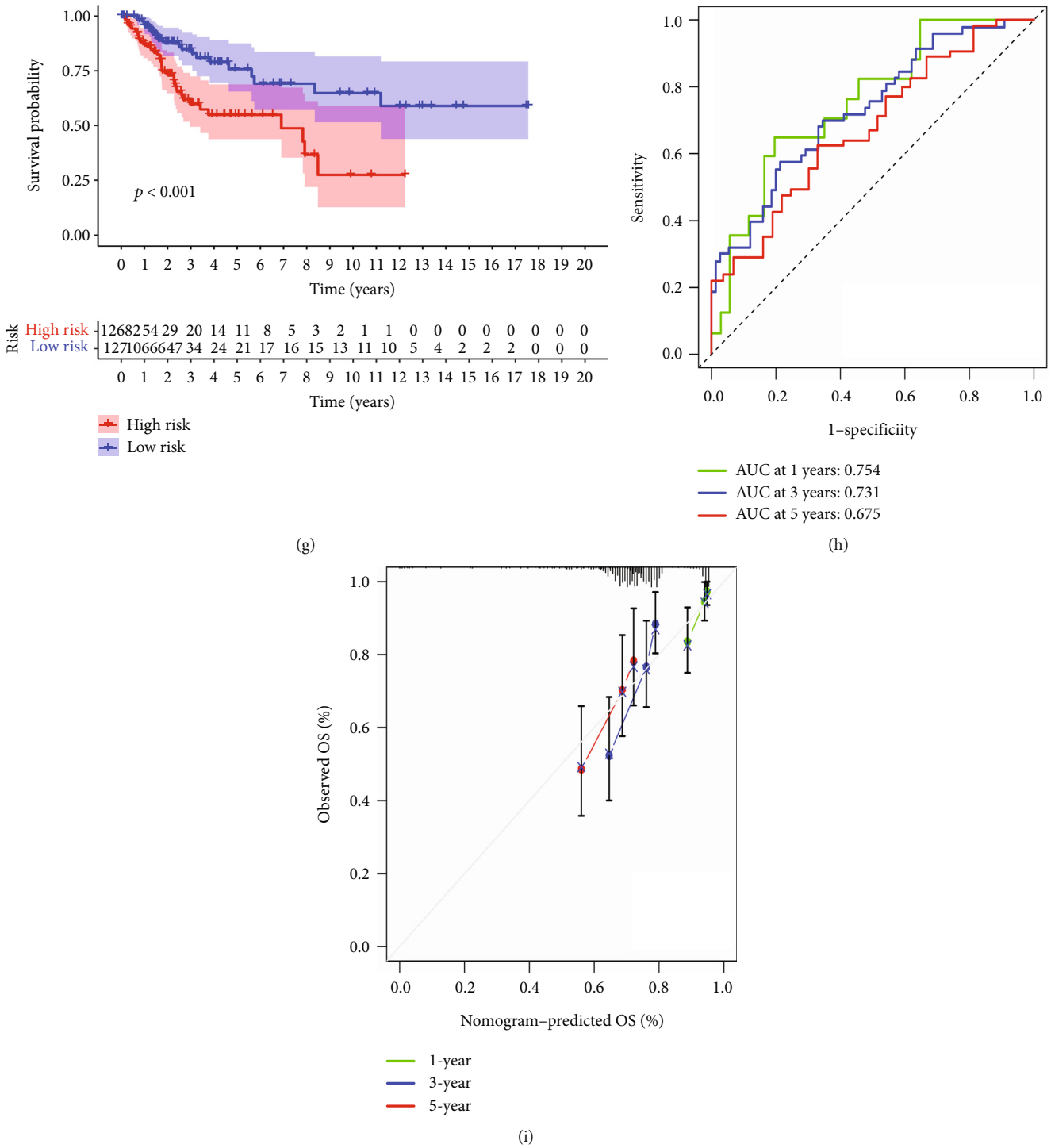

Figure 4: (a and b) The differentially expressed analysis between normal cohort and UCC patients; (c) the results of univariate COX regression analysis; (d and e) the lasso regression analysis; (f) the risk plot between low- and high-risk groups; (g) the survival analysis between low- and high-risk score groups; (h) the time-dependent ROC curve revealed the 1-year, 3-year, and 5-year AUC score of risk score; (i) the calibration score reveals the predictive value of risk score in UCC cohort.

3.4. Construction of the PPAR-Based Prognostic Prediction Model in UCC Patients. First, we obtained the mRNA expression data, as well as the clinical characteristics of UCC patients. Next, we performed the differentially expressed analysis between UCC patients and normal people. The results demonstrated that a total of 5980 genes showed significant differences, which includes 2033 up-regulated genes and 3947 down-regulated genes (Figure 4(a)). The heat map shows the top 50 differentially expressed genes (Figure 4(b)). Subsequently, we construct the prognostic prediction model based on the overall survival (OS) of UCC patients. The univariate COX regression analysis demonstrated that 19 genes are associated with the

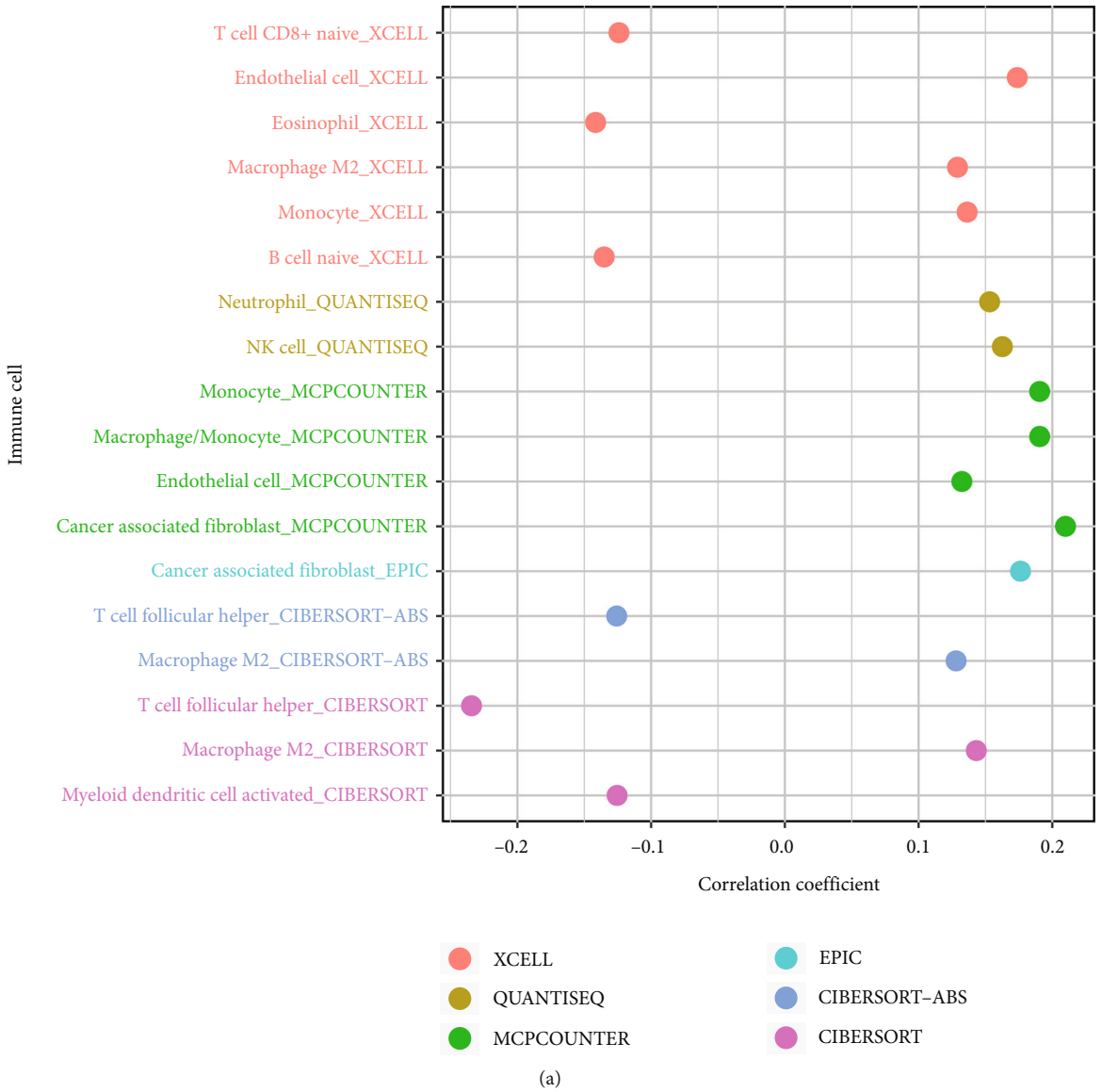

(a)

Figure 5: Continued.

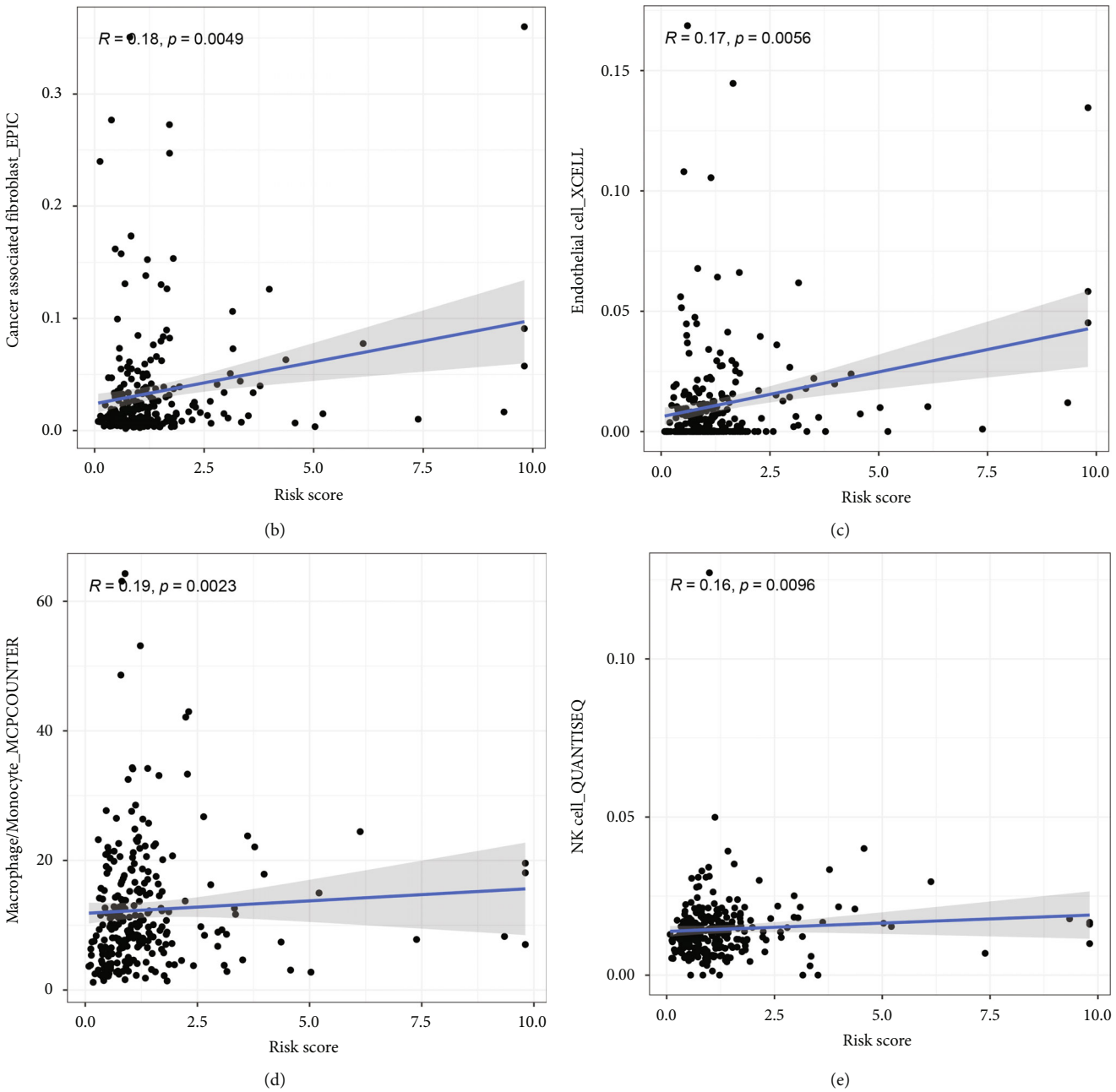

Figure 5: Continued.

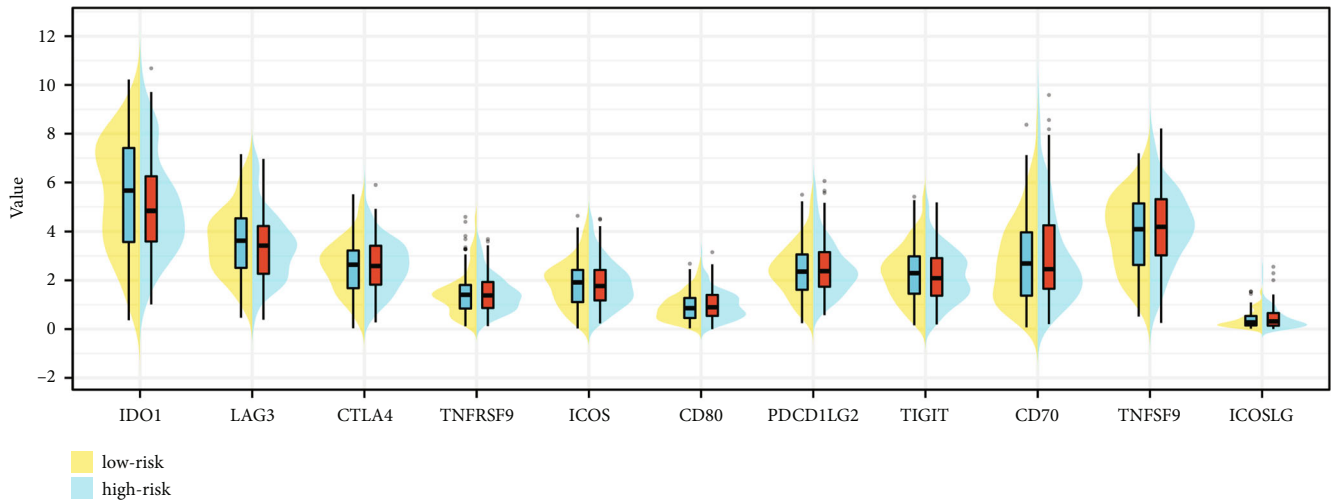

(f)

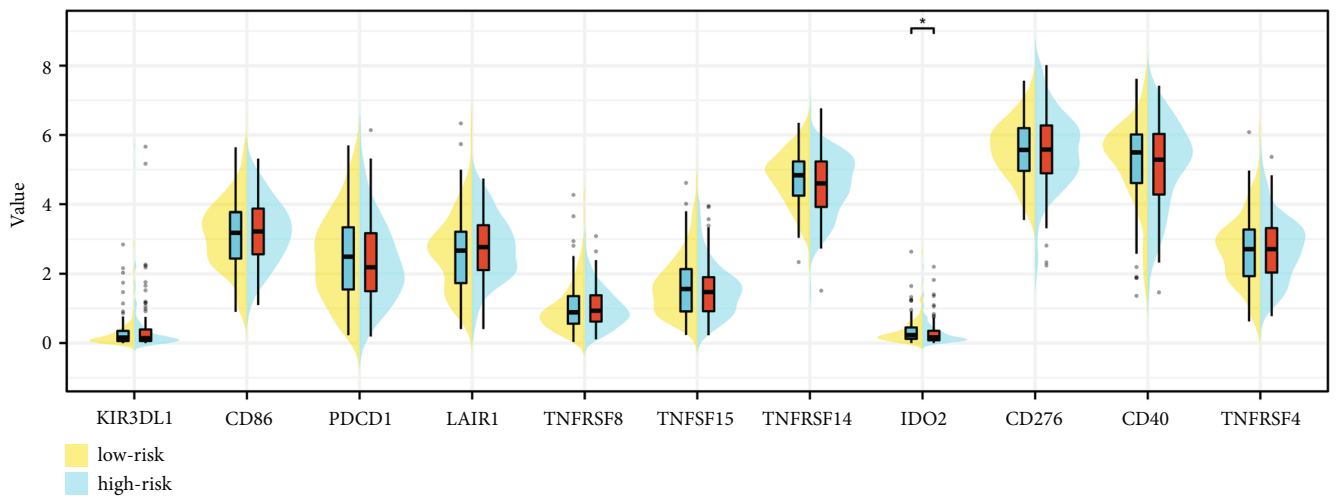

(g)

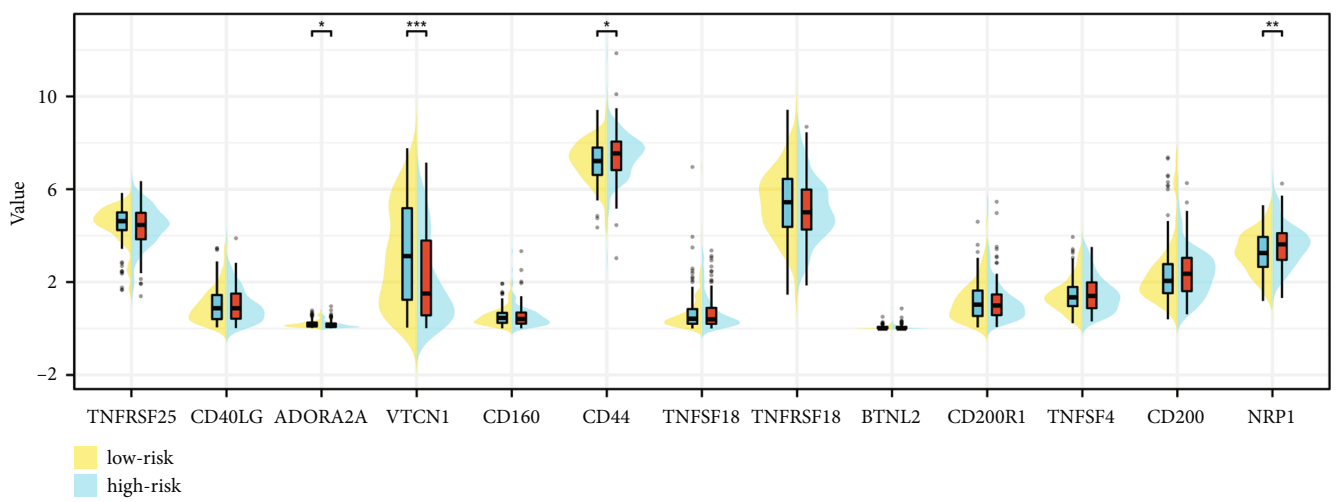

(h)

Figure 5: Continued.

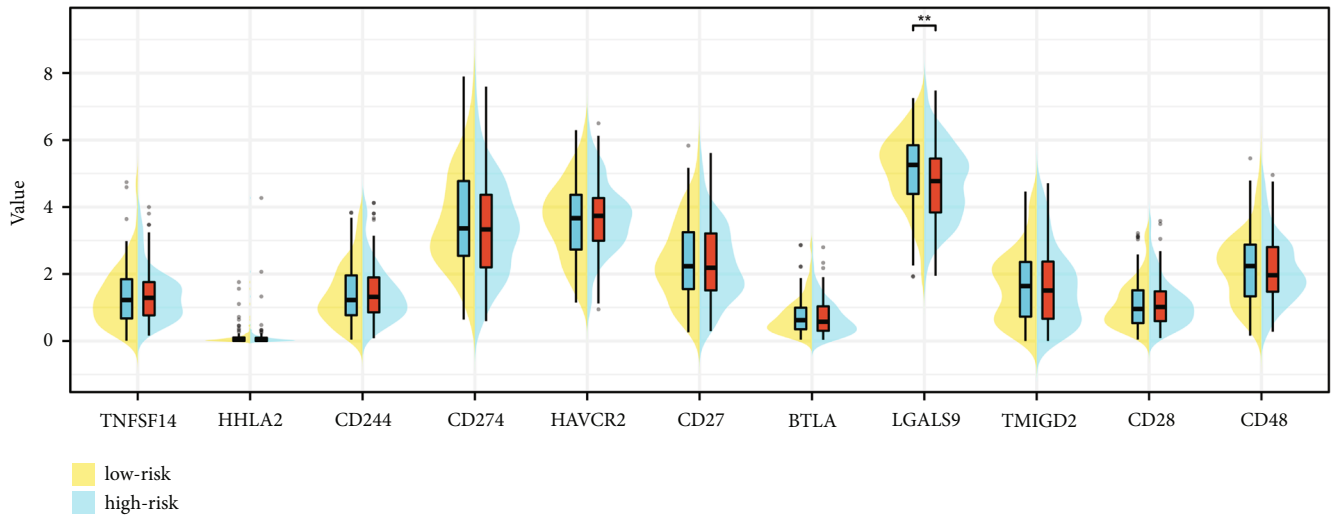

(i)

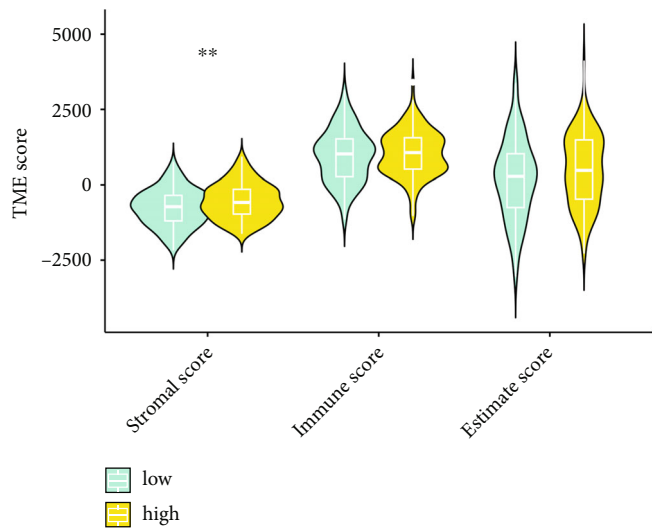

(j)

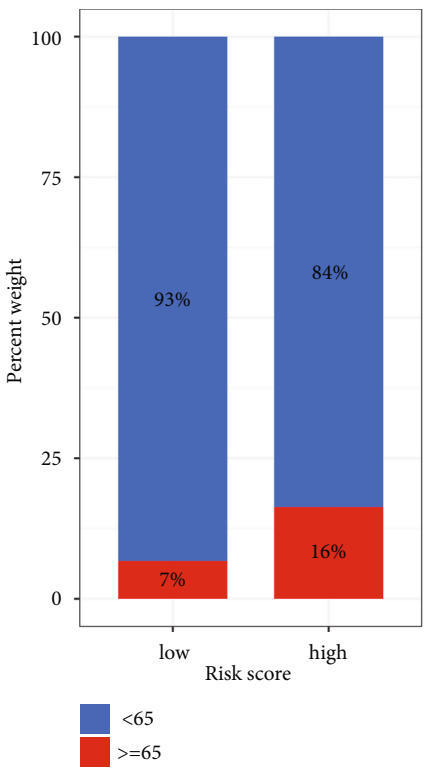

(k)

Figure 5: Continued.

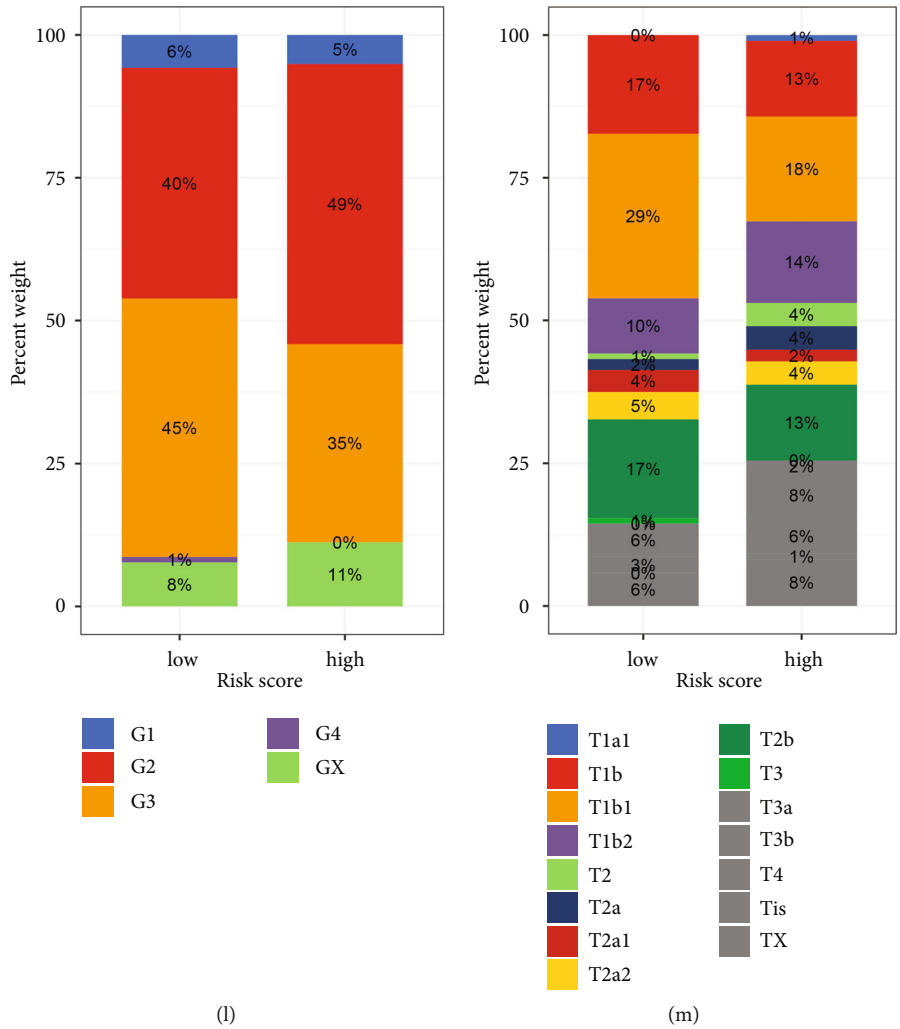

(l) (m)

Figure 5: Continued.

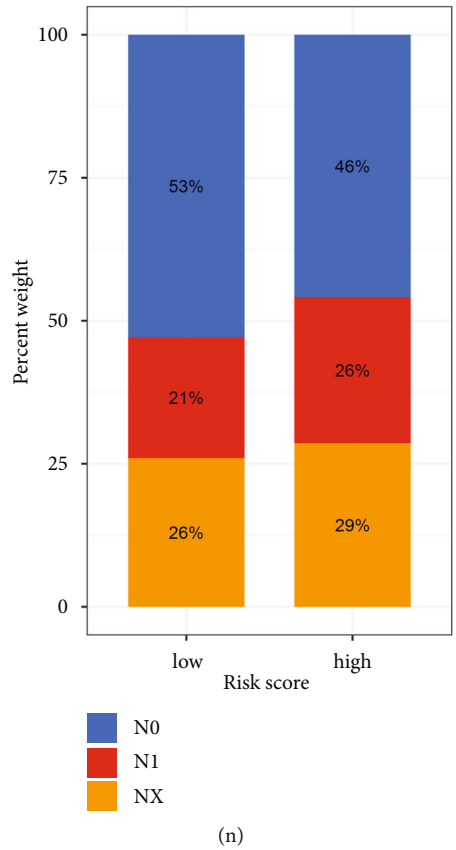

Figure 5: (a) The immune infiltration analysis based on the risk score; the correlation analysis between risk score and cancer-associated fibroblasts (b); endothelial cells (c); macrophages (d); NK cell (e); (f–i) the correlation analysis between risks score and immune checkpoint-related genes; (j) the correlation analysis between risk score and immune-related score; the correlation analysis between risk score and age (k); grade (l); T stage (m); N stage (n).

prognosis of UCC patients (Figure 4(c)). The LASSO regression analysis and multivariate COX regression analysis were then performed to further explore the biomarkers for the prognosis of UCC patients. The results demonstrated that PCK1, MT1A, AL096855.1, AC096711.2, FAR2P2, and AC099568.2 are mostly associated with the prognosis of UCC patients. We then successfully constructed the PPAR-based prognostic prediction model. Each UCC patient was assigned with the risk score as follows: Risk score = PCK1 × 0.371061037507491 + MT1A × 0.181870631948255 + AL096855.1 × 0.207868336512594 + AC096711.2 × 0.570820588371621 + FAR2P2 × 0.801187844986532 + AC099568.2 × −0.54499718389366 (Figures 4(d) and 4(e)). Based on the risk score, the UCC patients were divided into low- and high-risk groups (Figure 4(f)). The survival analysis revealed that patients with higher risk scores tend to show poorer OS (Figure 4(g)). In addition, the Area Under the Curve (AUC) value of the Receiver Operating Characteristic (ROC) curve was 0.751 at 1 year, 0.731 at 3 years, and 0.675 at 5 years, respectively (Figure 4(h)). The calibration curve proves that PPAR-based prognostic prediction model shows good predictive value in UCC patients (Figure 4(i)).

3.5. Validation of the Role of PPAR-Based Prognostic Prediction Model in Immune-Related Cells, Immune Checkpoint Genes, Immune-Related Score, and Clinical Characteristics. On the basis of the former analysis, we successfully obtained the PPAR-based prognostic prediction model, which involves six genes (PCK1, MT1A, AL096855.1, AC096711.2, FAR2P2, and AC099568.2). We then performed the immune infiltration analysis. The results demonstrated that the risk score is positively associated with endothelial cells, M2 macrophage, monocyte, Natural Killer (NK) cell, neutrophil, and cancer-associated fibroblasts. However, the risk score is negatively associated with CD8+ naïve T cell, eosinophil, naïve B cell, and T cell follicular helper (Figures 5(a), 5(b), 5(c), 5(d), and 5(e)). The immune checkpoint analysis demonstrated that the risk score is associated with IDO2, ADORA2A, VTCN1, CD44, NRP1, and LGALS9 (Figures 5(f), 5(g), 5(h), and 5(i)). In terms of immune score analysis, the higher risk score is associated with a high stromal score (Figure 5(j)). For clinical characteristics, the UCC patients with the high-risk score are associated with higher age, T stage, and N stage, while the grade is not associated with the risk score (Figures 5(k), 5(l), 5(m), and 5(n)).

3.6. Exploration of the Potential Pathways That Are Associated with Risk Score and PPAR-Related Genes. Then, we performed the pathway enrichment analysis based on the risk score. The GSVA analysis shows that the calcium

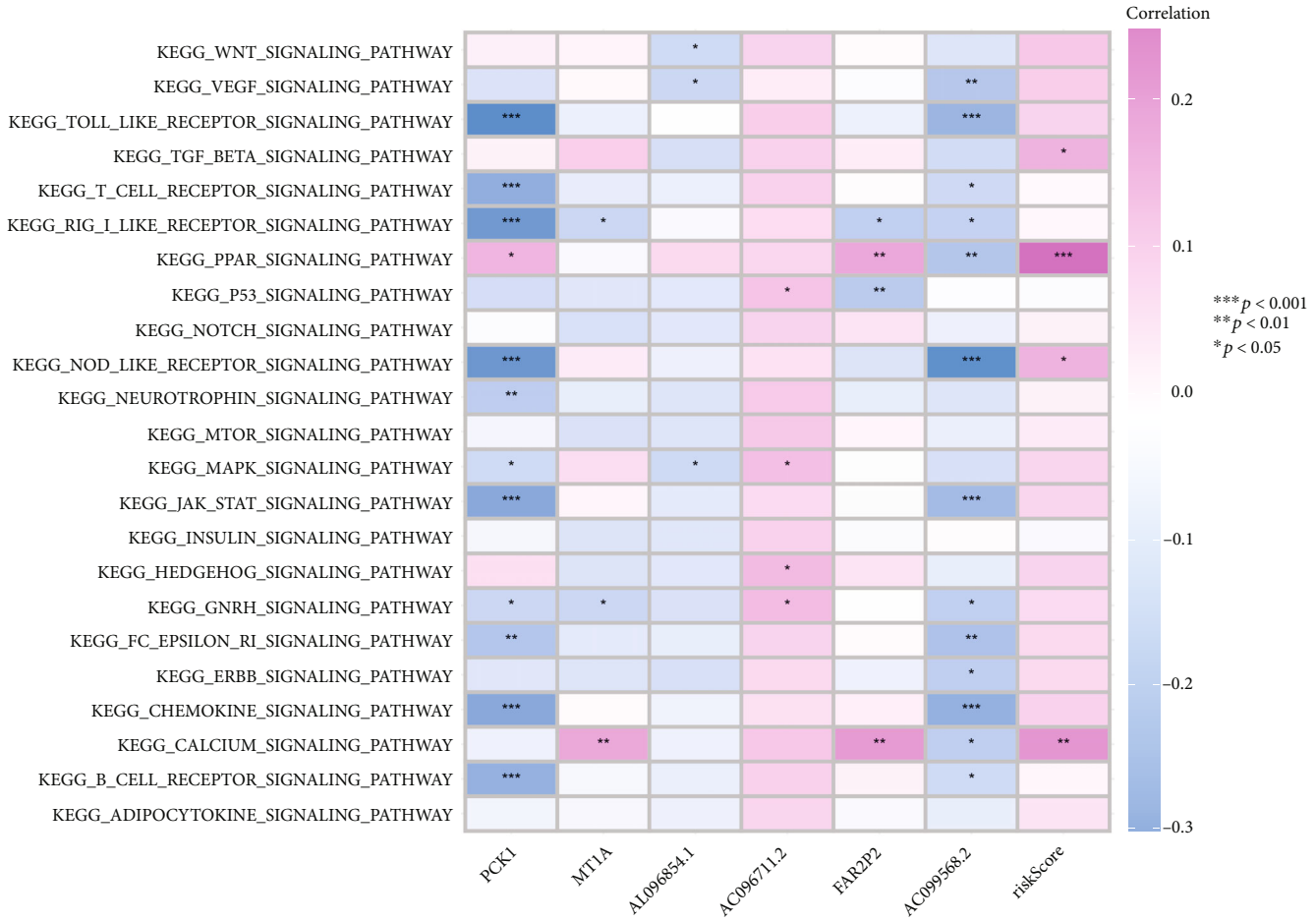

(a)

Figure 6: Continued.

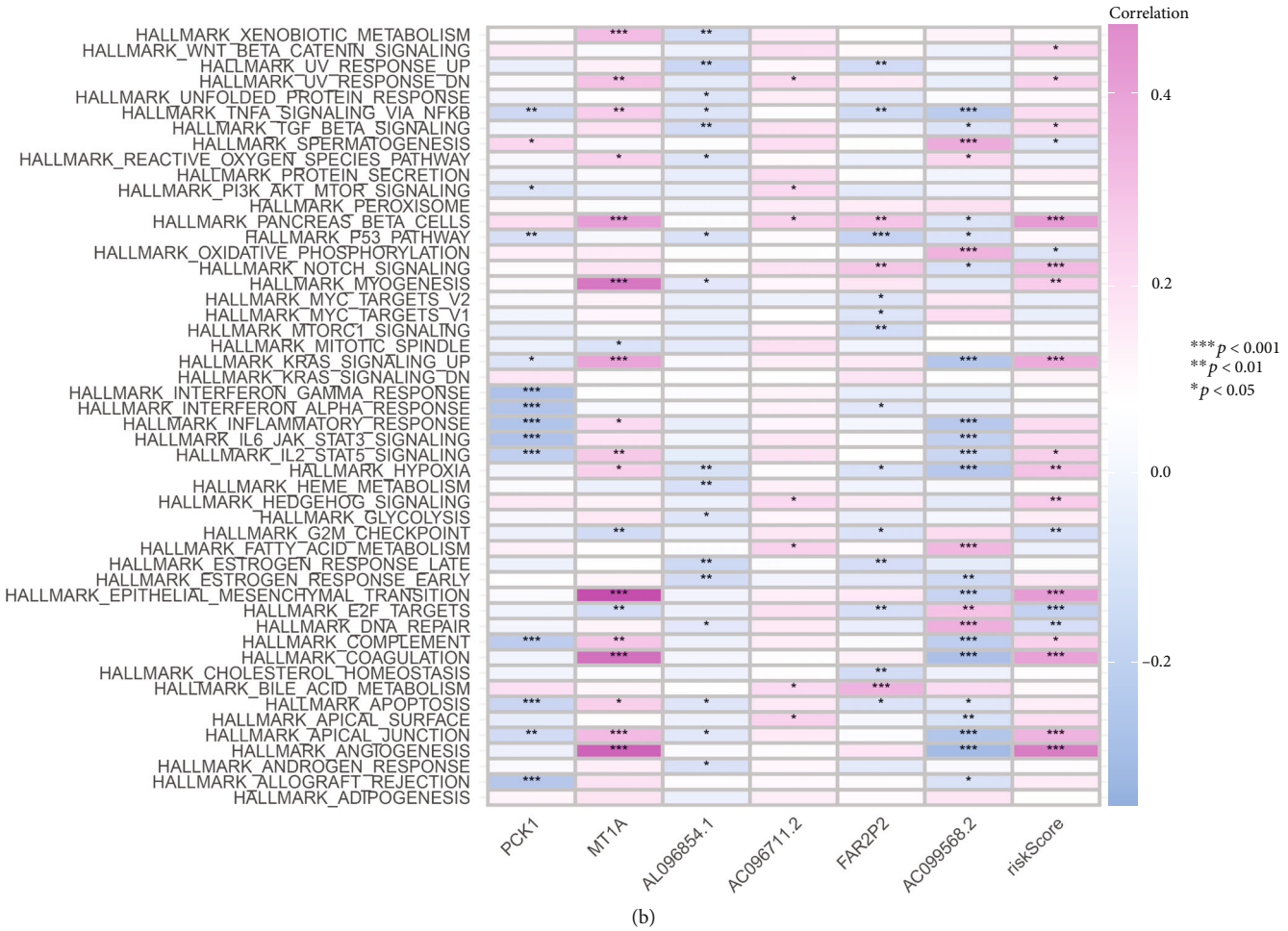

(b)

Figure 6: Continued.

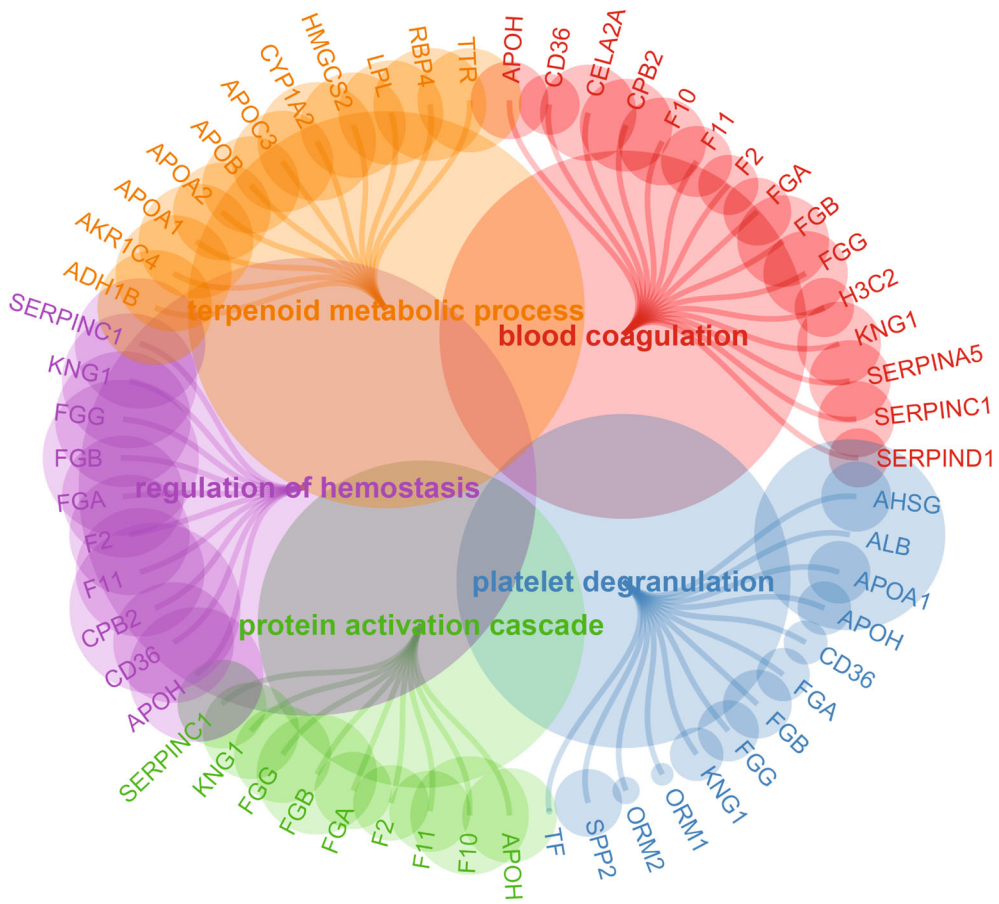

(c)

Figure 6: Continued.

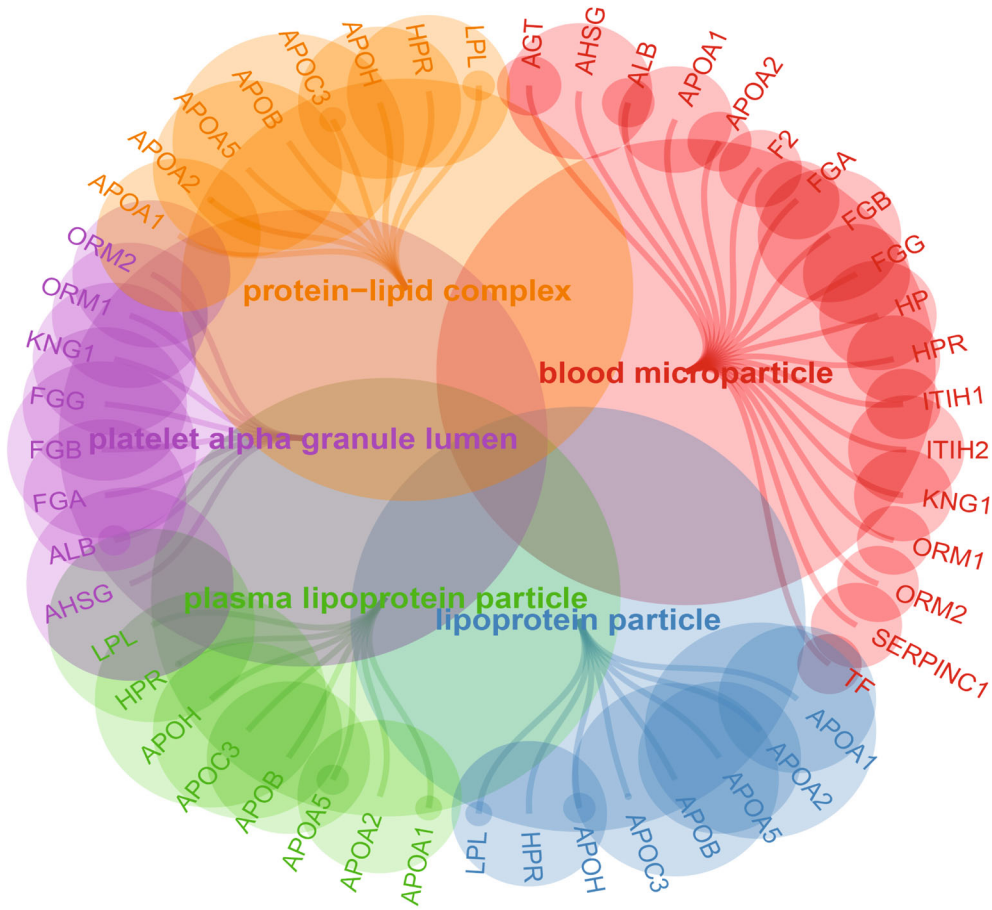

(d)

Figure 6: Continued.

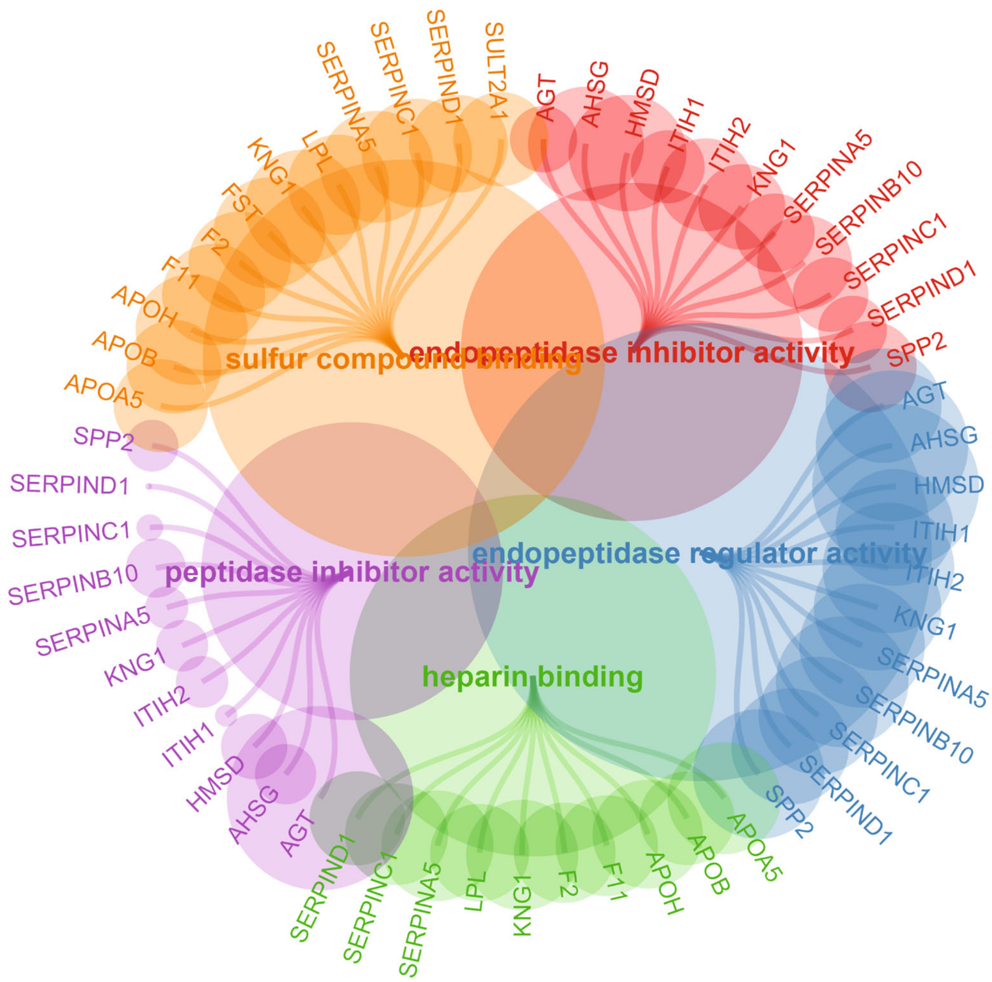

(e)

Figure 6: (a) The GSVA analysis based on the KEGG terms; (b) the GSVA analysis based on the Hallmark terms; (c) the GO BP enrichment analysis; (d) the GO CC enrichment analysis; (e) the GO MF enrichment analysis.

signaling pathway, receptor signaling pathway, PPAR signaling pathway, and Transforming Growth Factor (TGF)-beta signaling pathway are the most enriched KEGG terms (Figure 6(a)). For Hallmark terms, angiogenesis, apical junction, coagulation, complement, E2F target, KRAS signaling, and pancreas beta cells are the most enriched pathways. In addition, we also explore the GO enrichment pathways based on the PPAR-related genes (Figure 6(b)). For GO BP analysis, blood coagulation, platelet degranulation, protein activation cascade, regulation of hemostasis, and terpenoid metabolic process are the most enriched pathways (Figure 6(c)). The blood microparticle, lipoprotein particle, plasma lipoprotein particle, protein–lipid complex, and platelet alpha granule lumen are the most enriched GO CC enrichment pathways (Figure 6(d)). In addition, the GO MF enrichment analysis demonstrated that heparin binding, peptidase inhibitor activity, endopeptidase regulator activity, sulfur compound binding, and endopeptidase inhibitor activity are most associated with PPAR-related genes (Figure 6(e)).

3.7. AC099568.2 May Play a Key Role in the UCC and PPAR Signaling Pathway. Based on the PPAR-based prognostic prediction model constructed in the previous analysis, we successfully obtained six genes, which may be the biomarkers (PCK1, MT1A, AL096855.1, AC096711.2, FAR2P2, and AC099568.2) for UCC. Subsequently, we performed the survival analysis solely on these six genes. The results demonstrated that the high expression of AC099568.2 is associated with a better prognosis of UCC patients, while the other five genes are not associated with the OS of UCC patients (Figures 7(a), 7(b), 7(c), 7(d), 7(e), and 7(f)). In addition, the ROC curve also proved the good predictive value of AC099568.2 in the UCC cohort (Figure 7(g)). Additionally, the expression level of AC099568.2 in UCC patients is higher than normal cohort (Figures 7(h) and 7(i)). Subsequently, the GSVA analysis demonstrated that midbody, regulation of cell population proliferation, misfolded protein binding, response to oxidative stress, and cyclin binding are positively associated with AC099568.2. However, external encapsulating structure, smoothened signaling pathway, kinase binding, microtubule cytoskeleton, and response to xenobiotic stimulus are correlated with the down-regulation of AC099568.2 (Figure 7(j)). In addition, the GSEA analysis revealed that keratinization, NK activation involved in immune response, negative

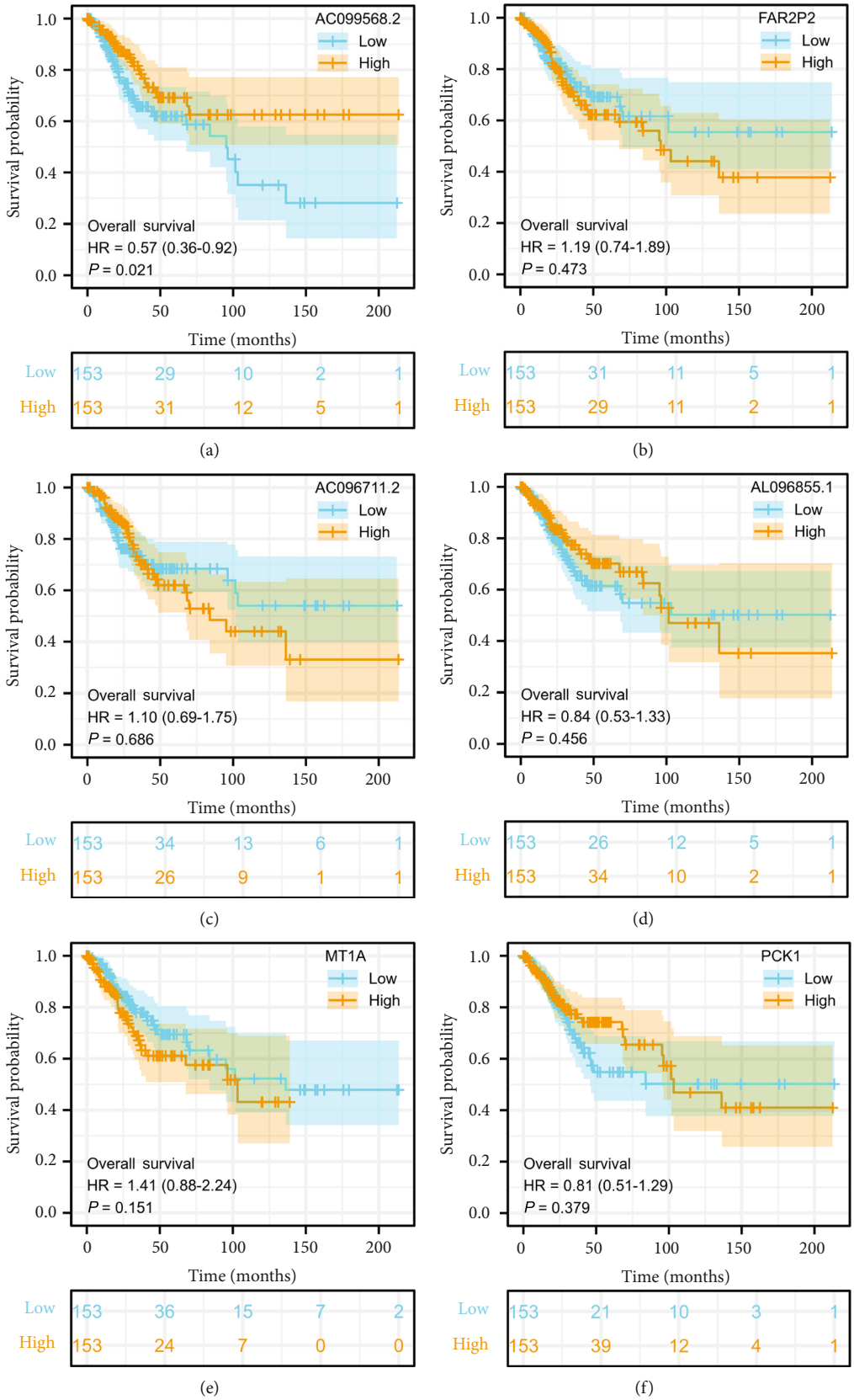

Figure 7: Continued.

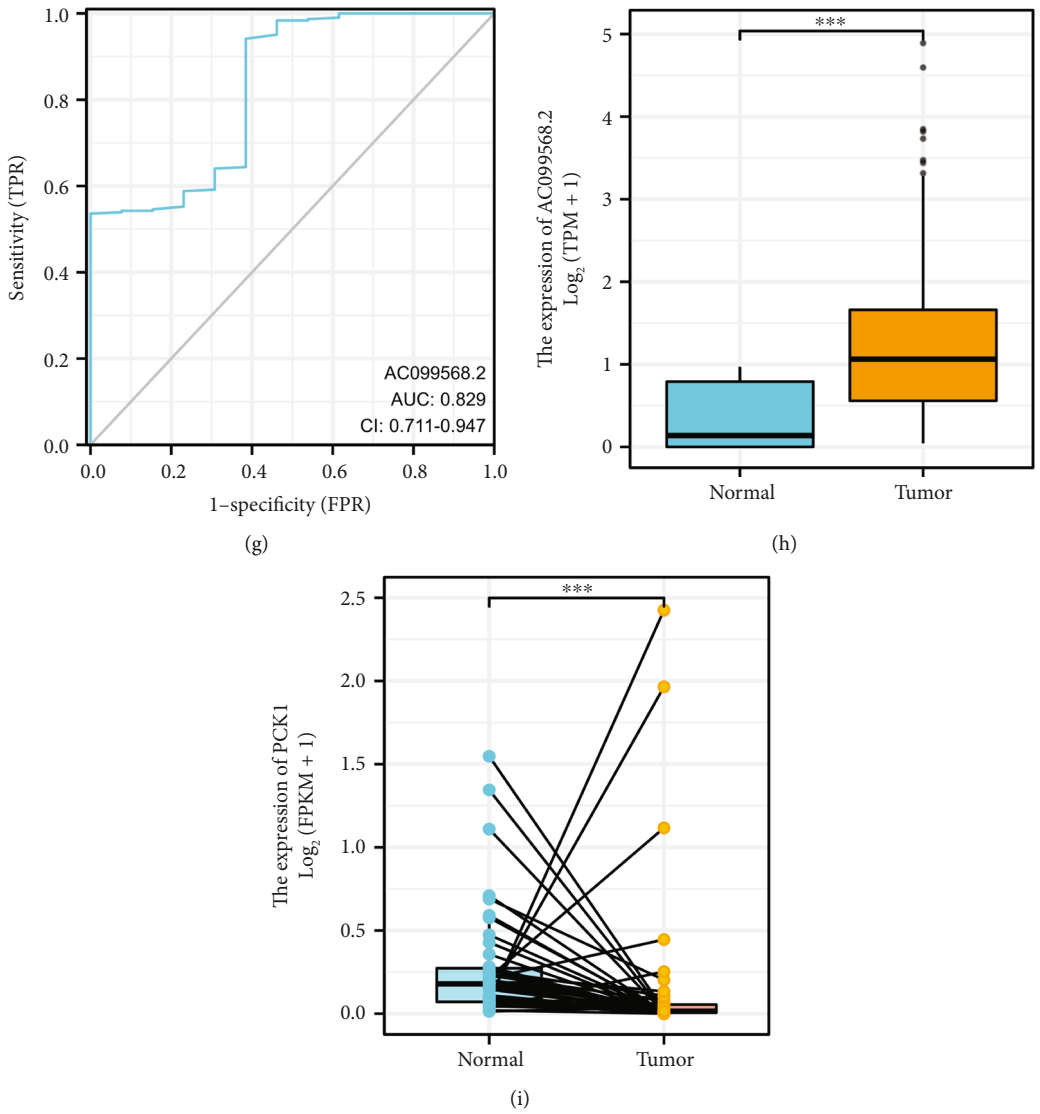

Figure 7: Continued.

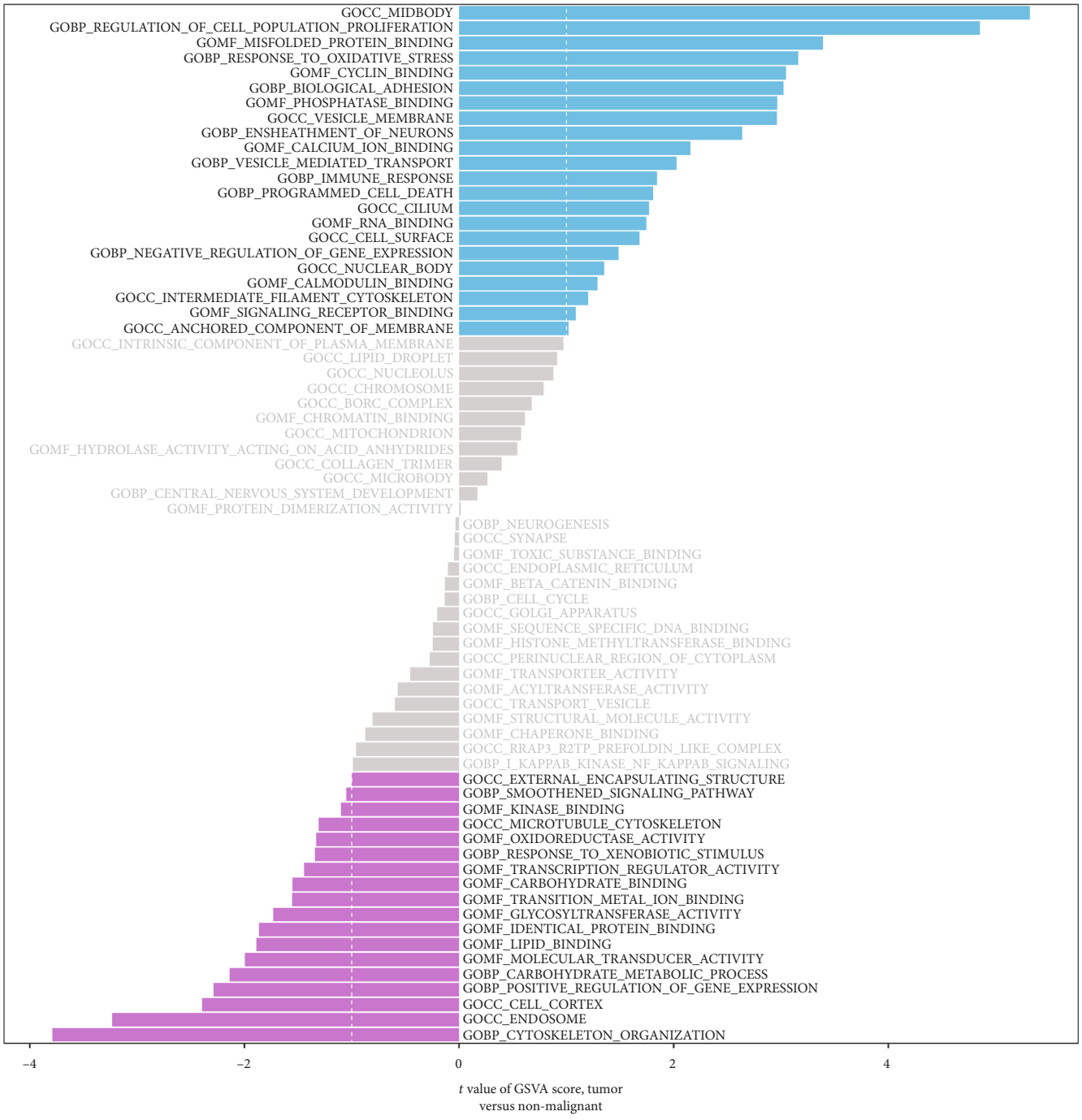

(j)

Figure 7: Continued.

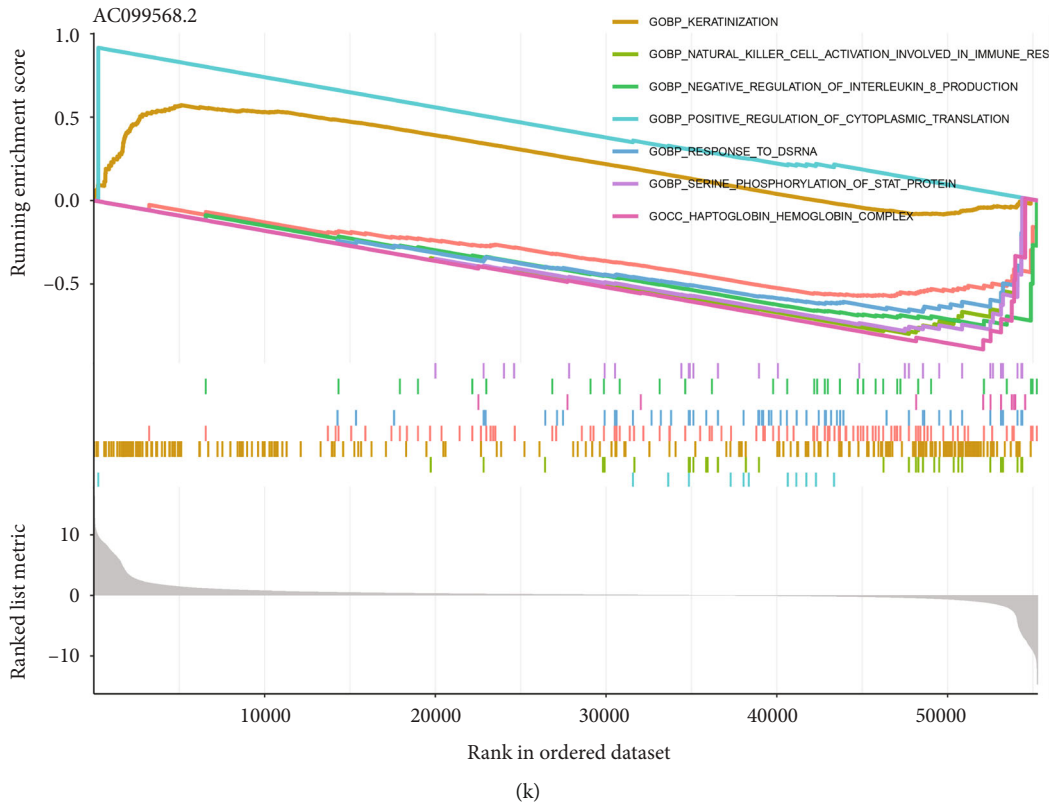

(k)

Figure 7: The survival analysis of AC099568.2 (a); FAR2P2 (b); AC096711.2 (c); AL096855.1 (d); MT1A (e); PCK1 (f) in UCC cohort; (g) the ROC curve of AC099568.2 in UCC cohort; (h) the box plot reflects the differentially expressed analysis of AC099568.2; (i) the results of the paired differently expressed analysis; (j) the GSVA analysis of AC099568.2; (k) the GSEA analysis of AC099568.2.

regulation of interleukin 8 productions, and positive regulation of cytoplasmic translation are closely associated with the AC099568.2 (Figure 7(k)).

4. Discussion

Every year, thousands of women die from cervical cancer. Approximately 273,000 women die from cervical cancer each year, despite preventive HPV vaccines and conventional cancer treatments [17]. Malignant cells evade immune surveillance by forming tumors, invading, and metastasizing when their immune systems are perturbed [18]. A deeper understanding of the immune system players that suppress or promote cervical cancer is essential to develop more targeted treatments with fewer side effects [19]. Using natural processes of action to stimulate the immune system to fight cancer cells, immunotherapy has become the most desirable method of targeting cancer [20]. It is possible to treat cervical cancer with a variety of immunotherapy approaches, including monoclonal antibodies, immune checkpoint blockade therapy, adoptive cell transfer therapy, and oncolytic viruses [21]. Recent studies have found that PPARs, which are nuclear hormone receptors, may be used as therapeutic targets for a variety of cancers, including lung cancer [22]. Furthermore, PPARs participate in various cellular functions, such as differentiation, proliferation, survival, apoptosis, and motility [23]. Cancer risk is increased when these cellular processes and metabolic disturbances are dysregulated in tumors [24]. In recent years, with the development of bioinformatics analysis, more and more research started to focus on the advantages of bioinformatics analysis in the treatment, prognosis prediction, and diagnosis of cancer patients [25–31]. In this work, we aim to explore the role of PPAR signaling pathways in UCC patients. By using the ssGSEA algorithm, the UCC cohort was successfully divided into PPAR-low and PPAR-high groups. In addition, the differentially expressed analysis revealed a total of 290 PPAR-related genes. The pathway enrichment analysis also proved that the PPAR signaling pathway is one of the most enriched pathways. Cancer prevention and treatment may be improved using PPAR modulators, including agonists and antagonists. A number of factors contribute to cancer risk, including dyslipidemia, obesity, glucose intolerance, and low-grade inflammation. Therefore, PPAR modulators can be used to treat cancer by promoting proliferation, differentiation, and apoptosis of cancerous cells. They have a significant role to play in preventing various types of cancer, such as cancer of the breast, lung, and pancreas.

Subsequently, by constructing the prognostic prediction model based on the PPAR-related genes, we successfully obtained a six-gene-based prognostic prediction model. The survival analysis and ROC curve demonstrated that the PPAR-based model shows good predictive value in UCC patients. In addition, the immune checkpoint analysis demonstrated that the expression level of many immune checkpoint-related genes is closely associated with the

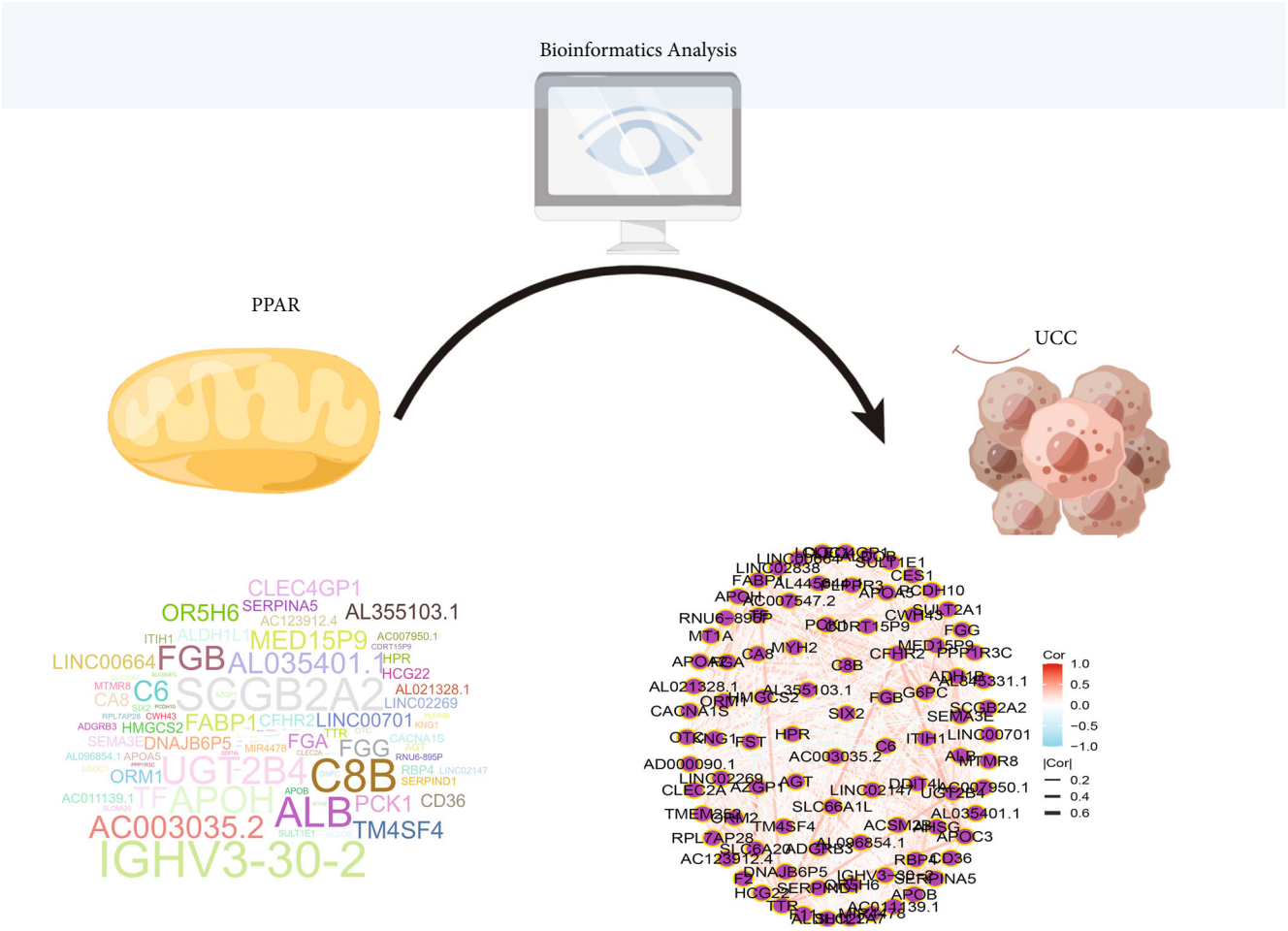

Figure 8: The flow chart of this work.

PPAR-based risk score, which may indicate that the PPAR signaling pathway map influences immune checkpoint therapy (Figure 8). As shown in the previous study, PPARα acts as a transcription factor influencing intracellular signaling events and cellular metabolism [32]. In conditions of various immunological backgrounds, PPAR-targeted therapies have become more commonly used due to their broad effects on the immune system [33].

Finally, further analysis revealed that AC099568.2 may be the most promising biomarker for the diagnosis, treatment, and prognosis in UCC patients. Both the survival analysis and ROC curve demonstrated that AC099568.2 plays a key role in UCC patients. However, to our knowledge, this is the first time a study focused on the role of AC099568.2 in UCC patients. Our work successfully revealed a new biomarker for UCC patients, which also provides a new direction for future research.

5. Conclusion

In this work, we construct the PPAR-based prognostic prediction model. PCK1, MT1A, AL096855.1, AC096711.2, FAR2P2, and AC099568.2 not only play a key role in the PPAR signaling pathway. Further analysis revealed that AC099568.2 may be the most promising biomarker for the diagnosis, treatment, and prognosis in cervical cancer patients.

Data Availability

The data used to support the findings of this study are included within the article.

Conflicts of Interest

The authors declare that they have no conflicts of interest.

Authors' Contributions

Yan Zhang collected the data and performed the analysis. Xing Li wrote the manuscript. All authors contributed to the article and approved the submitted version.

Acknowledgments

Lin Mao and Zou Wen performed the copyediting and translation services. This work was supported by the Key Research and Development Program of Hubei Province (Grant No. 2022BCA010).

References

[1] M. Kagabu, T. Nagasawa, C. Sato et al., "Immunotherapy for uterine cervical cancer using checkpoint inhibitors: future directions," *International Journal of Molecular Sciences*, vol. 21, no. 7, p. 2335, 2020.

[2] N. Murakami, K. Ando, M. Murata et al., "Why not de-intensification for uterine cervical cancer?," *Gynecologic Oncology*, vol. 163, no. 1, pp. 105–109, 2021.

[3] M. Kagabu, T. Nagasawa, D. Fukagawa et al., "Immunotherapy for uterine cervical cancer," *Healthcare*, vol. 7, no. 3, p. 108, 2019.

[4] Y. H. Hsiao, S. F. Yang, Y. H. Chen et al., "Updated applications of ultrasound in uterine cervical cancer," *Journal of Cancer*, vol. 12, no. 8, pp. 2181–2189, 2021.

[5] D. Champin, M. C. Ramírez-Soto, and J. Vargas-Herrera, "Use of smartphones for the detection of uterine cervical cancer: a systematic review," *Cancers*, vol. 13, no. 23, p. 6047, 2021.

[6] Y. H. Sun, Y. H. Chou, C. H. Wang et al., "Impact of pentraxin 3 genetic variants on uterine cervical cancer clinicopathologic characteristics," *International Journal of Medical Sciences*, vol. 18, no. 11, pp. 2339–2346, 2021.

[7] G. Valenti, S. G. Vitale, A. Tropea, A. Biondi, and A. S. Laganà, "Tumor markers of uterine cervical cancer: a new scenario to guide surgical practice?," *Updates in Surgery*, vol. 69, no. 4, pp. 441–449, 2017.

[8] A. Urushibara, T. Saida, K. Mori et al., "Diagnosing uterine cervical cancer on a single T2-weighted image: comparison between deep learning versus radiologists," *European Journal of Radiology*, vol. 135, p. 109471, 2021.

[9] S. Sato, H. Itamochi, and T. Sugiyama, "Fertility-sparing surgery for uterine cervical cancer," *Future Oncology*, vol. 12, no. 20, pp. 2345–2355, 2016.

[10] S. A. Mohd Isa, M. S. Md Salleh, M. P. Ismail, and S. M. Hairon, "ADAM9 expression in uterine cervical cancer and its associated factors," *Asian Pacific Journal of Cancer Prevention*, vol. 20, no. 4, pp. 1081–1087, 2019.

[11] M. Shimomura, T. Fukuda, Y. Awazu et al., "PRMT1 expression predicts response to neoadjuvant chemotherapy for locally advanced uterine cervical cancer," *Oncology Letters*, vol. 21, no. 2, p. 150, 2021.

[12] M. Hata, "Radiation therapy for elderly patients with uterine cervical cancer: feasibility of curative treatment," *International Journal of Gynecological Cancer*, vol. 29, no. 3, pp. 622–629, 2019.

[13] D. Montaigne, L. Butruille, and B. Staels, "PPAR control of metabolism and cardiovascular functions," *Nature Reviews. Cardiology*, vol. 18, no. 12, pp. 809–823, 2021.

[14] N. Latruffe, M. Cherkaoui Malki, V. Nicolas-Frances, M. C. Clemencet, B. Jannin, and J. P. Berlot, "Regulation of the peroxisomal beta-oxidation-dependent pathway by peroxisome proliferator-activated receptor alpha and kinases," *Biochemical Pharmacology*, vol. 60, no. 8, pp. 1027–1032, 2000.

[15] J. M. Stark, J. M. Coquet, and C. A. Tibbitt, "The role of PPAR-γ in allergic disease," *Current Allergy and Asthma Reports*, vol. 21, no. 11, p. 45, 2021.

[16] A. Christofides, E. Konstantinidou, C. Jani, and V. A. Boussiotis, "The role of peroxisome proliferator-activated receptors (PPAR) in immune responses," *Metabolism*, vol. 114, p. 154338, 2021.

[17] A. Biete and G. Oses, "Intraoperative radiation therapy in uterine cervical cancer: a review," *Reports of Practical Oncology and Radiotherapy*, vol. 23, no. 6, pp. 589–594, 2018.

[18] R. B. Vasques, L. L. Carramenha, I. Basílio et al., "Evaluation of uterine cervical cancer in pregnancy: a cross-sectional study," *European Journal of Obstetrics, Gynecology, and Reproductive Biology*, vol. 246, pp. 35–39, 2020.

[19] S. Mabuchi, Y. Matsumoto, M. Kawano et al., "Uterine cervical cancer displaying tumor-related leukocytosis: a distinct clinical entity with radioresistant feature," *Journal of the National Cancer Institute*, vol. 106, no. 7, p. dju147, 2014.

[20] J. L. Alcázar, S. Arribas, J. A. Mínguez, and M. Jurado, "The role of ultrasound in the assessment of uterine cervical cancer," *Journal of Obstetrics and Gynaecology of India*, vol. 64, no. 5, pp. 311–316, 2014.

[21] Y. Matsuura, M. Yoshioka, A. Nakata, M. Haraga, T. Hachisuga, and K. Mori, "Trends in uterine cervical cancer screening at physical health checkups for company employees in Japan," *Journal of UOEH*, vol. 41, no. 3, pp. 327–333, 2019.

[22] R. Marion-Letellier, G. Savoye, and S. Ghosh, "Fatty acids, eicosanoids and PPAR gamma," *European Journal of Pharmacology*, vol. 15, no. 785, pp. 44–49, 2016.

[23] G. Ercolano, A. Gomez-Cadena, N. Dumauthioz et al., "PPARɣ drives IL-33-dependent ILC2 pro-tumoral functions," *Nature Communications*, vol. 12, no. 1, p. 2538, 2021.

[24] L. Han, W. J. Shen, S. Bittner, F. B. Kraemer, and S. Azhar, "PPARs: regulators of metabolism and as therapeutic targets in cardiovascular disease. Part II: PPAR-β/δ and PPAR-γ," *Future Cardiology*, vol. 13, no. 3, pp. 279–296, 2017.

[25] T. Zhang, J. Wu, X. Zhang, X. Zhou, S. Wang, and Z. Wang, "Pharmacophore based in silico study with laboratory verification-environmental explanation of prostate cancer recurrence," *Environmental Science and Pollution Research International*, vol. 28, no. 43, pp. 61581–61591, 2021.

[26] X. Zhang, T. Zhang, X. Ren, X. Chen, S. Wang, and C. Qin, "Pyrethroids toxicity to male reproductive system and offspring as a function of oxidative stress induction: rodent studies," *Frontiers in Endocrinology*, vol. 27, no. 12, p. 656106, 2021.

[27] X. Ren, T. Zhang, X. Chen et al., "Early-life exposure to bisphenol A and reproductive-related outcomes in rodent models: a systematic review and meta-analysis," *Aging*, vol. 12, no. 18, pp. 18099–18126, 2020.

[28] S. Ye, Q. Liu, K. Huang, X. Jiang, and X. Zhang, "The comprehensive analysis based study of perfluorinated compounds—environmental explanation of bladder cancer progression," *Ecotoxicology and Environmental Safety*, vol. 1, no. 229, article 113059, 2022.

[29] X. Jiang, H. Zhang, J. Ni, X. Zhang, and K. Ding, "Identifying tumor antigens and immune subtypes of gastrointestinal MALT lymphoma for immunotherapy development," *Frontiers in Oncology*, vol. 12, p. 1060496, 2022.

[30] L. Ye, X. Zhang, P. Wang et al., "Low concentration triphenyl phosphate fuels proliferation and migration of hepatocellular carcinoma cells," *Environmental Toxicology*, vol. 37, no. 10, pp. 2445–2459, 2022.

[31] X. Zhai, X. Chen, Z. Wan et al., "Identification of the novel therapeutic targets and biomarkers associated of prostate cancer with cancer-associated fibroblasts (CAFs)," *Frontiers in Oncology*, vol. 13, p. 1136835, 2023.

[32] A. P. Kumar, P. Prabitha, B. R. P. Kumar, V. Jeyarani, S. P. Dhanabal, and A. Justin, "Glitazones, PPAR-γ and neuroprotection,"

Mini Reviews in Medicinal Chemistry, vol. 21, no. 12, pp. 1457–1464, 2021.

[33] M. Botta, M. Audano, A. Sahebkar, C. R. Sirtori, N. Mitro, and M. Ruscica, "PPAR agonists and metabolic syndrome: an established role?," *International Journal of Molecular Sciences*, vol. 19, no. 4, p. 1197, 2018.

Hindawi
PPAR Research
Volume 2023, Article ID 6637414, 23 pages
https://doi.org/10.1155/2023/6637414

Research Article

Comprehensive Analysis Identifies the PPAR-Targeted Genes Associated with Ovarian Cancer Prognosis and Tumor Microenvironment

Xiao-Fei Leng,[1] Gao-Fa Wang,[1] Hao Yin,[1] Feng Wei,[1] Kang-Kang Zeng,[1] and Yi-Qun Zhang[1,2,3]

[1]*Department of Obstetrics and Gynecology, Taihe Hospital, Hubei University of Medicine, Shiyan, China*
[2]*State Key Laboratory of Ultrasound in Medicine and Engineering, Chongqing Medical University, Chongqing 400016, China*
[3]*Department of Gynecologic Oncology, Beijing Obstetrics and Gynecology Hospital, Capital Medical University, No. 251, Yaojiayuan Road, Chaoyang District, Beijing, China*

Correspondence should be addressed to Yi-Qun Zhang; yiqunzhang892729@163.com

Received 5 December 2022; Revised 7 February 2023; Accepted 11 April 2023; Published 11 May 2023

Academic Editor: Jincheng Wang

Background. There is a significant role for peroxisome proliferator-activated receptors (PPARs) in the development of cancer. Nevertheless, the role of PPARs-related genes in ovarian cancer (OC) remains unclear. *Methods*. The open-accessed data used for analysis were downloaded from The Cancer Genome Atlas database, which was analyzed using the R software. *Results*. In our study, we comprehensively investigated the PPAR target genes in OC, including their biological role. Meanwhile, a prognosis signature consisting of eight PPAR target genes was established, including apolipoprotein A-V, UDP glucuronosyltransferase 2 family, polypeptide B4, TSC22 domain family, member 1, growth hormone inducible transmembrane protein, renin, dedicator of cytokinesis 4, enoyl CoA hydratase 1, peroxisomal (ECH1), and angiopoietin-like 4, which showed a good prediction efficiency. A nomogram was constructed by combining the clinical feature and risk score. Immune infiltration and biological enrichment analysis were applied to investigate the difference between high- and low-risk patients. Immunotherapy analysis indicated that low-risk patients might respond better to immunotherapy. Drug sensitivity analysis indicated that high-risk patients might respond better to bleomycin, nilotinib, pazopanib, pyrimethamine, and vinorelbine, yet worse to cisplatin and gefitinib. Furthermore, the gene ECH1 was selected for further analysis. *Conclusions*. Our study identified a prognosis signature that could effectively indicates patients survival. Meanwhile, our study can provide the direction for future studies focused on the PPARs in OC.

1. Introduction

Around the world, ovarian cancer (OC) remains one of the most lethal gynecological cancers [1]. With high mortality, the incidence rate of OC still shows an upward trend, making it a serious public health threat [2]. Nowadays, surgery and chemotherapy are the main treatments for OC. Meanwhile, as a result of hidden early symptoms, many patients have entered the progressive stage of the disease after their first diagnosis, missing the best time for treatment [3]. Consequently, exploring new targets with potential for clinical application is extremely important [4].

Peroxisome proliferator-activated receptors (PPARs) are a kind of nuclear receptors regulated by ligands and are involved in sensing nutrients, regulating metabolism, and regulating lipids [5]. Considering the wide regulatory effect of PPARs, researchers have begun paying attention to their role in a variety of diseases, especially in cancers [5]. Yang et al. found that the interaction between PPARγ and Nur77 can contribute to fatty acid uptake, therefore, promoting breast cancer development [6]. Zou et al. noticed that the PPARγ signaling could be activated by the polyunsaturated fatty acids from astrocytes, further facilitating the brain metastasis process of cancer [7]. Moreover, PPARs

Table 1: The baseline information of the enrolled patients.

Clinical features		Number	Percentage (%)
Age (years)	≤60	326	55.5
	>60	261	44.5
Grade	G1–G2	75	12.8
	G3–G4	496	84.5
	Unknown	16	2.7

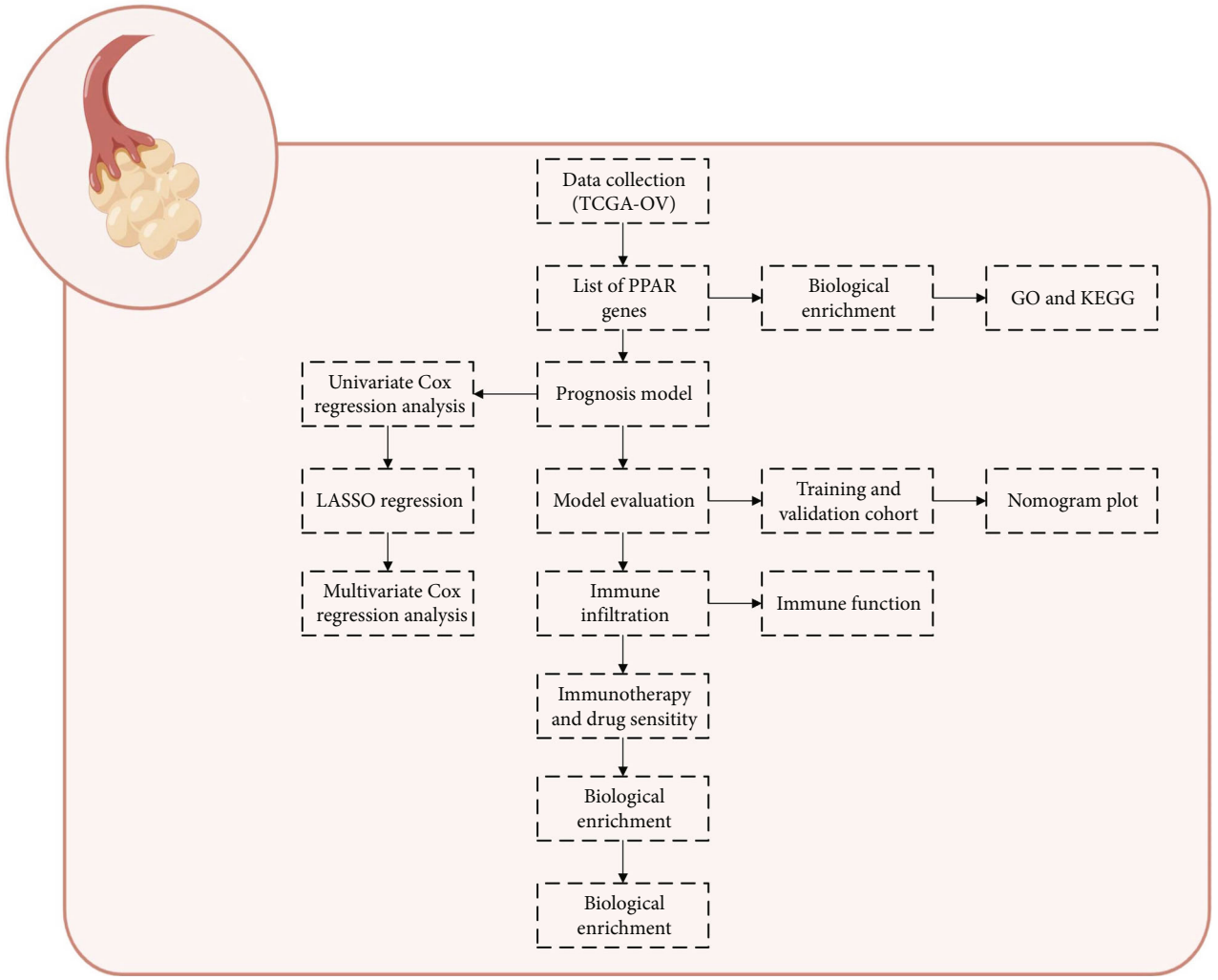

Figure 1: The flow chart of whole study.

signaling is associated with the immune cells in cancer tissue. Liu et al. indicated that S100A4 could regulate the fatty acid oxidation dependent on PPARγ and, therefore, induce M2 polarization in cancer [8]. Furthermore, various pieces of evidence indicate that cancer cells up-regulated PPARδ, which can be used as a defense mechanism against nutritional deprivation and energy stress to improve its survival rate and promote cancer progression [9]. In OC, some studies have preliminarily explored the potential mechanism of PPARs [10]. However, there are still few studies focusing on PPAR in OC.

In recent years, the development of bioinformatics is accompanied by the arrival of the big data era, which provides convenience for researchers [11–13]. In our study, we comprehensively investigated the PPAR target genes in OC, including their biological role. Meanwhile, a prognosis signature consisting of eight PPAR target genes was established, including apolipoprotein A-V (APOA5), UDP glucuronosyltransferase 2 family, polypeptide B4 (UGT2B4), TSC22 domain family, member 1 (TSC22D1), growth hormone inducible transmembrane protein (GHITM), renin (REN), dedicator of cytokinesis 4 (DOCK4), enoyl CoA hydratase 1, peroxisomal (ECH1), and angiopoietin-like 4 (ANGPTL4). Immune infiltration and biological enrichment analysis were applied to investigate the difference between high- and low-

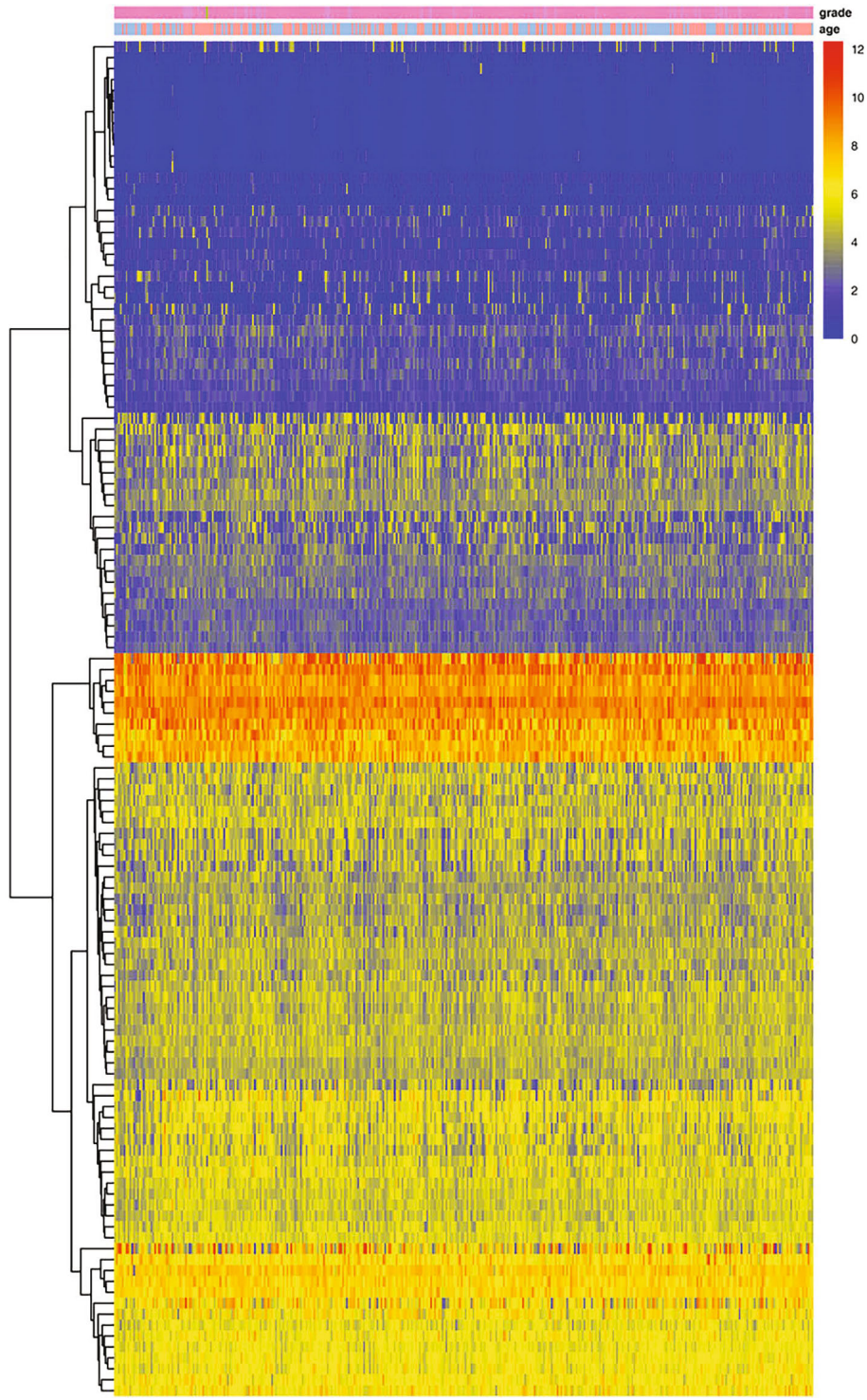

(a)

Figure 2: Continued.

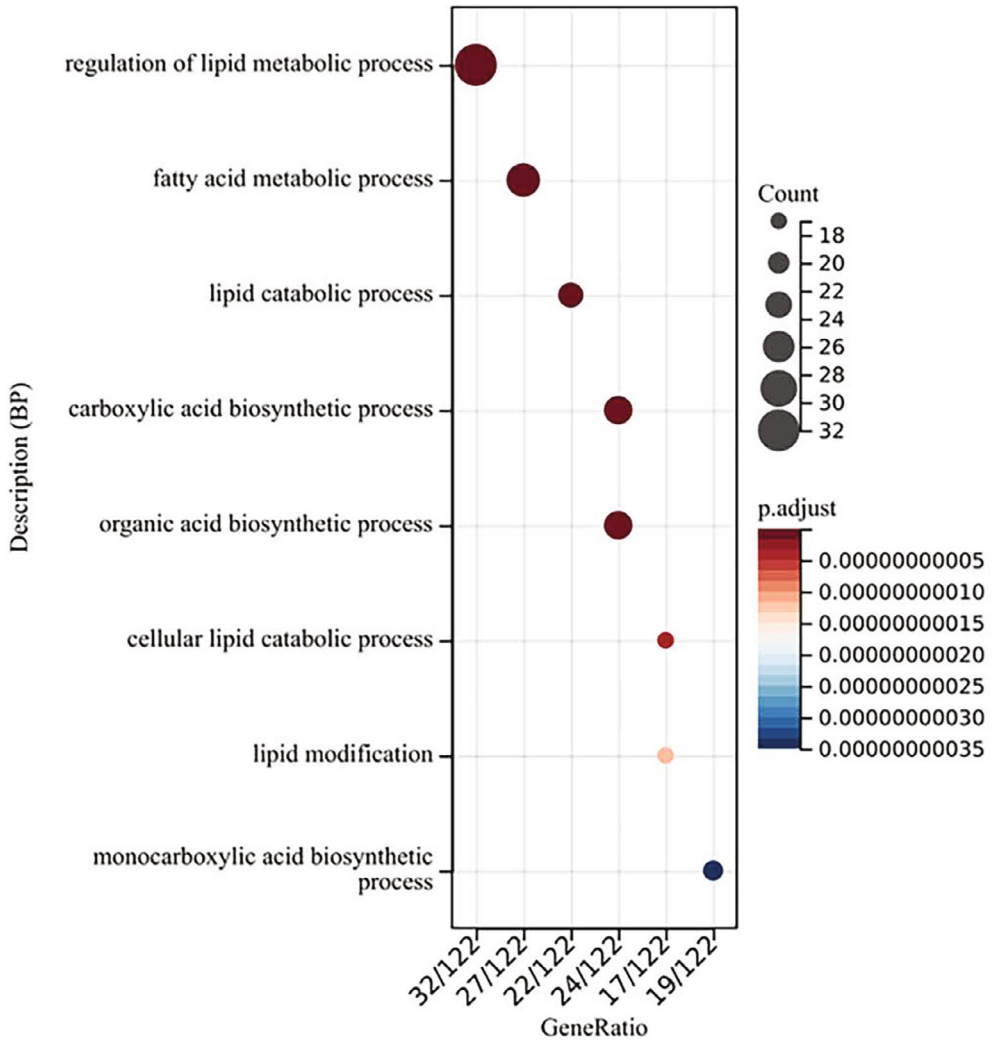

(b)

Figure 2: Continued.

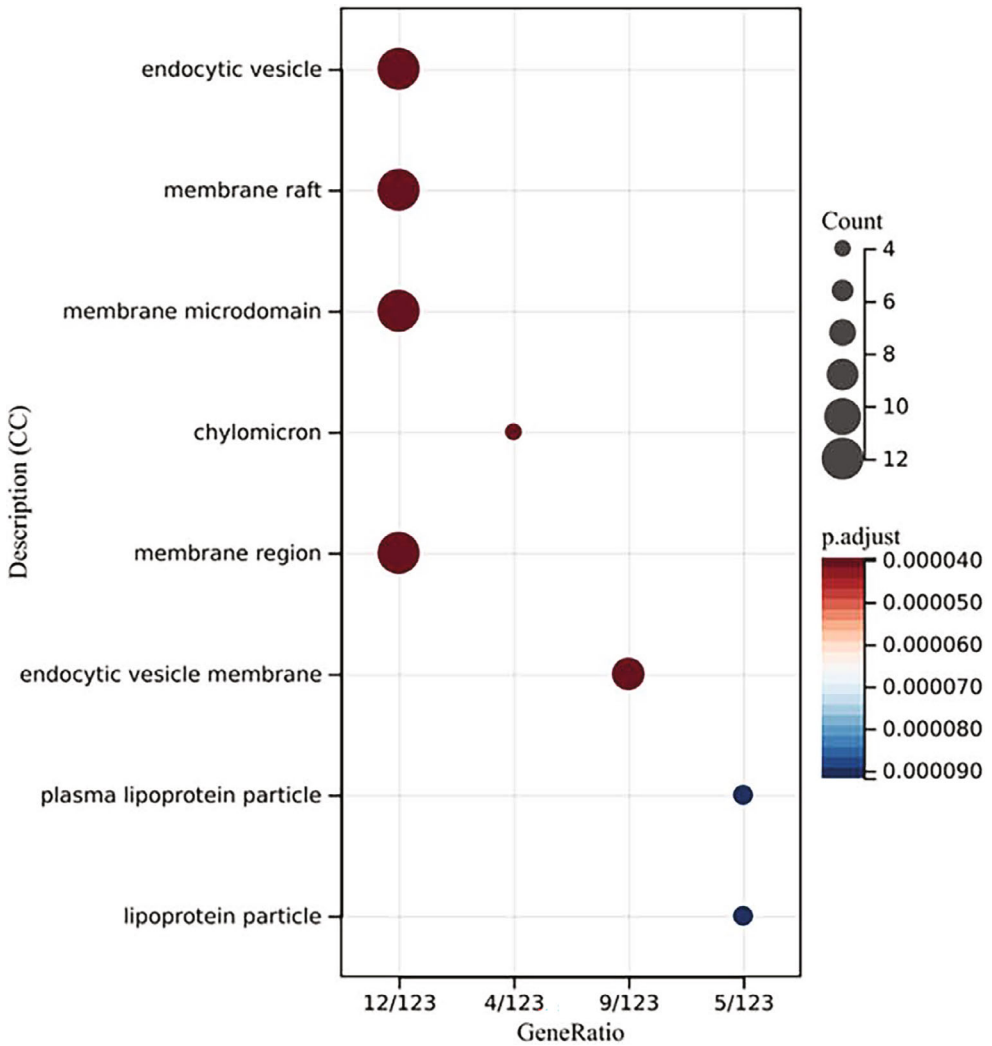

(c)

Figure 2: Continued.

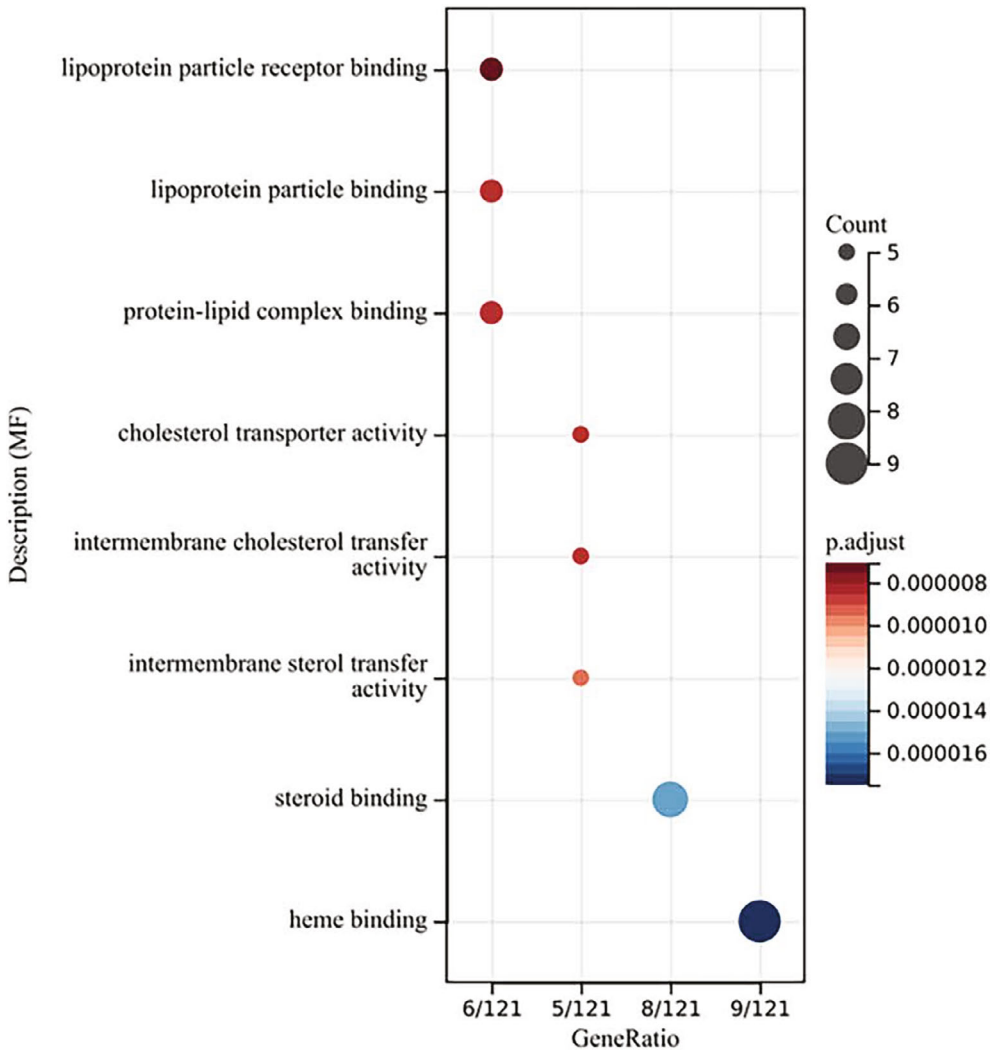

(d)

Figure 2: Continued.

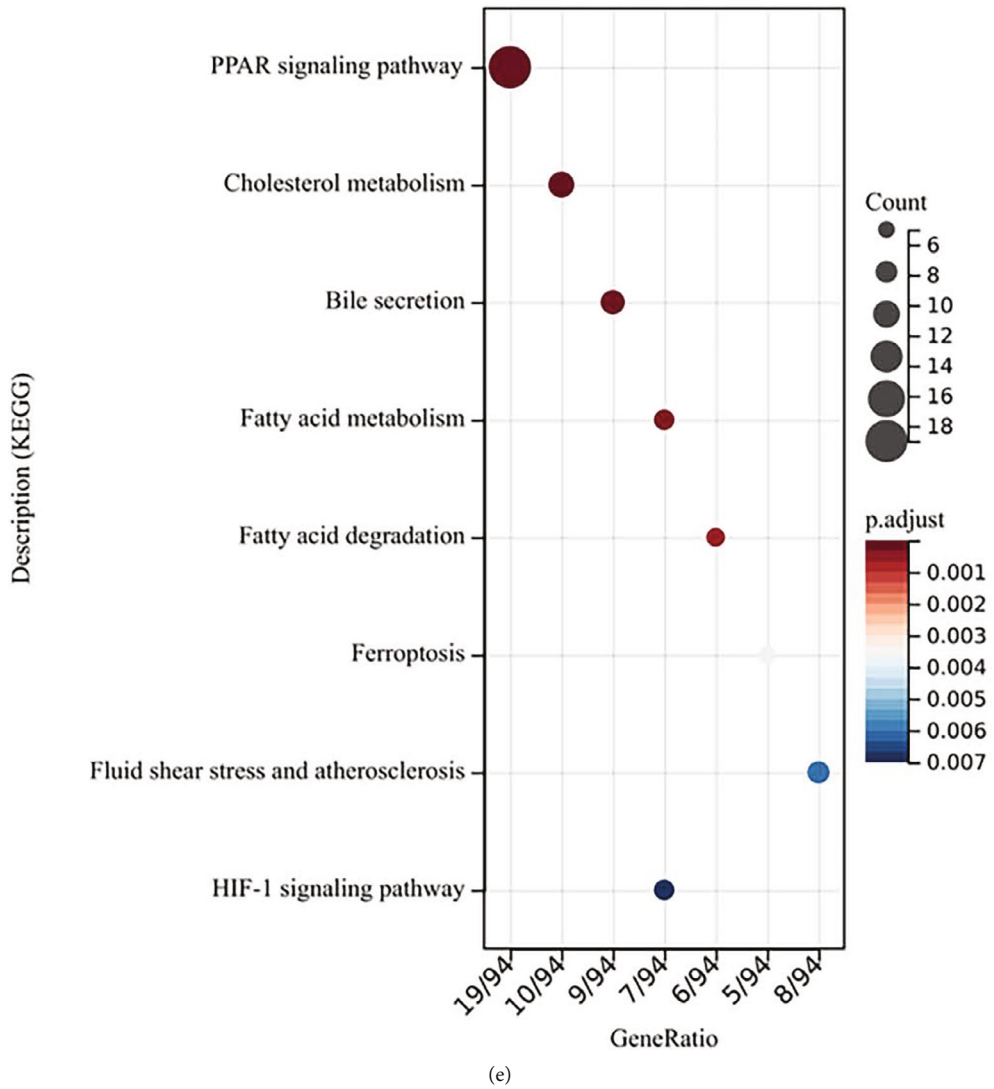

(e)

Figure 2: Role of PPAR target genes in OC. (a) The expression pattern of PPAR target genes in OC. (b) GO-BP analysis of these PPAR target genes. (c) GO-CC analysis of these PPAR target genes. (d) GO-MF analysis of these PPAR target genes. (e) KEGG analysis of these PPAR target genes.

risk patients. Immunotherapy and drug sensitivity analysis were then conducted. Furthermore, the gene ECH1 was selected for further analysis.

2. Methods

2.1. Acquisition of Open-Accessed Data. The expression profile and clinical characteristics of OC patients were downloaded from The Cancer Genome Atlas Program (TCGA) database (TCGA-OV project). The individual file was merged using the R code. Data pre-processing was conducted before the analysis. The list of 126 PPAR target genes was obtained from the PPARgene database (Supplementary Table S1) [14]. The baseline information of enrolled patients was shown in Table 1.

2.2. Biological Difference Investigation. Clusterprofiler was used in the R environment to perform Gene Ontology (GO) and Kyoto Encyclopedia of Genes and Genomes (KEGG) analysis [15]. Gene Set Enrichment Analysis (GSEA) was performed to identify the biological differences based on the specific gene set, including Hallmark and GO [16].

2.3. Prognosis Signature. First, patients were randomly divided into the training group and validation group according to the ratio of 1 : 1. Univariate Cox regression analysis was performed to identify the genes closely related with patients survival. The Least absolute shrinkage and selection operator (LASSO) regression algorithm was applied to screen the optimized variables through data dimension reduction. Ultimately, the multivariate Cox regression was utilized to identify a prognosis signature.

2.4. Model Evaluation and Nomogram. The performance of identified prognosis signature was completed using the Kaplan–Meier (KM) and receiver operating characteristic

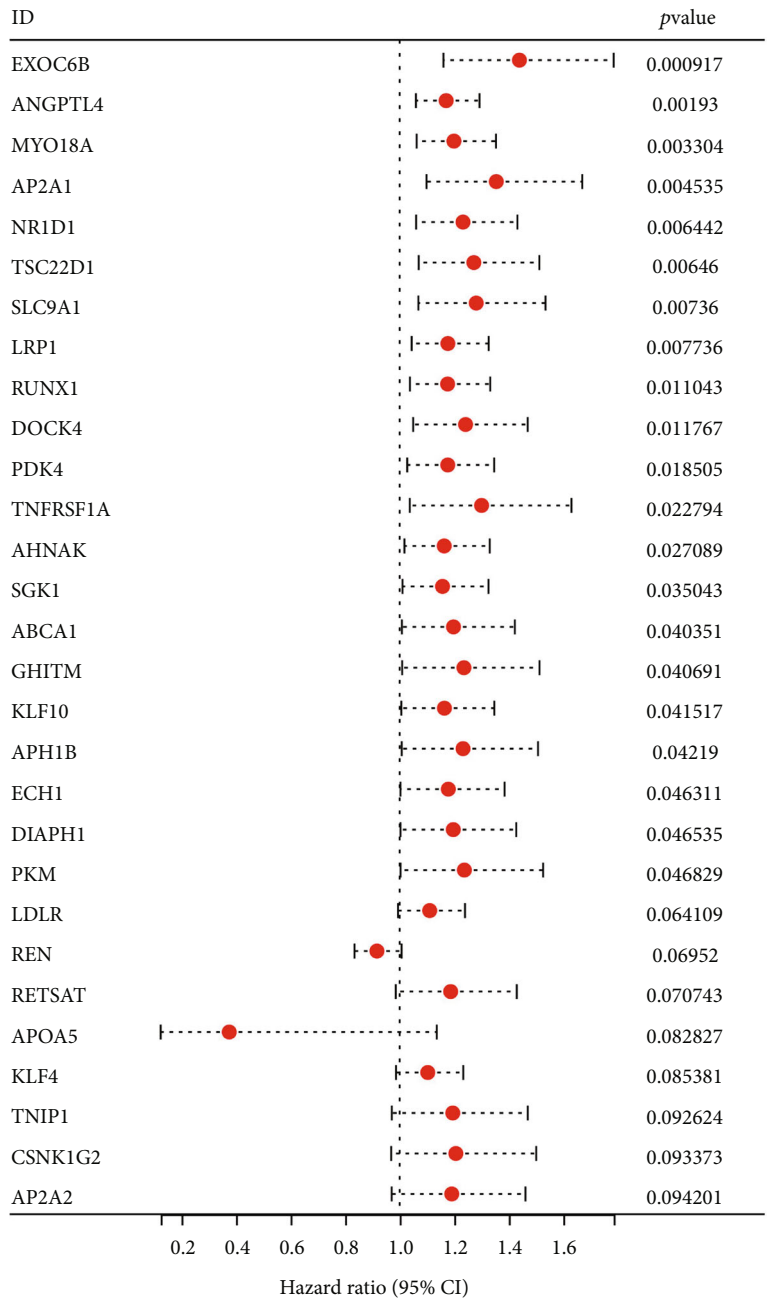

Figure 3: Continued.

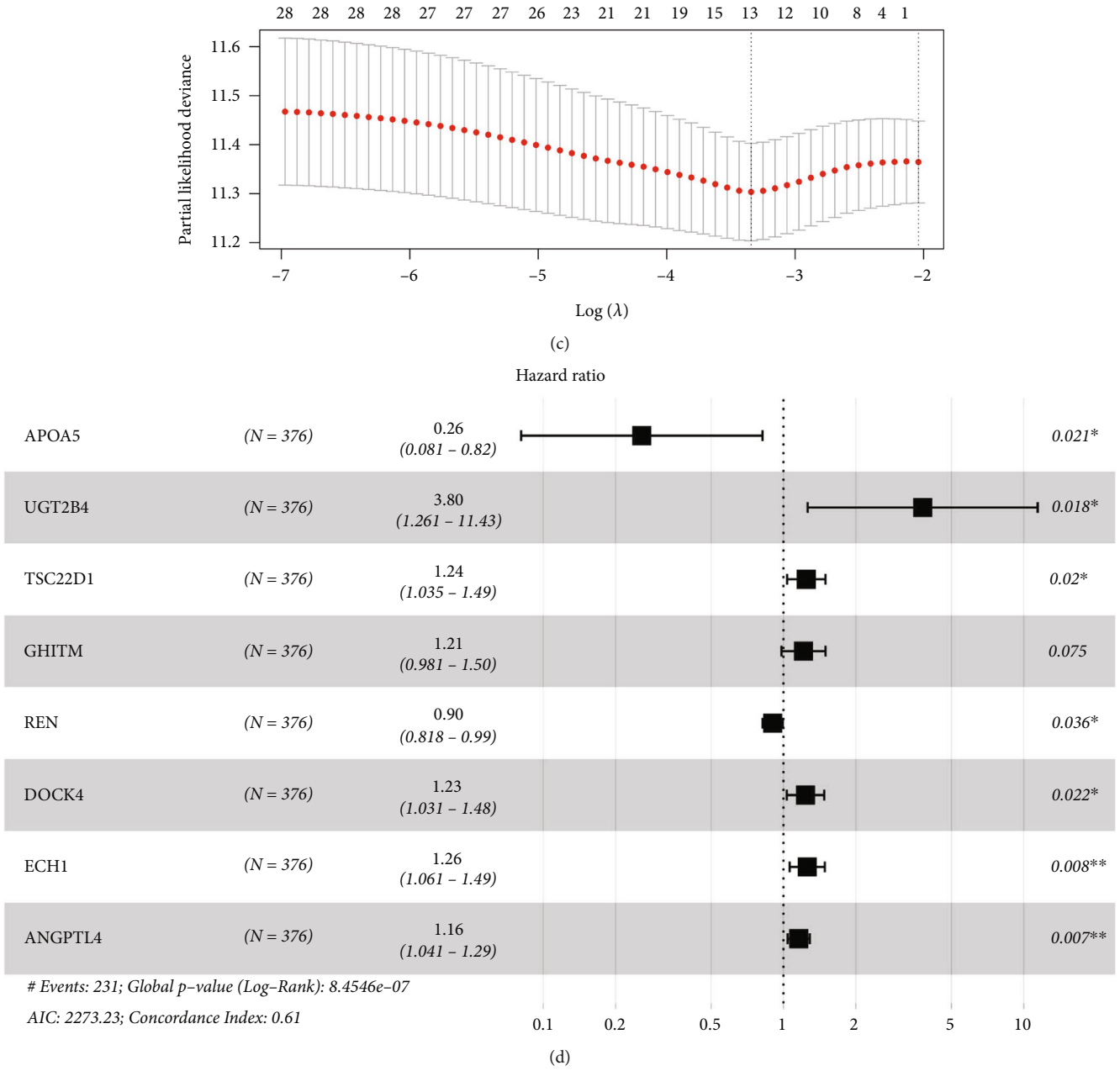

Figure 3: Identification a prognosis signature based on the PPAR target genes. (a) Univariate Cox regression analysis was performed to identify the prognosis-related genes. (b and c) LASSO regression analysis. (d) Multivariate Cox regression analysis was utilized to identify the prognosis signature.

(ROC) curves. A nomogram combining our prognosis signature and clinical features was established using the rms package. The calibration curve was used to compare the fit between nomogram-predicted and actual survival.

2.5. Immune Infiltration and Function Analysis. The quantification of the OC tumor microenvironment was evaluated using multiple algorithms, including CIBERSORT, EPIC, MCP-counter, quanTIseq, TIMER, and xCell [17]. The expression profile of OC patients was set as the input file. Immune function analysis was performed based on the single sample GSEA (ssGSEA) algorithm [18].

2.6. Evaluation of Immunotherapy and Drug Sensitivity. The assessment of patients on immunotherapy response was performed using the Tumor Immune Dysfunction and Exclusion (TIDE) algorithm [19]. Drug sensitivity analysis was conducted based on the data from the Genomics of Drug Sensitivity in Cancer database [20].

2.7. Statistical Analysis. Analysis based on public data was all analyzed using the R software. The threshold of statistical significance was set as 0.05. Different statistical methods are selected according to different data distribution forms. The data with normal distribution were analyzed using the

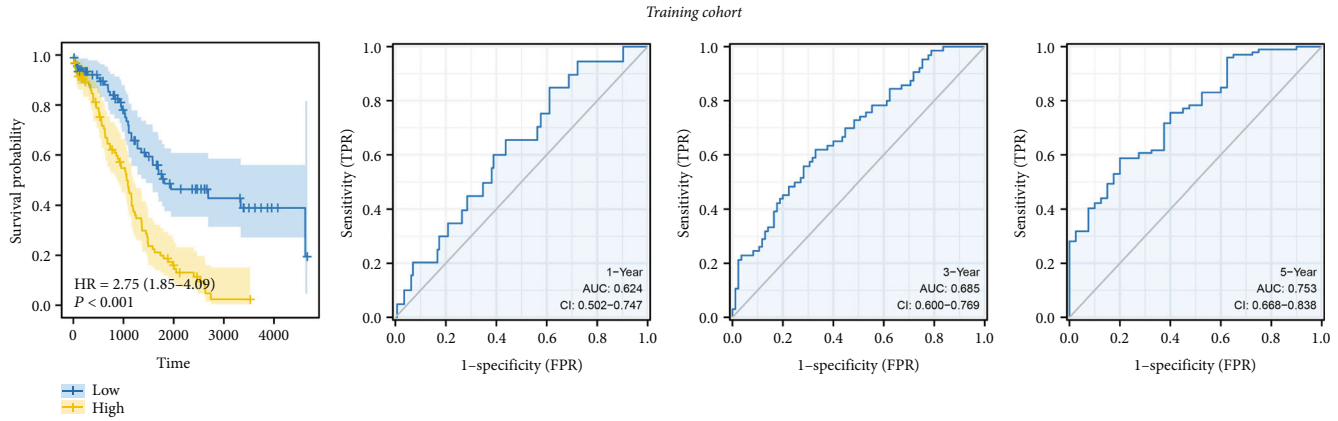

(a)

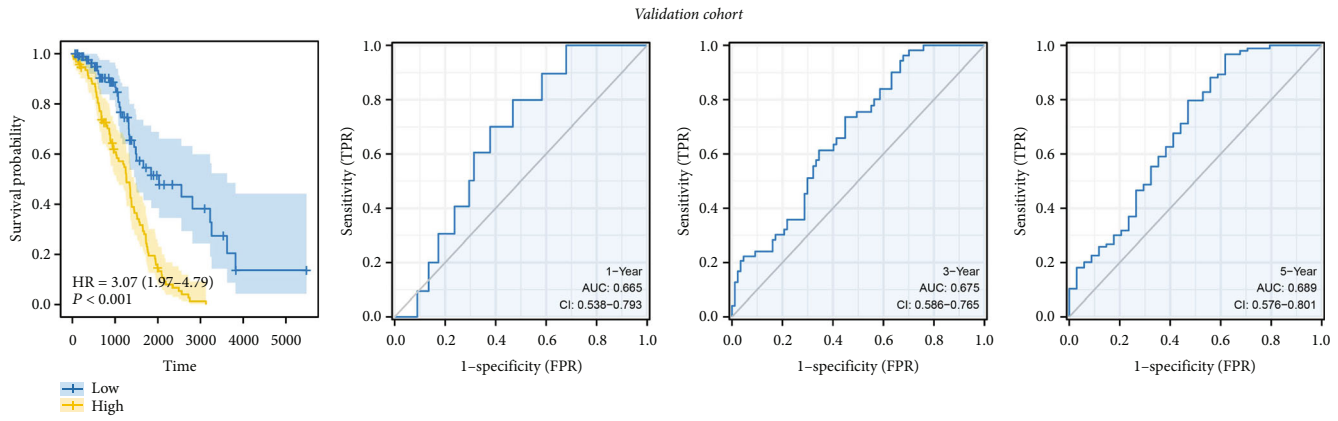

(b)

Figure 4: Continued.

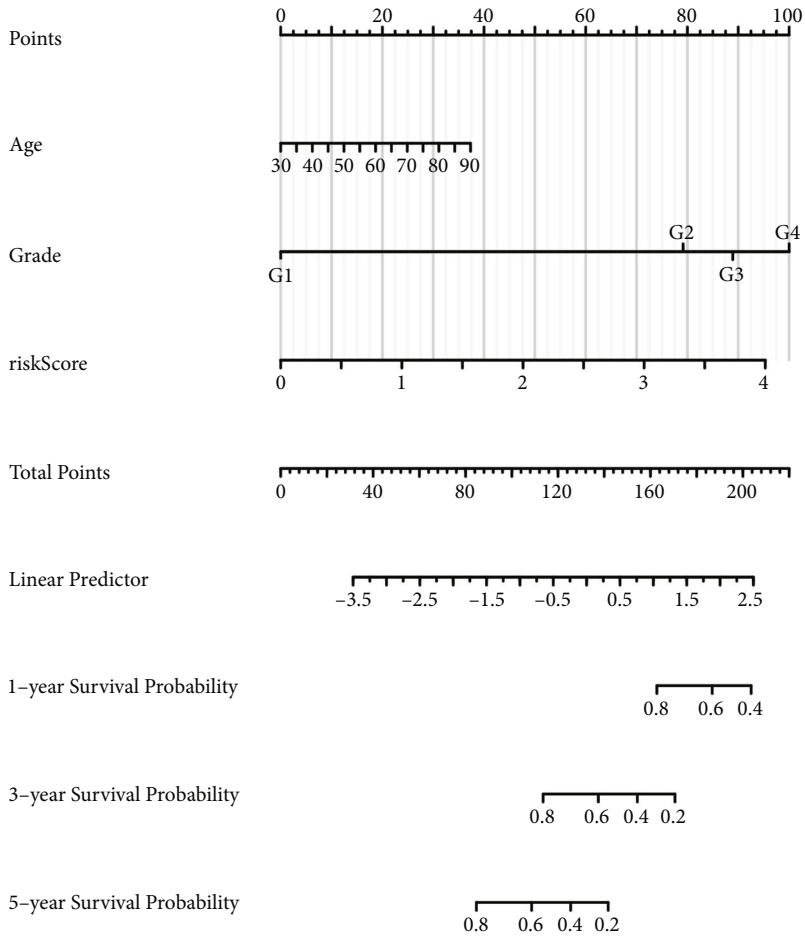

(c)

Figure 4: Continued.

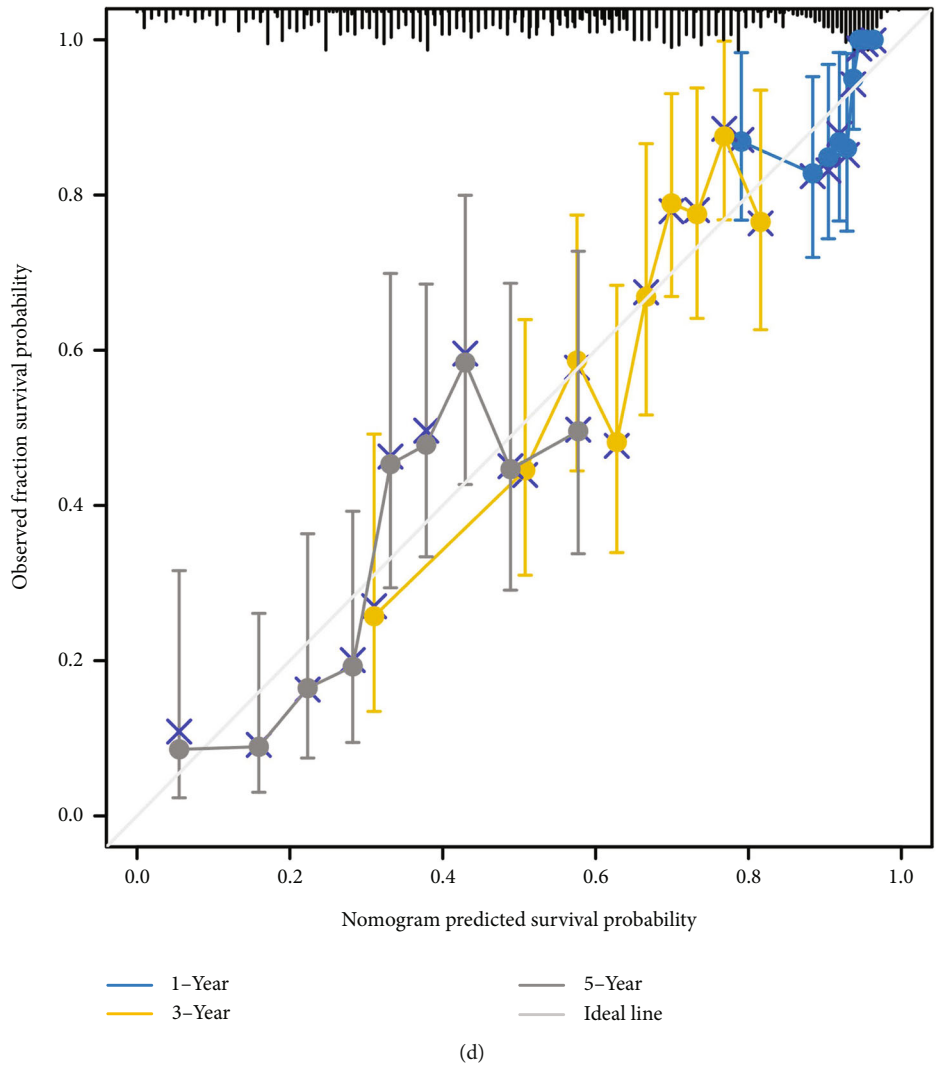

Figure 4: Evaluation of the prognosis model. (a) KM and ROC curves of our model in training cohort. (b) KM and ROC curves of our model in validation cohort. (c) A nomogram was established by combining the risk score and clinical features. (d) Calibration plots.

Students T test, and the non-normal distribution data was analyzed using the Mann–Whitney U test.

3. Results

The flow chart of the whole study was shown in Figure 1.

3.1. Collection of PPAR Target Genes in OC. First, the expression data of 126 PPAR targets were extracted, which was shown in Figure 2(a). Results of GO-Biological Process (BP) showed that the regulation of the lipid catabolic process, lipid metabolic process, and carboxylic acid biosynthetic process were top enriched terms of these genes (Figure 2(b)). For the GO-Cell Component (CC), these genes were primarily enriched in the endocytic vesicle, membrane raft, membrane microdomain, and chylomicron (Figure 2(c)). For the GO-Molecular Function (MF), these genes were mainly enriched in lipoprotein particle receptor binding, lipoprotein particle binding, protein–lipid complex binding, and cholesterol-transported activity (Figure 2(d)). For the KEGG analysis, these genes were mainly enriched in the PPAR signaling pathway, cholesterol metabolism, bile secretion, and fatty acid metabolism (Figure 2(e)).

3.2. Identification of a Prognosis Signature Robustly Indicating Patients Survival. Then, based on these PPAR target genes, the univariate Cox regression analysis was utilized to identify the genes close to patients survival with $P < 0.1$ (Figure 3(a)). Subsequently, the LASSO regression analysis was utilized to screen the optimized variables through data dimension reduction (Figures 3(b) and 3(c)). Finally, multivariate Cox regression analysis identified a prognosis signature consisting of eight PPAR target genes, including APOA5, UGT2B4, TSC22D1, GHITM, REN, DOCK4, ECH1, and ANGPTL4 (Figure 3(d)). The formula of "Risk score = APOA5 × −1.358 + UGT2B4 × 1.334 + TSC22D1 × 0.218 + GHITM × 0.192 + REN × −0.134 + DOCK4 × 0.211 + ECH1 × 0.228 + ANGPTL4 × 0.146" was utilized to calculate the risk score. The median value of risk score was used to divide high- and low-risk patients. The biological enrichment analysis of these model genes was

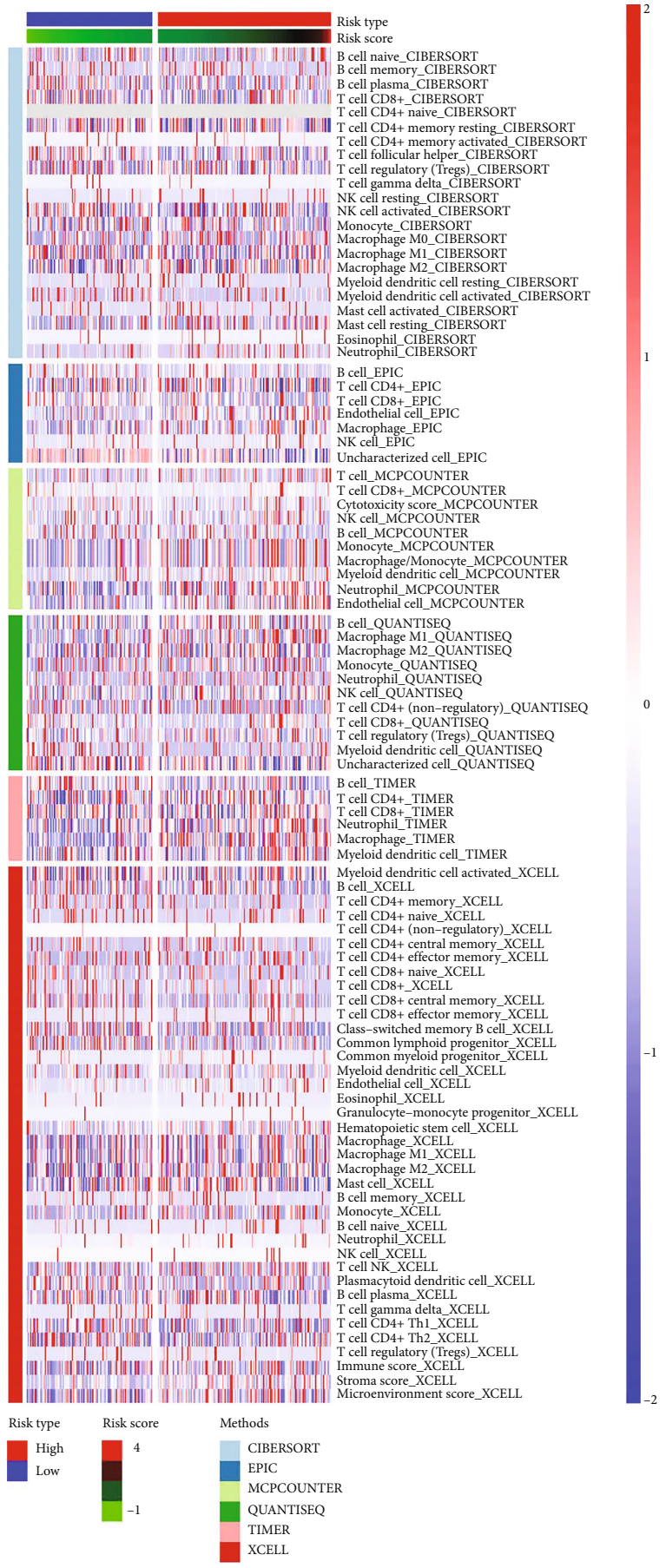

(a)

Figure 5: Continued.

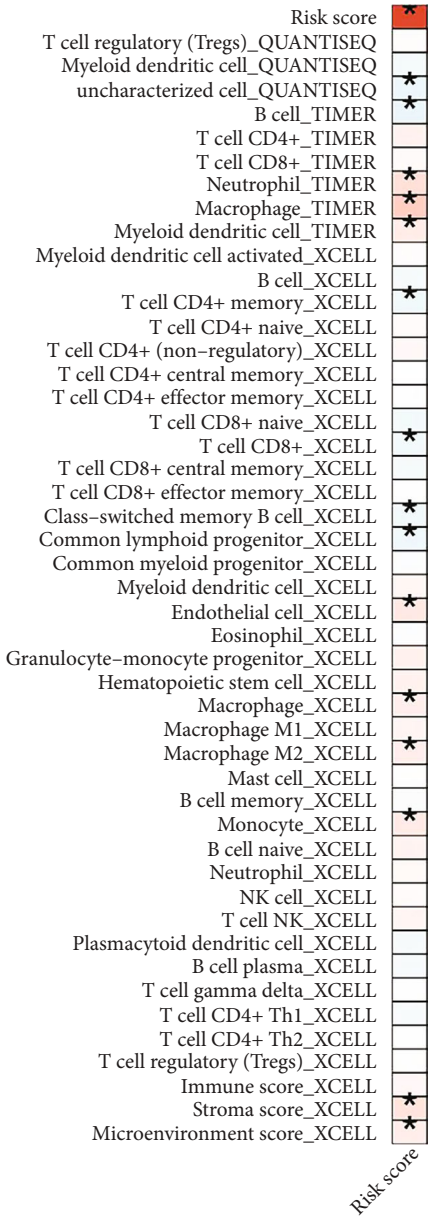

(b)

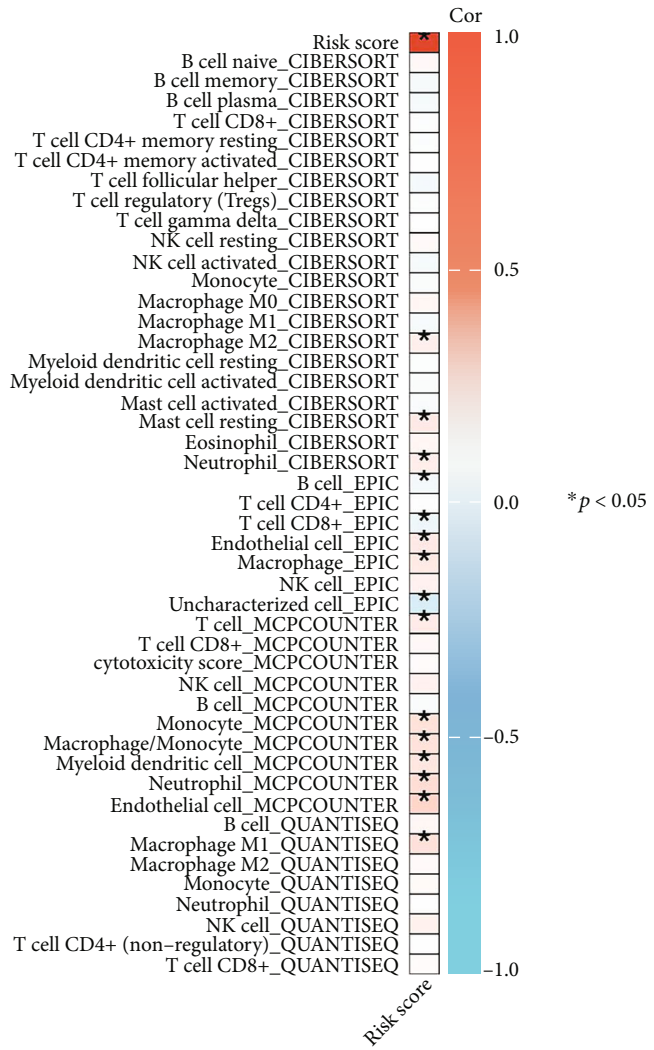

(c)

Figure 5: Continued.

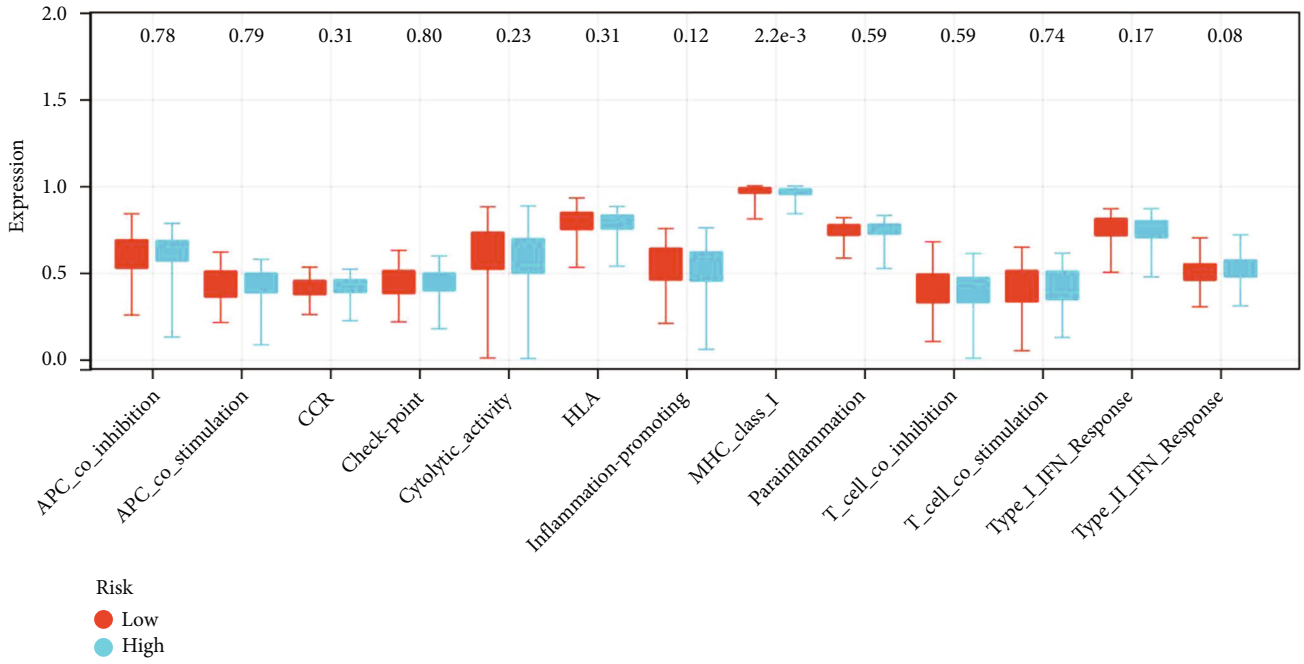

(d)

Figure 5: Immune microenvironment difference between high and low risk patients. (a) The tumor microenvironment of OC was quantified using the multiple algorithm. (b and c) Correlation between risk score and quantified cells. (d) The level of immune function in high- and low-risk patients.

shown in Figure S1. Results indicated that for the patients with high ANGPTL4 expression, the top 3 enriched pathways were angiogenesis, cholesterol hemoostasis, and interleukin 6/Janus kinase/signal transducer and activator of transcription 3 signaling (Figure S1(a)); for the patients with high APOA5 expression, the top 3 enriched pathways were V-Ki-ras2 Kirsten ratsarcoma viral oncogene homolog (KRAS) signaling, spermatogenesis, and pancreatic beta cells (Figure S1(b)); for the patients with high DOCK4 expression, the top 3 enriched pathways were angiogenesis, hedgehog signaling, and transforming growth factor-beta signaling (Figure S1(c)); for the patients with high ECH1 expression, the top 3 enriched pathways were KRAS signaling DN, E2F targets, and G2M checkpoint (Figure S1(d)); for the patients with high GHITM expression, the top 3 enriched pathways were reactive oxygen species pathway, MYC targets, and cholesterol homeostasis (Figure S1(e)); for the patients with high REN expression, the top 3 enriched pathways were estrogen response late, KRAS signaling, and G2M checkpoint (Figure S1(f)); for the patients with high TSC22D1 expression, the top 3 enriched pathways were angiogenesis, hedgehog signaling, and Wnt/β-catenin signaling (Figure S1(g)); and for the patients with high UGT2B4 expression, the top 3 enriched pathways were epithelial–mesenchymal transition (EMT), mitotic spindle, and ultraviolet (UV) response DN (Figure S1(h)).

3.3. Model Evaluation. Our training cohort showed that patients with a high-risk score may have a worse survival rate (Figure 4(a)). ROC curves presented a satisfactory prediction efficiency of our signature on patients survival (Figure 4(a); the area under the curve (AUC) value of 1-, 3-, and 5-year survival were 0.624, 0.685, and 0.753). The same result was also observed in the validation cohort (Figure 4(b); the AUC value of 1-, 3-, and 5-year survival were 0.665, 0.675, and 0.689). A nomogram was constructed by combining the risk score and clinical features to better predict patients survival (Figure 4(c)). The calibration curve indicated a good fit between the actual and nomogram-predicted survival (Figure 4(d)).

3.4. Microenvironment Quantification. We next quantified the cell infiltration of OC patients using multiple algorithms, including CIBERSORT, EPIC, MCP-counter, quanTIseq, TIMER, and xCell (Figure 5(a)). Results indicated that the risk score was positively correlated with neutrophils, macrophages, monocyte, myeloid dendritic cells, and endothelial cells, whereas negatively correlated with B cells and CD8-positive T-lymphocytes (CD8+ T) cells (Figures 5(b) and 5(c)). Immune function analysis showed that the high-risk patients might have a lower activity of major histocompatibility complex (MHC) class I (Figure 5(d)).

3.5. Evaluation of Immunotherapy and Drug Sensitivity. We next evaluated the immunotherapy sensitivity differences. The result indicated a positive correlation between the risk score and the TIDE score (Figure 6(a), $r = 0.207$, $P < 0.001$). Meanwhile, we noticed that the immunotherapy non-responders might have a higher risk score (Figure 6(b)). Moreover, we noticed a higher level of immune exclusion and Carcinoma-associated fibroblasts (CAFs) infiltration in high-risk patients (Figure 6(c)). Drug sensitivity analysis indicated that high-risk

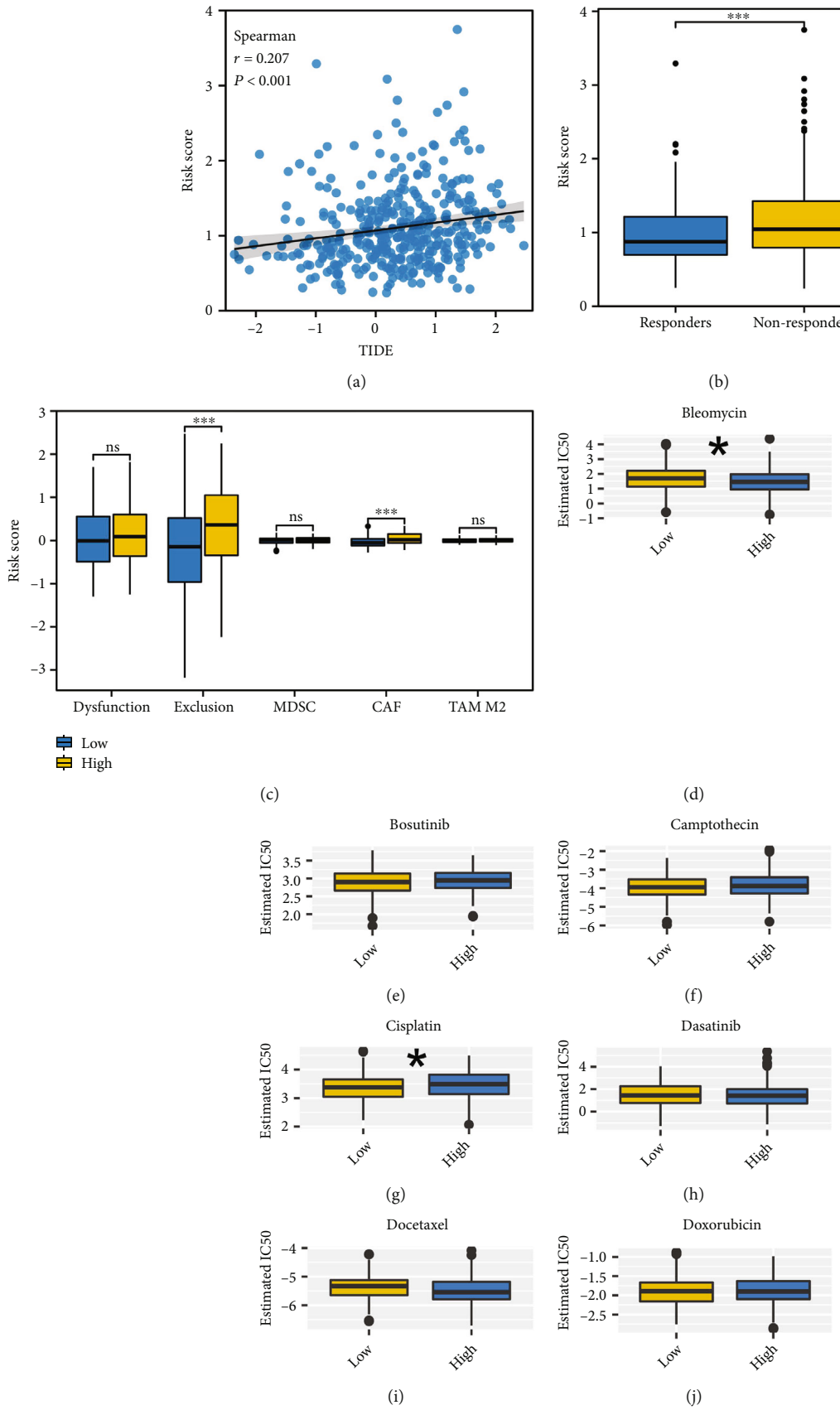

Figure 6: Continued.

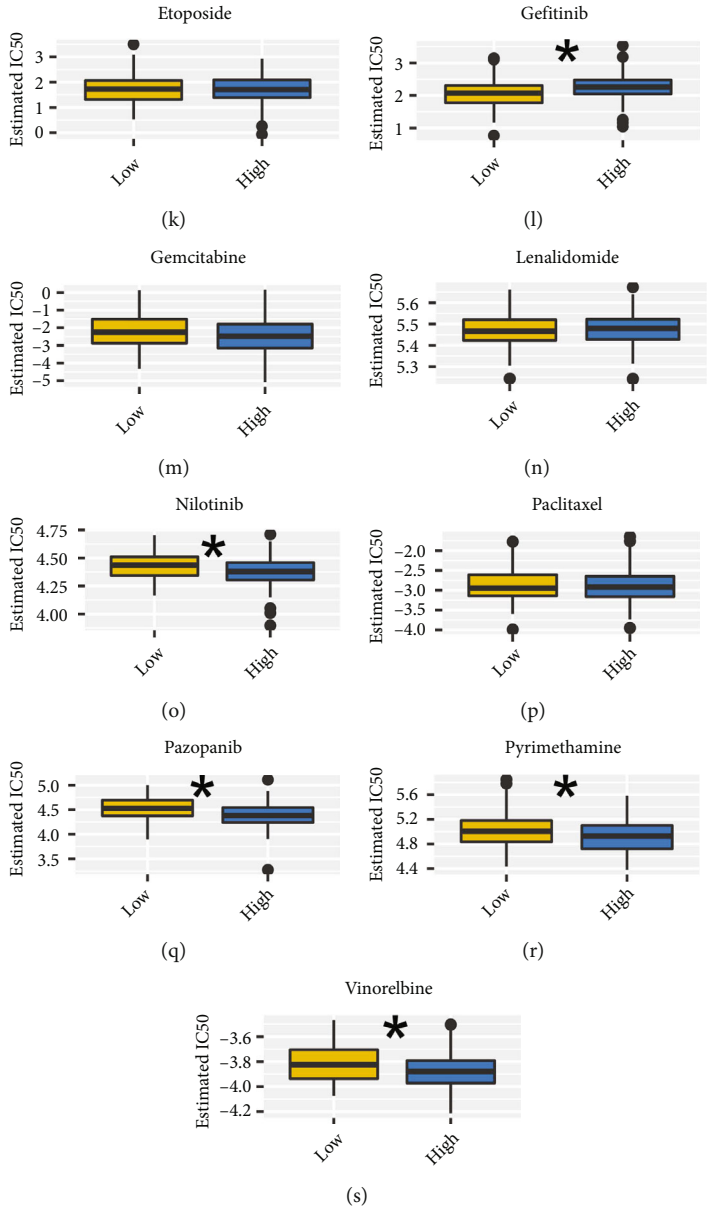

Figure 6: Immunotherapy and drug sensitivity analysis. (a) Correlation between the risk score and TIDE score. (b) The level of risk score in immunotherapy responders and non-responders. (c) The level of dysfunction, exclusion, MDSC, CAF, and TAM M2 in high- and low-risk patients. (d–s) Drug sensitivity analysis.

patients might respond better to bleomycin, nilotinib, pazopanib, pyrimethamine, and vinorelbine, yet resistant to cisplatin and gefitinib (Figures 6(d), 6(e), 6(f), 6(g), 6(h), 6(i), 6(j), 6(k), 6(l), 6(m), 6(n), 6(o), 6(p), 6(q), 6(r), and 6(s)).

3.6. Biological Enrichment Analysis. The GSEA analysis based on the Hallmark gene set indicated that the pathways of EMT, myogenesis, KRAS signaling, apical junction, and inflammatory response were activated in high-risk patients (Figure 7(a)). The GSEA analysis based on the GO gene set showed that the terms of external encapsulating structure organization, forebrain development, and muscle system process were activated (Figure 7(b)).

3.7. Further Investigation of ECH1. The ECH1 was then selected for further analysis. Although not statistically significant, considering the significant difference between KM curves, we believed that the patients with high ECH1 tend to have a worse prognosis (Figures 8(a), 8(b), and 8(c)). Immune infiltration analysis showed that ECH1 was positively correlated with Th2 cells, yet negatively correlated with T helper cell 17 (Th17) cells, CD8+ T cells, plasmacytoid DC (pDC), Central Memory T cell (Tcm), and CD56dim NK cells (Figure 8(d)). GSEA analysis indicated that the top 3 pathways ECH1 was involved in were E2F targets, G2M checkpoints, and estrogen response late (Figures 8(e), 8(f), and 8(g)).

Pathway	Gene ranks	NES	*p* val	*p* adj
HALLMARK_EPITHELIAL_MESENCHYMAL_TRANSITION		1.60	1.0e–04	5.0e–03
HALLMARK_MYOGENESIS		1.40	1.4e–03	3.5e–02
HALLMARK_KRAS_SIGNALING_UP		1.34	4.9e–03	8.2e–02
HALLMARK_KRAS_SIGNALING_DN		1.35	7.0e–03	8.8e–02
HALLMARK_APICAL_JUNCTION		1.29	1.3e–02	1.3e–01
HALLMARK_INFLAMMATORY_RESPONSE		1.27	2.5e–02	2.1e–01
HALLMARK_HYPOXIA		1.22	5.9e–02	3.0e–01
HALLMARK_ANGIOGENESIS		1.35	6.5e–02	3.0e–01
HALLMARK_UV_RESPONSE_DN		1.19	1.1e–01	4.1e–01
HALLMARK_PANCREAS_BETA_CELLS		1.27	1.4e–01	4.8e–01
HALLMARK_DNA_REPAIR		–0.71	1.0e+00	1.0e+00
HALLMARK_PEROXISOME		–0.94	6.5e–01	1.0e+00
HALLMARK_INTERFERON_ALPHA_RESPONSE		–1.05	3.8e–01	8.6e–01
HALLMARK_MYC_TARGETS_V1		–1.93	1.0e–01	3.8e–01
HALLMARK_E2F_TARGETS		–1.45	7.7e–02	3.2e–01
HALLMARK_OXIDATIVE_PHOSPHORYLATION		–1.54	6.7e–02	3.0e–01
HALLMARK_G2M_CHECKPOINT		–1.51	6.7e–02	3.0e–01
HALLMARK_MYC_TARGETS_V2		–1.28	5.6e–02	3.0e–01

0 10000 20000 30000

(a)

Pathway	Gene ranks	NES	*p* val	*p* adj
GOBP_CELL_CELL_ADHESION_VIA_PLASMA_MEMBRANE_ADHESION_MOLECULES		1.61	1.0e–04	5.3e–03
GOBP_CELL_JUNCTION_ASSEMBLY		1.40	1.0e–04	5.3e–03
GOBP_EXTERNAL_ENCAPSULATING_STRUCTURE_ORGANIZATION		1.67	1.0e–04	5.3e–03
GOBP_FOREBRAIN_DEVELOPMENT		1.41	1.0e–04	5.3e–03
GOBP_MUSCLE_SYSTEM_PROCESS		1.45	1.0e–04	5.3e–03
GOBP_OSSIFICATION		1.39	1.0e–04	5.3e–03
GOBP_REGULATION_OF_ION_TRANSMEMBRANE_TRANSPORT		1.39	1.0e–04	5.3e–03
GOBP_REGULATION_OF_MEMBRANE_POTENTIAL		1.59	1.0e–04	5.3e–03
GOBP_REGULATION_OF_NEURON_PROJECTION_DEVELOPMENT		1.38	1.0e–04	5.3e–03
GOBP_REGULATION_OF_TRANS_SYNAPTIC_SIGNALING		1.53	1.0e–04	5.3e–03
GOBP_ENDOSOME_TRANSPORT_VIA_MULTIVESICULAR_BODY_SORTING_PATHWAY		–1.96	1.6e–03	3.3e–02
GOBP_EXTRACELLULAR_TRANSPORT		–2.07	1.3e–03	2.9e–02
GOCC_AXONEMAL_MICROTUBULE		–2.74	1.1e–03	2.6e–02
GOBP_AXONEMAL_DYNEIN_COMPLEX_ASSEMBLY		–2.25	1.0e–03	2.5e–02
GOBP_SPLICEOSOMAL_TRI_SNRNP_COMPLEX_ASSEMBLY		–2.28	9.3e–04	2.4e–02
GOBP_DNA_REPLICATION_DEPENDENT_CHROMATIN_ASSEMBLY		–2.50	9.3e–04	2.4e–02
GOCC_U12_TYPE_SPLICEOSOMAL_COMPLEX		–1.91	9.0e–04	2.4e–02
GOCC_PROTON_TRANSPORTING_ATP_SYNTHASE_COMPLEX		–2.45	7.7e–04	2.1e–02
GOCC_DYNEIN_AXONEMAL_PARTICLE		–2.38	6.4e–04	1.8e–02
GOCC_CHROMOSOME_CENTROMERIC_CORE_DOMAIN		–2.30	6.4e–04	1.8e–02

0 10000 20000 30000

(b)

Figure 7: Biological enrichment analysis. (a) GSEA analysis based on Hallmark gene set. (b) GSEA analysis based on GO gene set.

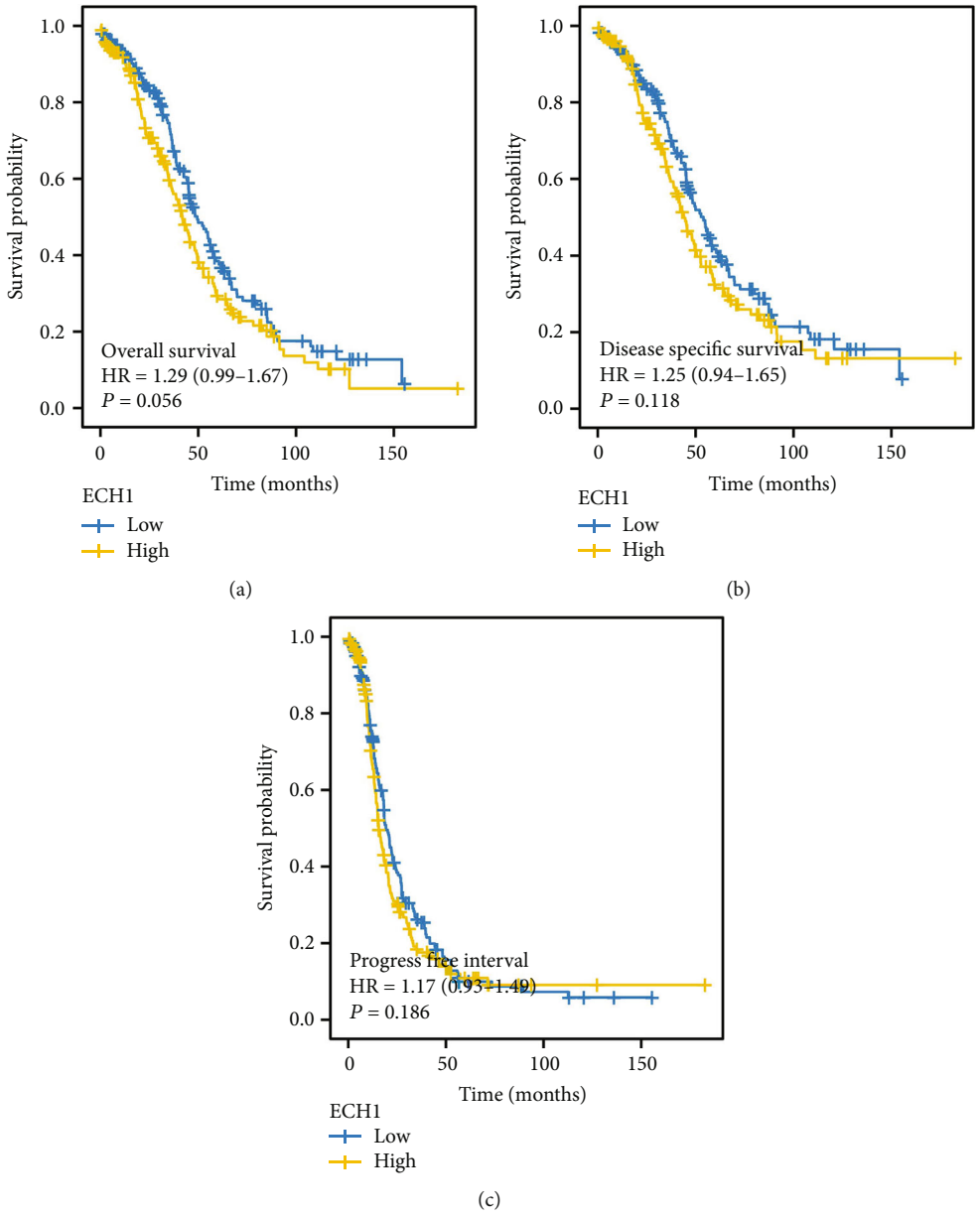

Figure 8: Continued.

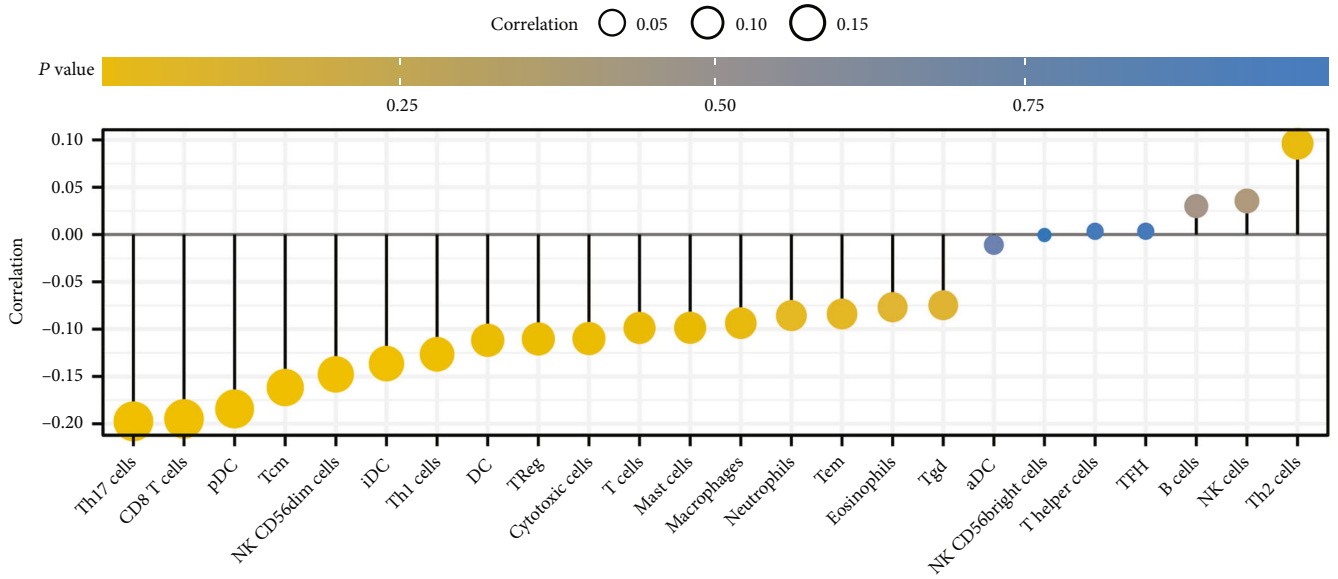

(d)

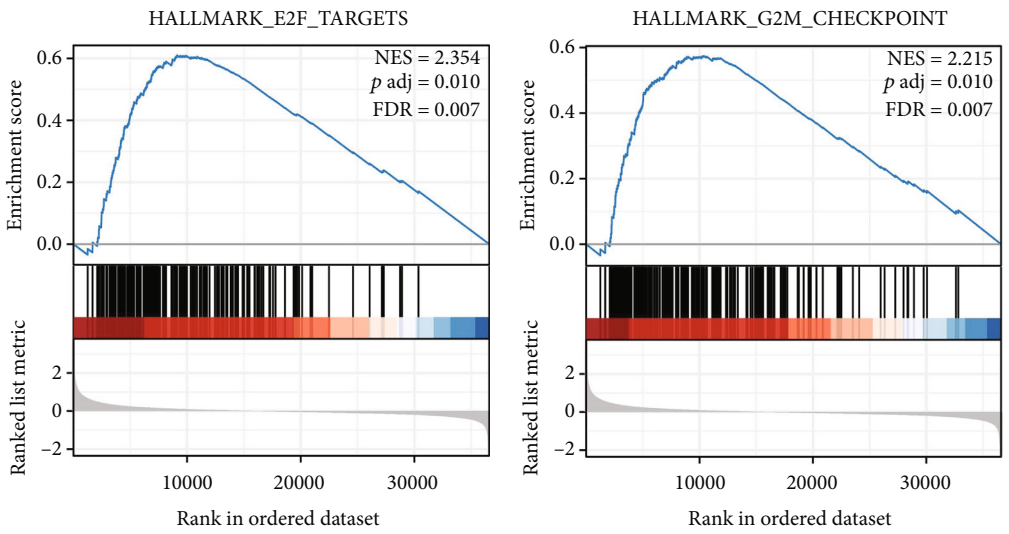

(e) (f)

Figure 8: Continued.

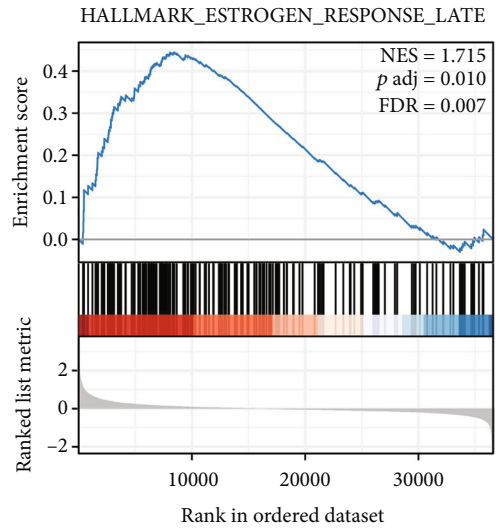

(g)

Figure 8: Further exploration of the ECH1. (a–c) KM survival curves of ECH1 (OS, DSS, and PFI). (d) Immune cell correlation of ECH1. (e–g): The top 3 enriched Hallmark pathways.

4. Discussion

OC remains the primary threat to women's health globally [21]. OC often occurs in perimenopausal women. Due to the lack of early symptoms and effective diagnostic methods, the mortality of OC ranks first among gynecological malignancies [22]. Moreover, the recurrence of OC can be considered a fatal chronic disease with limited treatment. Therefore, exploring its internal mechanism from a molecular perspective can effectively promotes the clinical application of OC.

The development of bioinformatics provides us with an opportunity to deeply understand the mechanism of disease [23]. In our study, we comprehensively investigated the PPAR target genes in OC, including their biological role. Meanwhile, a prognosis signature consisting of eight PPAR target genes was established, including APOA5, UGT2B4, TSC22D1, GHITM, REN, DOCK4, ECH1, and ANGPTL4. A nomogram was constructed by combining the clinical feature and risk score. Immune infiltration and biological enrichment analysis were applied to investigate the difference between high- and low-risk patients. Immunotherapy and drug sensitivity analysis were then conducted. Furthermore, the gene ECH1 was selected for further analysis.

Our prognosis signature consists of eight PPAR genes, including APOA5, UGT2B4, TSC22D1, GHITM, REN, DOCK4, ECH1, and ANGPTL4. Some studies have explored their role in cancers. For instance, the polymorphisms of UGT2B4 were reported to be associated with pancreatic cancer, breast cancer, and esophageal cancer [24–26]. In breast cancer, Meijer et al. found that the TSC22D1 could predict the clinical outcome of patients treated with tamoxifen [27]. Zhao et al. noticed that DOCK4 is a biomarker indicating the prognosis and sensitivity to platinum [28]. Kobayashi et al. revealed that the complex formed by DOCK4 and SH3YL1 could induce Rac1 activation and promote cell migration [29]. Zhang et al. found that ECH1 is an effective inhibitor for lymphatic metastasis of liver cancer [30]. Hui et al. noticed that the long non-coding RNA (lncRNA) AGAP2-AS1 induced by RREB1 could affect the malignant behaviors of pancreatic cancer by suppressing the ankyrin repeat domain 1 and ANGPTL4 [31]. Our results present the role of these genes in OC, which can provide direction for future studies.

GSEA analysis indicated that the pathways of the inflammatory response, EMT, myogenesis, and KRAS signaling were activated in high-risk patients. Liang et al. indicated that in OC, by competitively binding miR-101-3p, lncRNA PTAR promotes EMT and invasion-metastasis [32]. Wu et al. showed that ST3GAL1 could facilitate OC cancer progression through EMT signaling [33]. Kim et al. indicated that the silence of the KRAS gene could indicate a novel treatment strategy for OC [34]. Our result indicated that the poor prognosis of high-risk patients might be due to the abnormal activation of these pathways.

Results indicated that the risk score was positively correlated with neutrophils, macrophages, monocyte, myeloid dendritic cells, and endothelial cells, whereas negatively correlated with B cells and CD8+ T cells. Endothelial cells could promote angiogenesis in the tumor microenvironment, which is a key factor in tumor metastasis [35]. In OC, Li et al. found that the chemoresistant OC cells could promote angiogenesis through exosome manners [36]. Macrophages have also been found to exert an important role in OC. For example, Song et al. noticed that the ubiquitin protein ligase E3 component n-recognin 5 derived from the immunosuppressive macrophages could facilitate the OC progression [37]. Zeng et al. demonstrated that the EGF secreted by the M2 macrophages could enhance OC metastasis by activating epidermal growth factor receptor–extracellular regulated protein kinases signaling and inhibiting the expression of lncRNA LIMIT [38]. Muthuswamy et al. noticed that the

CXCR6 could promote immunosurveillance and control in the OC microenvironment through increasing the retention of memory CD8+ T cells [39]. Our results indicated that the diverse immune cell infiltration pattern can be partly responsible for the difference in prognosis.

ECH1 was selected for our further analysis. Previous studies have shown its role in cancers. Zhang et al. revealed that ECH1 is a potent inhibitor in the process of lymphatic metastasis in liver cancer [30]. Dai et al. found that the ECH1 and HNRNPA2B1 could be a biomarkers for the early diagnosis of lung cancer [40]. Our study illustrated the role of ECH1 in OC, which could provide direction for follow-up research.

Some limitations should be noticed. First, since most of the patients included are from Western populations, this study is inevitably affected by race bias. Second, the results of bioinformatics can not directly reflect the real biological role. Consequently, further biological validation is necessary for the future.

Data Availability

Data supporting this research article are available from the corresponding author or first author on reasonable request.

Conflicts of Interest

The authors declare that they have no conflicts of interest.

Authors' Contributions

Xiao-Fei Leng and Gao-Fa Wang are co-first authors.

Acknowledgments

This work was supported by the Foundation of State Key Laboratory of Ultrasound in Medicine and Engineering (Grant No. 2022KFKT012).

Supplementary Materials

Figure S1. The biological enrichment analysis of APOA5, UGT2B4, TSC22D1, GHITM, REN, DOCK4, ECH1, and ANGPTL4. (a) GSEA analysis of ANGPTL4 based on Hallmark gene set. (b) GSEA analysis of APOA5 based on Hallmark gene set. (c) GSEA analysis of DOCK4 based on Hallmark gene set. (d) GSEA analysis of ECH1 based on Hallmark gene set. (e) GSEA analysis of GHITM based on Hallmark gene set. (f) GSEA analysis of REN based on Hallmark gene set. (g) GSEA analysis of TSC22D1 based on Hallmark gene set. (h) GSEA analysis of UGT2B4 based on Hallmark gene set. Table S1. The list of PPAR-related genes. *(Supplementary Materials)*

References

[1] K. R. Cho and I. M. Shih, "Ovarian cancer," *Annual Review of Pathology*, vol. 4, no. 1, pp. 287–313, 2009.

[2] P. M. Webb and S. J. Jordan, "Epidemiology of epithelial ovarian cancer," *Best Practice and Research Clinical Obstetrics and Gynaecology*, vol. 41, pp. 3–14, 2017.

[3] S. Gupta, S. Nag, S. Aggarwal, A. Rauthan, and N. Warrier, "Maintenance therapy for recurrent epithelial ovarian cancer: current therapies and future perspectives - a review," *Journal of Ovarian Research*, vol. 12, no. 1, p. 103, 2019.

[4] Y. Wei, X. Chen, X. Ren et al., "Identification of MX2 as a novel prognostic biomarker for sunitinib resistance in clear cell renal cell carcinoma," *Frontiers in Genetics*, vol. 12, article 680369, 2021.

[5] J. Porcuna, J. Mínguez-Martínez, and M. Ricote, "The PPARα and PPARγ epigenetic landscape in cancer and immune and metabolic disorders," *International Journal of Molecular Sciences*, vol. 22, no. 19, p. 10573, 2021.

[6] P. B. Yang, P. P. Hou, F. Y. Liu et al., "Blocking PPARγ interaction facilitates Nur77 interdiction of fatty acid uptake and suppresses breast cancer progression," *Proceedings of the National Academy of Sciences of the United States of America*, vol. 117, no. 44, pp. 27412–27422, 2020.

[7] Y. Zou, A. Watters, N. Cheng et al., "Polyunsaturated fatty acids from astrocytes activate PPARγ signaling in cancer cells to promote brain metastasis," *Cancer Discovery*, vol. 9, no. 12, pp. 1720–1735, 2019.

[8] S. Liu, H. Zhang, Y. Li et al., "S100A4 enhances protumor macrophage polarization by control of PPAR-γ-dependent induction of fatty acid oxidation," *Journal for Immunotherapy of Cancer*, vol. 9, no. 6, p. e002548, 2021.

[9] Y. Liu, J. K. Colby, X. Zuo, J. Jaoude, D. Wei, and I. Shureiqi, "The role of PPAR-δ in metabolism, inflammation, and cancer: many characters of a critical transcription factor," *International Journal of Molecular Sciences*, vol. 19, no. 11, p. 3339, 2018.

[10] J. Dupont, M. Reverchon, L. Cloix, P. Froment, and C. Ramé, "Involvement of adipokines, AMPK, PI3K and the PPAR signaling pathways in ovarian follicle development and cancer," *The International Journal of Developmental Biology*, vol. 56, no. 10–12, pp. 959–967, 2012.

[11] X. Wei, Y. Dong, X. Chen et al., "Construction of circRNA-based ceRNA network to reveal the role of circRNAs in the progression and prognosis of metastatic clear cell renal cell carcinoma," *Aging*, vol. 12, no. 23, pp. 24184–24207, 2020.

[12] X. Zhang, T. Zhang, X. Ren, X. Chen, S. Wang, and C. Qin, "Pyrethroids toxicity to male reproductive system and offspring as a function of oxidative stress induction: rodent studies," *Frontiers in Endocrinology*, vol. 12, article 656106, 2021.

[13] T. Zhang, X. Zhou, X. Zhang et al., "Gut microbiota may contribute to the postnatal male reproductive abnormalities induced by prenatal dibutyl phthalate exposure," *Chemosphere*, vol. 287, no. Point 1, p. 132046, 2022.

[14] L. Fang, M. Zhang, Y. Li, Y. Liu, Q. Cui, and N. Wang, "PPARgene: a database of experimentally verified and computationally predicted PPAR target genes," *PPAR Research*, vol. 2016, p. 6042166, 2016.

[15] G. Yu, L. G. Wang, Y. Han, and Q. Y. He, "ClusterProfiler: an R package for comparing biological themes among gene clusters," *OMICS*, vol. 16, no. 5, pp. 284–287, 2012.

[16] A. Subramanian, P. Tamayo, V. K. Mootha et al., "Gene set enrichment analysis: a knowledge-based approach for interpreting genome-wide expression profiles," *Proceedings of the National Academy of Sciences of the United States of America*, vol. 102, no. 43, pp. 15545–15550, 2005.

[17] D. Aran, Z. Hu, and A. J. Butte, "xCell: digitally portraying the tissue cellular heterogeneity landscape," *Genome Biology*, vol. 18, no. 1, p. 220, 2017.

[18] S. Hänzelmann, R. Castelo, and J. Guinney, "GSVA: gene set variation analysis for microarray and RNA-seq data," *BMC Bioinformatics*, vol. 14, no. 1, p. 7, 2013.

[19] J. Fu, K. Li, W. Zhang et al., "Large-scale public data reuse to model immunotherapy response and resistance," *Genome Medicine*, vol. 12, no. 1, p. 21, 2020.

[20] W. Yang, J. Soares, P. Greninger et al., "Genomics of drug sensitivity in cancer (GDSC): a resource for therapeutic biomarker discovery in cancer cells," *Nucleic Acids Research*, vol. 41, no. Database issue, pp. D955–D961, 2013.

[21] M. A. Roett and P. Evans, "Ovarian cancer: an overview," *American Family Physician*, vol. 80, no. 6, pp. 609–616, 2009.

[22] X. Dong, X. Men, W. Zhang, and P. Lei, "Advances in tumor markers of ovarian cancer for early diagnosis," *Indian Journal of Cancer*, vol. 51, no. Suppl 3, pp. e72–e76, 2014.

[23] D. Wu, Z. Yin, Y. Ji et al., "Identification of novel autophagy-related lncRNAs associated with a poor prognosis of colon adenocarcinoma through bioinformatics analysis," *Scientific Reports*, vol. 11, no. 1, p. 8069, 2021.

[24] X. Che, D. Yu, Z. Wu et al., "Polymorphisms in UGT2B4 and susceptibility to pancreatic cancer," *International Journal of Clinical and Experimental Medicine*, vol. 8, no. 2, pp. 2702–2710, 2015.

[25] C. Sun, D. Huo, C. Southard et al., "A signature of balancing selection in the region upstream to the human UGT2B4 gene and implications for breast cancer risk," *Human Genetics*, vol. 130, no. 6, pp. 767–775, 2011.

[26] P. Dura, J. Salomon, R. H. Te Morsche et al., "High enzyme activity UGT1A1 or low activity UGT1A8 and UGT2B4 genotypes increase esophageal cancer risk," *International Journal of Oncology*, vol. 40, no. 6, pp. 1789–1796, 2012.

[27] D. Meijer, M. P. Jansen, M. P. Look et al., "TSC22D1 and PSAP predict clinical outcome of tamoxifen treatment in patients with recurrent breast cancer," *Breast Cancer Research and Treatment*, vol. 113, no. 2, pp. 253–260, 2009.

[28] Q. Zhao, J. Zhong, P. Lu et al., "DOCK4 is a platinum-chemosensitive and prognostic-related biomarker in ovarian cancer," *PPAR Research*, vol. 2021, p. 6629812, 2021.

[29] M. Kobayashi, K. Harada, M. Negishi, and H. Katoh, "Dock4 forms a complex with SH3YL1 and regulates cancer cell migration," *Cellular Signalling*, vol. 26, no. 5, pp. 1082–1088, 2014.

[30] J. Zhang, M. Sun, R. Li et al., "Ech1 is a potent suppressor of lymphatic metastasis in hepatocarcinoma," *Biomedicine and Pharmacotherapy = Biomedecine and Pharmacotherapie*, vol. 67, no. 7, pp. 557–560, 2013.

[31] B. Hui, H. Ji, Y. Xu et al., "RREB1-induced upregulation of the lncRNA AGAP2-AS1 regulates the proliferation and migration of pancreatic cancer partly through suppressing ANKRD1 and ANGPTL4," *Cell Death and Disease*, vol. 10, no. 3, p. 207, 2019.

[32] H. Liang, T. Yu, Y. Han et al., "LncRNA PTAR promotes EMT and invasion-metastasis in serous ovarian cancer by competitively binding miR-101-3p to regulate ZEB1 expression," *Molecular Cancer*, vol. 17, no. 1, p. 119, 2018.

[33] X. Wu, J. Zhao, Y. Ruan, L. Sun, C. Xu, and H. Jiang, "Sialyltransferase ST3GAL1 promotes cell migration, invasion, and TGF-β1-induced EMT and confers paclitaxel resistance in ovarian cancer," *Cell Death and Disease*, vol. 9, no. 11, p. 1102, 2018.

[34] M. J. Kim, S. J. Lee, J. H. Ryu, S. H. Kim, I. C. Kwon, and T. M. Roberts, "Combination of KRAS gene silencing and PI3K inhibition for ovarian cancer treatment," *Journal of Controlled Release*, vol. 318, pp. 98–108, 2020.

[35] J. Bolik, F. Krause, M. Stevanovic et al., "Inhibition of ADAM17 impairs endothelial cell necroptosis and blocks metastasis," *The Journal of Experimental Medicine*, vol. 219, no. 1, 2022.

[36] Z. Li, W. Yan-Qing, Y. Xiao et al., "Exosomes secreted by chemoresistant ovarian cancer cells promote angiogenesis," *Journal of Ovarian Research*, vol. 14, no. 1, p. 7, 2021.

[37] M. Song, O. O. Yeku, S. Rafiq et al., "Tumor derived UBR5 promotes ovarian cancer growth and metastasis through inducing immunosuppressive macrophages," *Nature Communications*, vol. 11, no. 1, p. 6298, 2020.

[38] X. Y. Zeng, H. Xie, J. Yuan et al., "M2-like tumor-associated macrophages-secreted EGF promotes epithelial ovarian cancer metastasis via activating EGFR-ERK signaling and suppressing lncRNA LIMT expression," *Cancer Biology and Therapy*, vol. 20, no. 7, pp. 956–966, 2019.

[39] R. Muthuswamy, A. R. McGray, S. Battaglia et al., "CXCR6 by increasing retention of memory CD8(+) T cells in the ovarian tumor microenvironment promotes immunosurveillance and control of ovarian cancer," *Journal for Immunotherapy of Cancer*, vol. 9, no. 10, p. e003329, 2021.

[40] L. Dai, J. Li, J. J. Tsay et al., "Identification of autoantibodies to ECH1 and HNRNPA2B1 as potential biomarkers in the early detection of lung cancer," *Oncoimmunology*, vol. 6, no. 5, article e1310359, 2017.

Hindawi
PPAR Research
Volume 2023, Article ID 6797694, 17 pages
https://doi.org/10.1155/2023/6797694

Research Article

Nuclear Protein 1 Expression Is Associated with PPARG in Bladder Transitional Cell Carcinoma

Chao Lu, Shenglin Gao, Li Zhang, Xiaokai Shi, Yin Chen, Shuzhang Wei, Li Zuo, and Lifeng Zhang

Department of Urology, Changzhou Second People's Hospital, 29 Xinglong Road, Changzhou 213003, China

Correspondence should be addressed to Li Zuo; zuoli@njmu.edu.cn and Lifeng Zhang; nj-likky@aliyun.com

Received 3 November 2022; Revised 20 March 2023; Accepted 20 April 2023; Published 8 May 2023

Academic Editor: Xiao-Jie Lu

Background. The *Nuclear protein 1* gene was first discovered in acute pancreatitis and functions as an oncogene in cancer progression and drug resistance. However, the role of *Nuclear protein 1* in bladder transitional cell carcinoma (BTCC) is still unclear. *Methods*. The Cancer Genome Atlas database and immunohistochemical analysis were adopted to evaluate *Nuclear protein 1* expression in BTCC. We applied lentivirus-mediated small-interfering RNA to down-regulate the expression of *Nuclear protein 1* in BTCC cell lines. We further performed an Affymetrix microarray and Gene Set Enrichment Analysis (GSEA) to assess the genes and signaling pathways related to *Nuclear protein 1*. *Results*. We found that *Nuclear protein 1* expression was up-regulated in BTCC and positively related to the degree of BTCC malignancy. Compared with Caucasian patients with BTCC, *Nuclear protein 1* expression was attenuated in Asian patients. The Affymetrix microarray showed that lipopolysaccharide was the upstream regulatory factor of *Nuclear protein 1* in BTCC. The GSEA indicated that *Nuclear protein 1* expression was associated with signaling pathways in cancer, peroxisome proliferator-activated receptor (PPAR) pathways, and RNA degradation. The expression of *Nuclear protein 1* was negatively correlated with PPARG ($R = -0.290$, $P < 0.001$), but not with PPARA ($R = 0.047$, $P = 0.344$) and PPARD ($R = -0.055$, $P = 0.260$). *Conclusions*. The study findings indicate that *Nuclear protein 1* is positively associated with the malignancy degree of BTCC and that *Nuclear protein 1* expression is negatively correlated with PPARG.

1. Introduction

Bladder transitional cell carcinoma (BTCC) is one of the most common malignancies of the urinary system. In the United States, 61,700 new cases of BTCC in men and 19,480 new cases in women were estimated in 2022. A total of 12,120 men and 4,980 women died in the same year as a result of BTCC [1]. BTCC is also one of the five most common malignancies in the United States. Given its high recurrence rate, BTCC remains one of the most expensive malignancies to treat [2]. With about 550,000 new patients each year, BTCC is one of the 10 most common malignancies worldwide. Currently, developed communities have the heaviest burden of BTCC [3], and hence, strategies are required for the prevention and control of BTCC and to alleviate the exorbitant burden on the society and economy. The gradual understanding of urinary biomarkers in BTCC has facilitated the employment of non-invasive biomarkers to replenish urine cytology. However, none is effective enough when performed alone, and pathology remains to be the gold standard method to detect and diagnose BTCC [4].

The *Nuclear protein 1* (also named Com-1) is a gene strongly up-regulated in the acute stage of pancreatitis. The *Nuclear protein 1* mRNA is activated in response to a variety of stress responses, and its activation is not limited to pancreatic cells. Restoration of *Nuclear protein 1* expression in transformed fibroblasts results in the formation of carcinoma, suggesting that the expression of *Nuclear protein 1* is essential for tumor development [5, 6]. The *Nuclear protein 1* is a protein associated with a high-migration subgroup of transcriptional regulatory proteins and plays a hinge role in cellular stress response and metastasis [7]. The CAAT-enhancer binding protein (C/EBP) is a cis-acting element at the nucleotide −111 position of *Nuclear protein 1* and

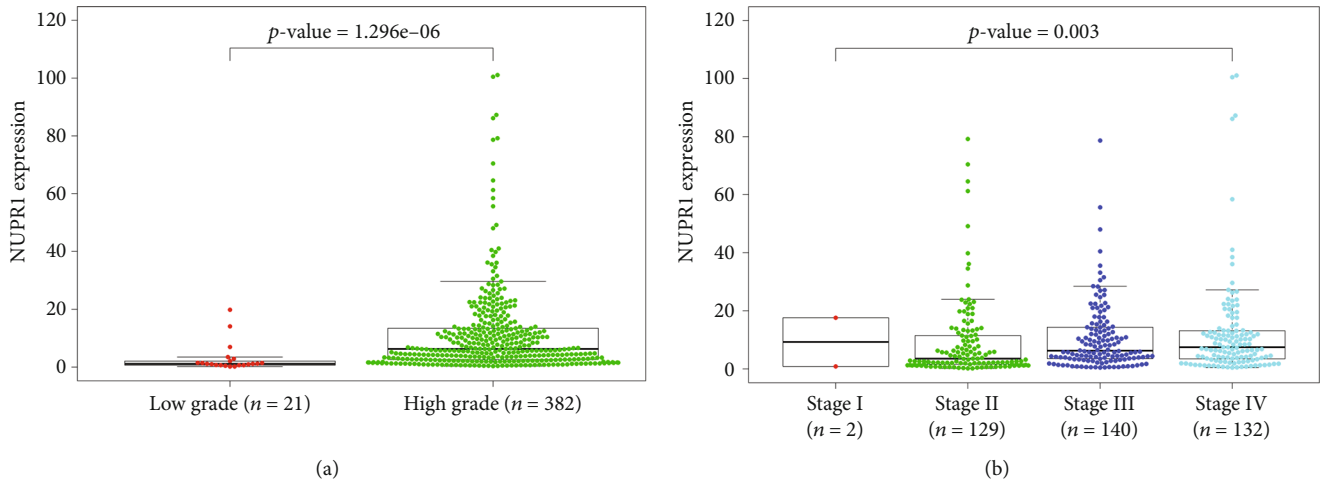

Figure 1: Association between *Nuclear protein 1* expression and clinical manifestation of bladder transitional cell carcinoma (BTCC) evaluated by TCGA database. (a) The *Nuclear protein 1* in high-grade BTCC was enhanced in low-grade BTCC ($P < 0.05$). (b) The *Nuclear protein 1* was positively associated with the stage of BTCC ($P < 0.05$).

can facilitate the transcription of the *Nuclear protein 1* gene in mice [8]. The anomalous expression of *Nuclear protein 1* in many benign disorders can cause renal mesangial cell hypertrophy, cardiac fibrosis, and higher autophagy [9–11]. Additionally, as a transcription regulator, *Nuclear protein 1* can participate in DNA damage response, cell cycle, apoptosis, and chromatin remodeling in response to chemotherapeutic resistance in carcinoma [12]. Understanding the regulation of multifaceted functions of *Nuclear protein 1* can provide new insights, which could help in the creation of new therapies for cancer and other pathologies [13]. Moreover, conclusions from existing *in vitro* studies may not be in line with those from *in vivo* studies [14].

Initially, *Nuclear protein 1* was thought to regulate pancreatic cancer cell growth through growth suppression-related pathways and the inhibition of cell growth promoting factors [15]. To a certain extent, *Nuclear protein 1* adjusts the migration, invasion, and adhesion of pancreatic cancer cells through cytoskeletal regulatory factors [16]. Results from breast cancer studies revealed that *Nuclear protein 1* interacts with p53 to up-regulate the anti-apoptotic protein Bcl-2, giving breast epithelial cells an advantage in growth and survival [17]. As a transcriptional co-regulator, *Nuclear protein 1* plays a key role in the endocrine therapy of breast cancer, thus representing a sensitive therapeutic target for the study of endocrine resistance of breast cancer [18]. *In vitro* studies revealed *Nuclear protein 1* to be a potential tumor suppressor in human prostate cancer, and that *Nuclear protein 1* expression is inversely associated with prostate cancer aggressiveness and growth [19]. The specific mechanism of *Nuclear protein 1* action in BTCC cells and tissues remains unclear till date. Therefore, the present study assessed the expression of *Nuclear protein 1* in clinical BTCC tissues. In addition, the regulatory factors of *Nuclear protein 1* and the signaling pathway of their interaction were identified through functional experiments. Bioinformatic tools were used to verify *Nuclear protein 1*-related genes and signaling pathways in BTCC.

2. Materials and Methods

2.1. Study Population. RNA sequencing data and corresponding clinicopathological data of 414 cases of BTCC were extracted from The Cancer Genome Atlas (TCGA) database. The baseline data sheet of patients with BTCC who were enrolled for the study is summarized in Supplemental Table 1. The specimens collected from these patients were first examined by pathological examination. Patients who had received chemotherapy or radiation before operation were excluded. In addition, we recruited patients with BTCC from our research center and conducted clinical verification on the tissue samples of these patients. Changzhou Second People's Hospital's Ethics Committee approved the study protocol.

2.2. Immunohistochemical Analysis. Immunohistochemical analysis was employed to verify the clinical samples of patients with BTCC enrolled in our center. The control groups were derived from cancer-free mucosal tissue from patients with BTCC. The slices were stained with anti-*Nuclear protein 1* antibody using standard immunoperoxidase-staining protocols. Two pathologists were invited to evaluate the tissue sections and obtain the corresponding staining scores. We independently chose five fields of view for each section. The staining intensity score was recorded as four scales (0–3) according to the number of immune response cells.

2.3. Cell Culture. We used the human BTCC cell line (5637 Cell Line, Shanghai, China) for functional experiments. This cell line was cultured in a RPMI-1640 medium (Gibco, USA). The medium consisted of 10% fetal bovine serum as well as 100 U/mL penicillin and streptomycin. The cells were stored in a humidified incubator with 5% CO_2 at 37°C.

2.4. Transfection of Lentivirus and Affymetrix Microarray Analysis. To construct lentivirus with low *Nuclear protein 1* expression, we designed the RNA interference sequence (RNAi) system using a part of *Nuclear protein 1* sequence (CCAAGC TGCAGAATTCAGA). A non-silencing small-interfering RNA

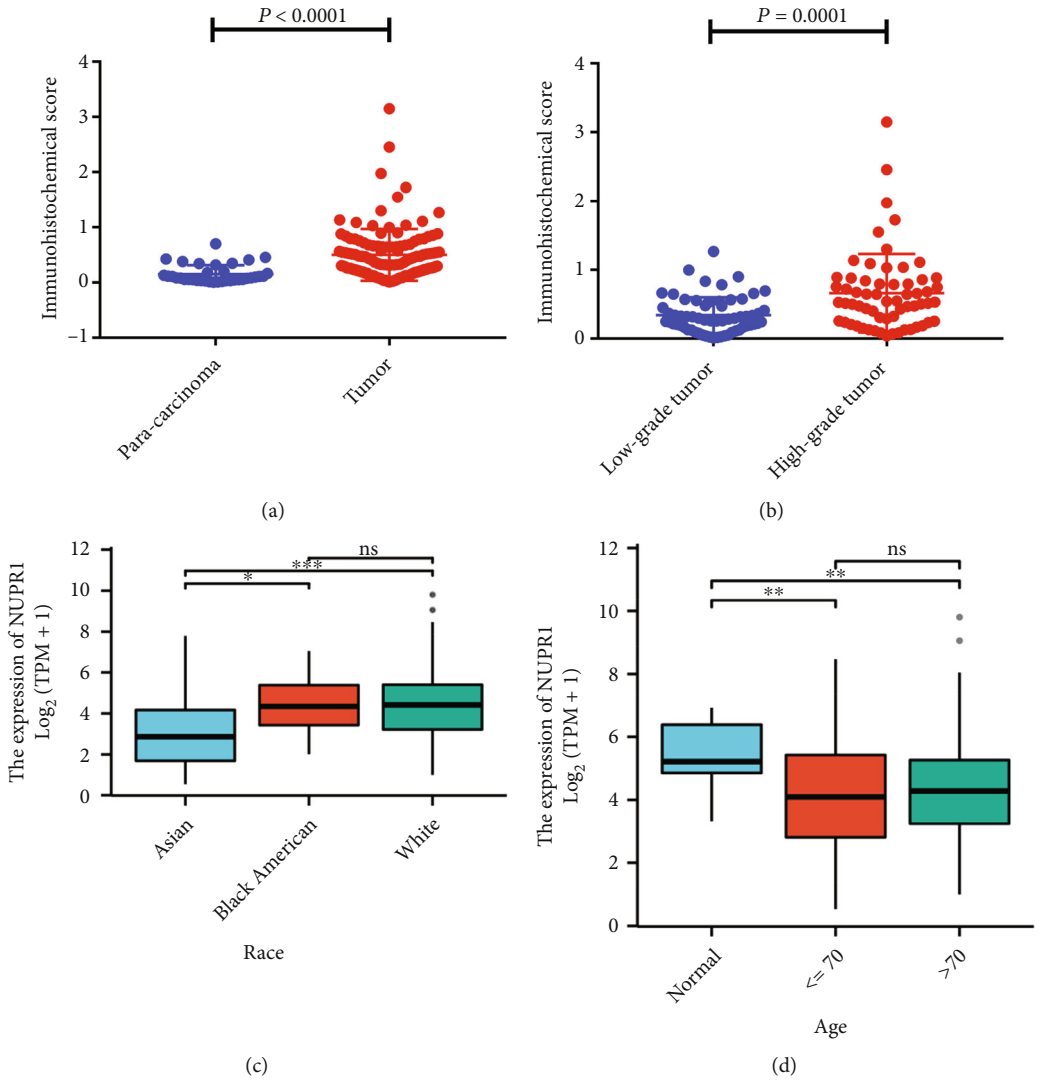

Figure 2: Expression of *Nuclear protein 1* in different subgroups of BTCC. (a) The expression of *Nuclear protein 1* was down-regulated in para-carcinoma tissues ($P < 0.001$). (b) The *Nuclear protein 1* in high-grade BTCC was significantly augmented than that in low-grade BTCC ($P < 0.001$). (c) Compared with Caucasian patients with BTCC, the *Nuclear protein 1* expression was attenuated in Asian patients. (d) There was no difference in the expression of *Nuclear protein 1* in patients with different ages.

(siRNA) sequence (TTCTCCGAACGTGTCACGT) was used as negative control. We employed the PrimeView Human Gene Expression Array (Affymetrix, Thermo Fisher Scientific, USA) and conducted gene chip assays to explore the differential expression profile after *Nuclear protein 1* interference. Total RNA was retrieved from *Nuclear protein 1* interference and control cells. The NanoDrop 2000 (NanoDrop Technologies, Wilmington, USA) was used to evaluate the quality of the total RNA, and the GeneChip kit (Affymetrix, Thermo Fisher Scientific, USA) was used to perform gene hybridization, washing, and staining based on the manufacturer's instructions. Subsequently, an ingenuity pathway analysis (IPA) was carried out to annotate the gene microarray expression profiles.

2.5. Western Blotting. After quantification, the total protein (<100 μg) was mixed with protein marker and buffer. The buffer was subsequently added into the wells of a sodium dodecyl sulfate–polyacrylamide gel electrophoresis gel for electrophoretic separation. Afterwards, we transferred the samples to a polyvinylidene fluoride membrane, which was further blocked with 5% skim milk. The *Nuclear protein 1* antibody was purchased from Proteintech Group. The BCL-2, BAX, E-cadherin, vimentin, P21, N-cadherin, cyclin-D1, C-caspase 3, CDK2, and GAPDH antibodies were bought from Abcam company. GAPDH was used as the internal control. The membranes were then incubated with an appropriate primary antibody overnight at 4°C. After a thorough wash, the samples were reacted with a secondary antibody for 2 hours (20°C). We used the chemiluminescence reagent (Millipore, USA) to evaluate the protein bands.

2.6. GSEA and Bioinformatic Analyses of Nuclear Protein 1. We used the Gene Set Enrichment Analysis (GSEA) to

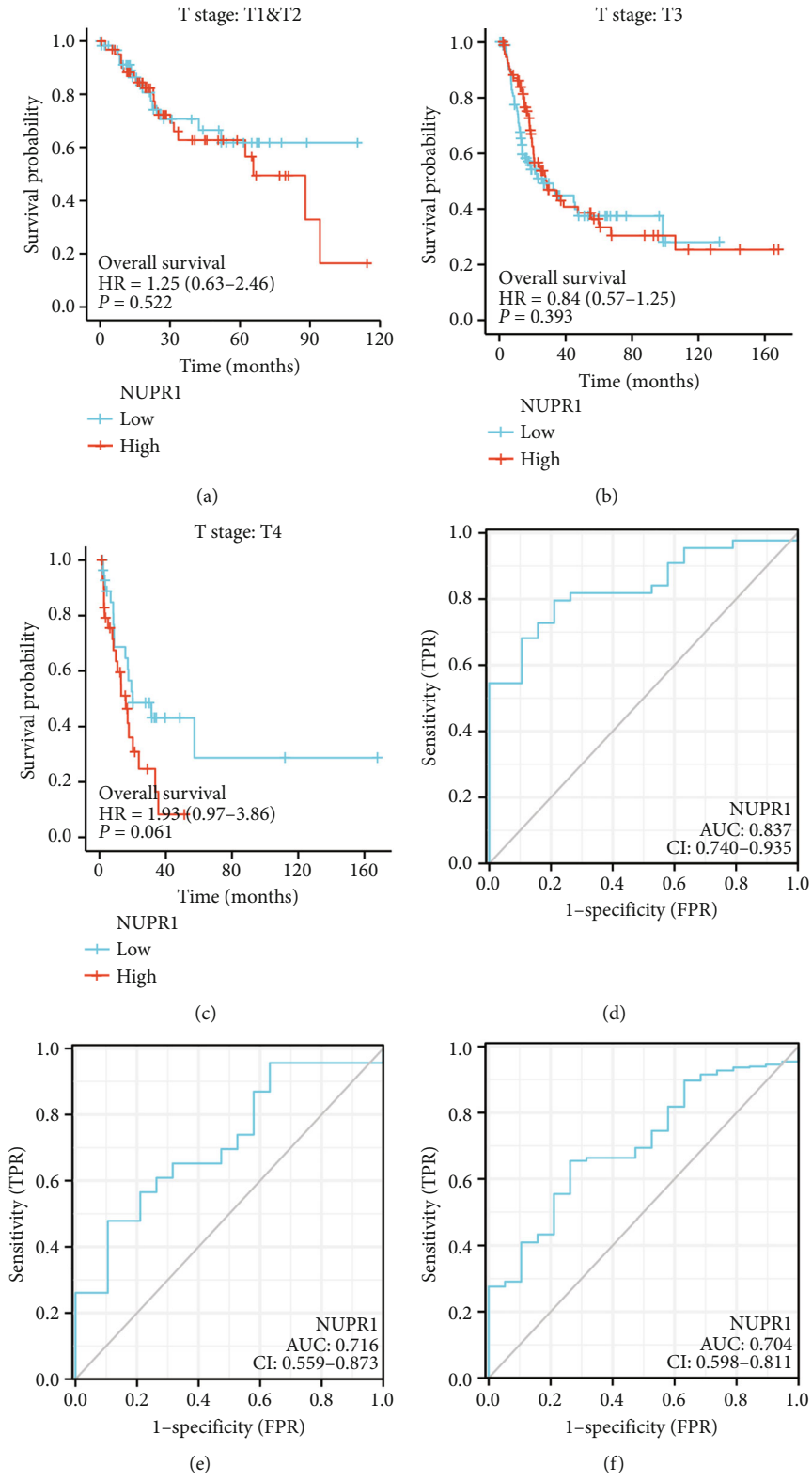

Figure 3: Prognosis analysis of *Nuclear protein 1* in different stage of BTCC. High *Nuclear protein 1* expression had a worse prognosis in patients with advanced BTCC (c) compared to relatively early cancer (a) and (b). ROC curve of *Nuclear protein 1* expression in Asian, Caucasian, and Black American subgroup was revealed in (d), (e), and (f).

assess the possible pathways associated with *Nuclear protein 1*. A gene set, c2.cp.kegg.v7.1.symbols.gmt, was chosen as the reference gene set [20]. We adopted the R language to analyze the clinical data acquired from the TCGA database and applied the Search Tool for the Retrieval of Interaction Gene/Proteins (STRING) server to explore the

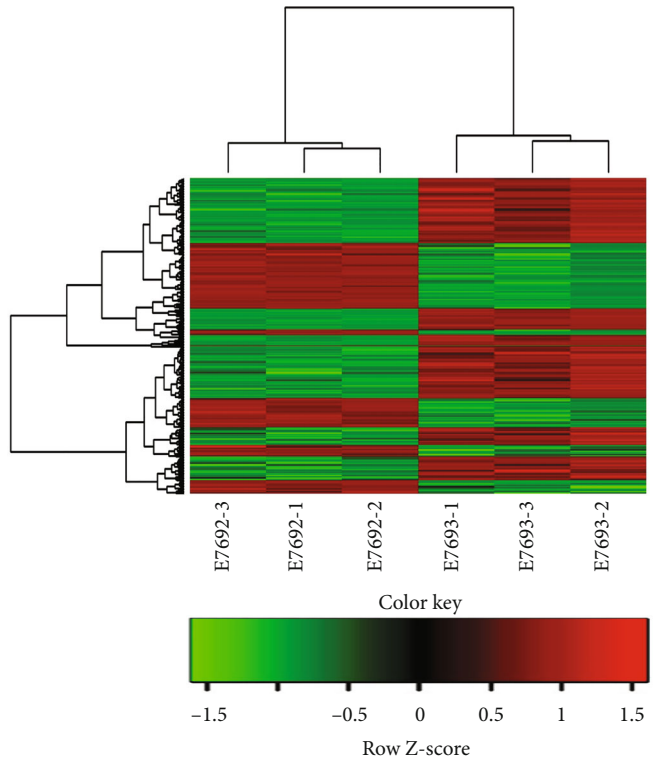

(a)

Figure 4: Continued.

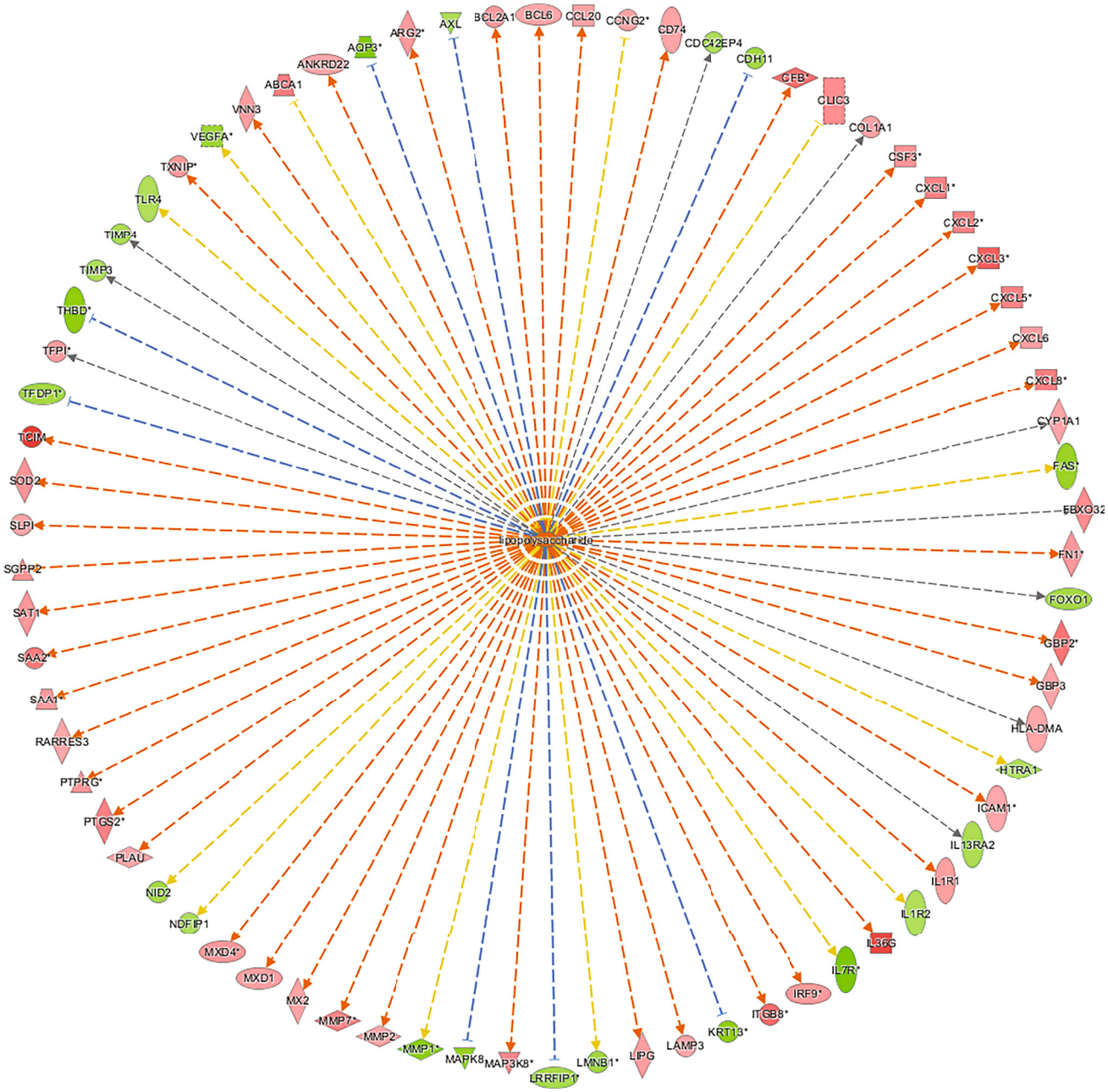

(b)

Figure 4: Continued.

Upstream Regulator	Molecule Type	Predicted Activation State	Activation z-score	p-value
beta-estradiol	chemical - endogenous mammalian	Inhibited	-2.518	1.60E-24
IFNG	cytokine	Activated	2.517	1.39E-22
TNF	cytokine	Activated	2.679	1.44E-21
estrogen receptor	group		0.694	4.94E-20
OSM	cytokine	Activated	2.430	2.13E-18
dexamethasone	chemical drug		-1.572	1.07E-17
IL1B	cytokine	Activated	3.643	1.16E-17
LY294002	chemical - kinase inhibitor	Inhibited	-2.652	2.60E-17
lipopolysaccharide	chemical drug	Activated	4.766	2.00E-16
IL17A	cytokine	Activated	2.403	2.81E-15
JUN	transcription regulator	Activated	2.160	3.74E-15
ERK	group	Activated	2.456	5.73E-15
NFKBIA	transcription regulator		0.471	7.80E-15
ESR1	ligand-dependent nuclear receptor	Inhibited	-2.168	1.19E-14
IL6	cytokine	Activated	3.335	3.73E-14
VCAN	other		0.134	4.15E-14
P38 MAPK	group	Activated	2.244	9.35E-14
STAT3	transcription regulator	Activated	2.453	1.33E-13
TGFB1	growth factor		1.699	2.95E-13
pyrrolidine dithiocarbamate	chemical reagent	Inhibited	-2.415	4.51E-13

(c)

Figure 4: Continued.

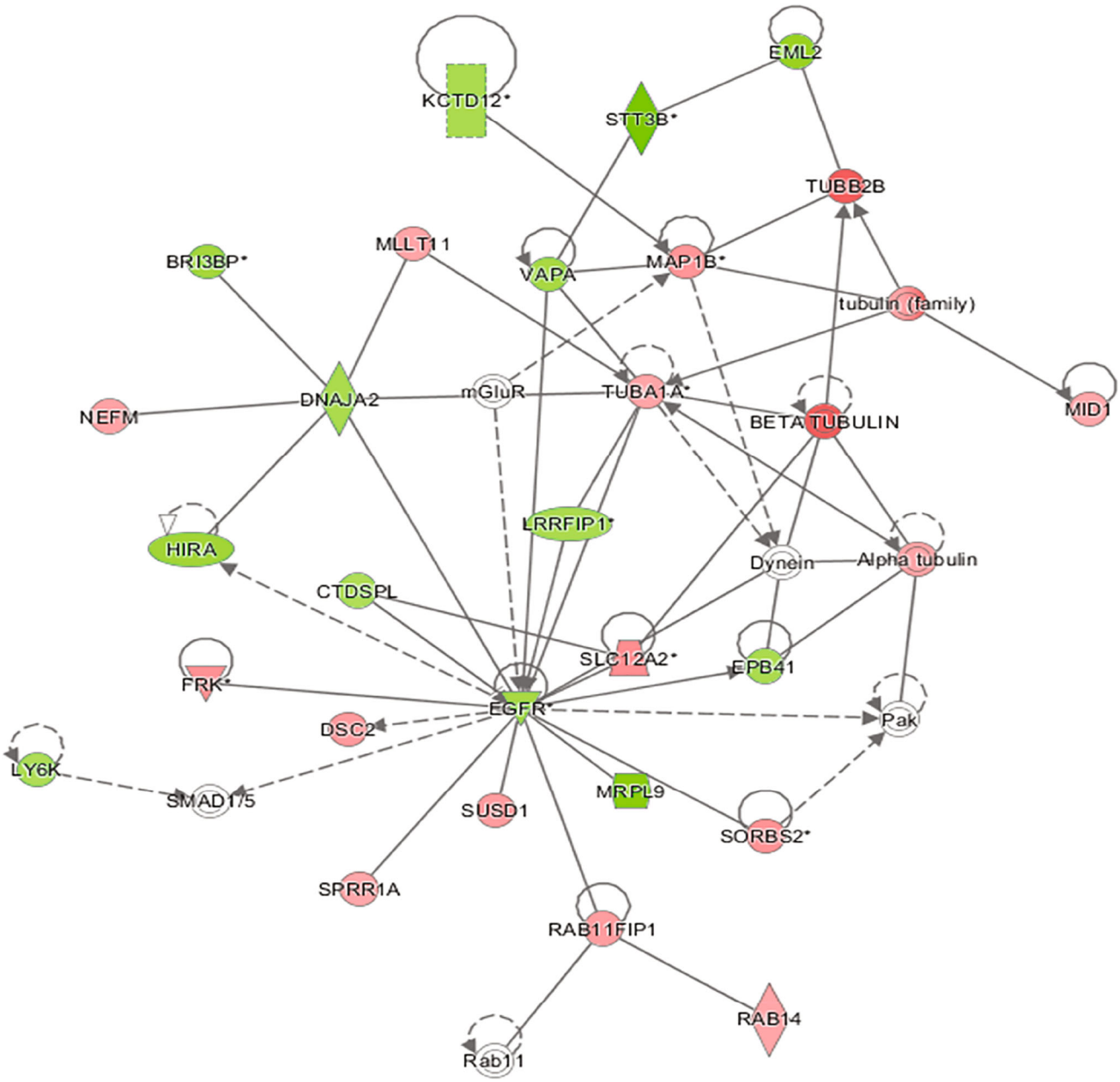

(d)

Figure 4: The relative regulatory molecules of *Nuclear protein 1* evaluated by microarray. We used gene chip to explore the expression profile of relative molecules after *Nuclear protein 1* interference. Cluster map panoramic display of differential molecule distribution was indicated in (a). Among them, one of the most up-regulated molecules was lipopolysaccharide (c). Network diagram of lipopolysaccharide was shown in (b). The downstream path network diagram with significant changes was deprived in (d).

protein–protein crosstalk of *Nuclear protein 1* in Homo sapiens (https://string-db.org/cgi/input.pl). We then used the GraphPad Prism software to evaluate the findings of immunohistochemical analyses. Participants were classified into two groups according to the *Nuclear protein 1* expression. We employed a prognostic classifier to explore whether the expression of *Nuclear protein 1* influences the clinical outcomes in patients with BTCC. The rank of differentially expressed genes associated with *Nuclear protein 1* was measured by R (3.6.3). We applied the predictive receiver operating characteristic package to create receiver operating characteristic (ROC) curves, and multivariate Cox analysis was used to evaluate the influence of *Nuclear protein 1* expression on prognosis. We employed the University of ALabama at Birmingham CANcer data analysis Portal (http://ualcan.path.uab.edu/analysis.html) to explore the expression profile of PPARG in bladder cancer. The influence of different PPARG expression levels on overall survival and disease-free survival time was investigated by Gene Expression Profiling Interactive Analysis (GEPIA, http://gepia.cancer-pku.cn/index.html) database. We further used a correlation chord diagram to outline the degree of correlation between *Nuclear*

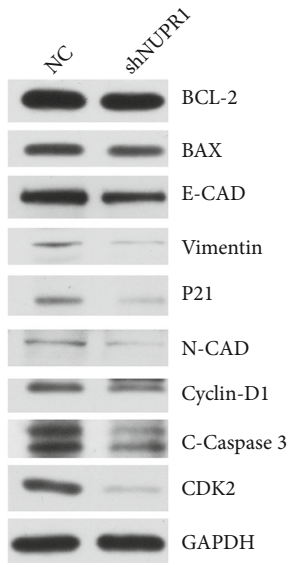

FIGURE 5: Verification of downstream proteins after *Nuclear protein 1* interference investigated by western blotting. In *Nuclear protein 1* interference group, key proteins in apoptosis (BCL-2), cell cycle (cyclin-D1, CDK2), and epithelial–mesenchymal transformation (vimentin, N-cadherin) were all diminished ($P < 0.05$).

protein 1, PPARG, PPARA, and PPARD. The nomogram chart was based on multivariate regression analysis. Statistical significance was set at $P < 0.05$.

3. Results

3.1. Expression of Nuclear Protein 1 in Clinical Tissue of BTCC. The TCGA database was employed to demonstrate the association between *Nuclear protein 1* and clinical traits of BTCC. The expression of *Nuclear protein 1* in high-grade BTCC was higher than that in low-grade BTCC (Figure 1(a), $P < 0.05$). Moreover, *Nuclear protein 1* expression was positively associated with the clinical stage of BTCC (Figure 1(b), $P < 0.05$). Further, the tissues collected from patients with BTCC were subjected to immunohistochemical analysis of *Nuclear protein 1*. Our results provide evidence that *Nuclear protein 1* is down-regulated in paracarcinoma tissues (Figure 2(a), $P < 0.001$). Furthermore, *Nuclear protein 1* expression in high-grade BTCC was significantly augmented compared to that in low-grade BTCC (Figure 2(b), $P < 0.001$).

3.2. Nuclear Protein 1 Expression in Different Subgroups of BTCC. We further utilized the R language to explore the expression of *Nuclear protein 1* in different subgroups of BTCC. Details of the *Nuclear protein 1* expression in different ethnic groups were summarized in Supplemental Table 1. The logistic regression model was used to analyze the odds ratio (OR) in different subgroups of BTCC (Supplemental Table 2). Compared with Caucasian patients with BTCC, *Nuclear protein 1* expression was attenuated in Asian patients (Figure 2(c), $P < 0.001$). No difference was observed in the expression of *Nuclear protein 1* among patients with different ages (Figure 2(d), $P > 0.05$). Additionally, we analyzed the prognosis potential of *Nuclear protein 1* in different stages of BTCC. High *Nuclear protein 1* expression had a worse prognosis in patients with advanced BTCC (Figure 3(c)) compared with patients with relatively early cancer (Figures 3(a) and 3(b)). The ROC curves of *Nuclear protein 1* expression in Asian, Caucasian, and Black American subgroups are shown in Figures 3(d), 3(e), and 3(f).

3.3. Investigation of the Relative Regulatory Molecules of Nuclear Protein 1 via Microarray. We used Affymetrix microarray assays to explore the expression profiles of relative molecules after RNAi silencing of *Nuclear protein 1*. The heat maps of hierarchical clustering of the two groups of samples of KD and normal control (NC) were selected by using the expression profiles of differential genes screened according to the criteria of fold change ≥1.5 and false discovery rate (FDR) <0.05. The cluster panoramic map of differential molecule distribution is shown in Figure 4(a). The tree structure indicated the aggregation of the expression patterns of different genes: red represented that the expression of genes was relatively up-regulated, green represented that the expression of genes was relatively down-regulated, and black indicated no significant change in gene expression. One of the most up-regulated molecules was lipopolysaccharide (Figure 4(c)). Figure 4(b) shows the network diagram of lipopolysaccharide, and Figure 4(d) shows the downstream path network diagram with significant changes.

3.4. Identification of Nuclear Protein 1-Related Proteins. We used western blotting to explore the downstream proteins after *Nuclear protein 1* interference. In the *Nuclear protein 1* interference group, key proteins in apoptosis (BCL-2), cell cycle (cyclin-D1, CDK2), and Epithelial–Mesenchymal Transition (EMT) (vimentin, N-cadherin) were all diminished ($P < 0.05$, Figure 5). We applied the STRING database to demonstrate more related proteins associated with *Nuclear protein 1*, indicating that more than 30 proteins were involved in the correlation with *Nuclear protein 1* (Figure 6(a)). In addition, peroxisome proliferator-activated receptor γ (PPARG) was found to be associated with *Nuclear protein 1* (Figure 6(b)).

3.5. GSEA and Bioinformatic Analyses of Nuclear Protein 1-Related Signaling Pathways. In order to verify whether the PPAR signaling pathway is associated with *Nuclear protein 1* expression, we employed GSEA to investigate the signaling pathways associated with *Nuclear protein 1*. Results from the GSEA revealed that the signaling pathways in cancer (Figure 7(a)) were associated with the expression of *Nuclear protein 1*, especially for BTCC (Figure 7(b)). The PPAR (Figure 7(c)) signaling pathway and RNA degradation (Figure 7(d)) were associated with high *Nuclear protein 1* expression. We further utilized the R language to explore the differentially expressed genes associated with *Nuclear protein 1*. Figure 8(a) shows the correlations between *Nuclear protein 1* and PPARA, PPARD, and PPARG. The *Nuclear protein 1* expression was significantly correlated with PPARG in BTCC (Figure 8(b)). The correlation chord diagram of *Nuclear protein 1*, PPARG, PPARA, and PPARD was shown in Figure 8(c). Furthermore, we employed

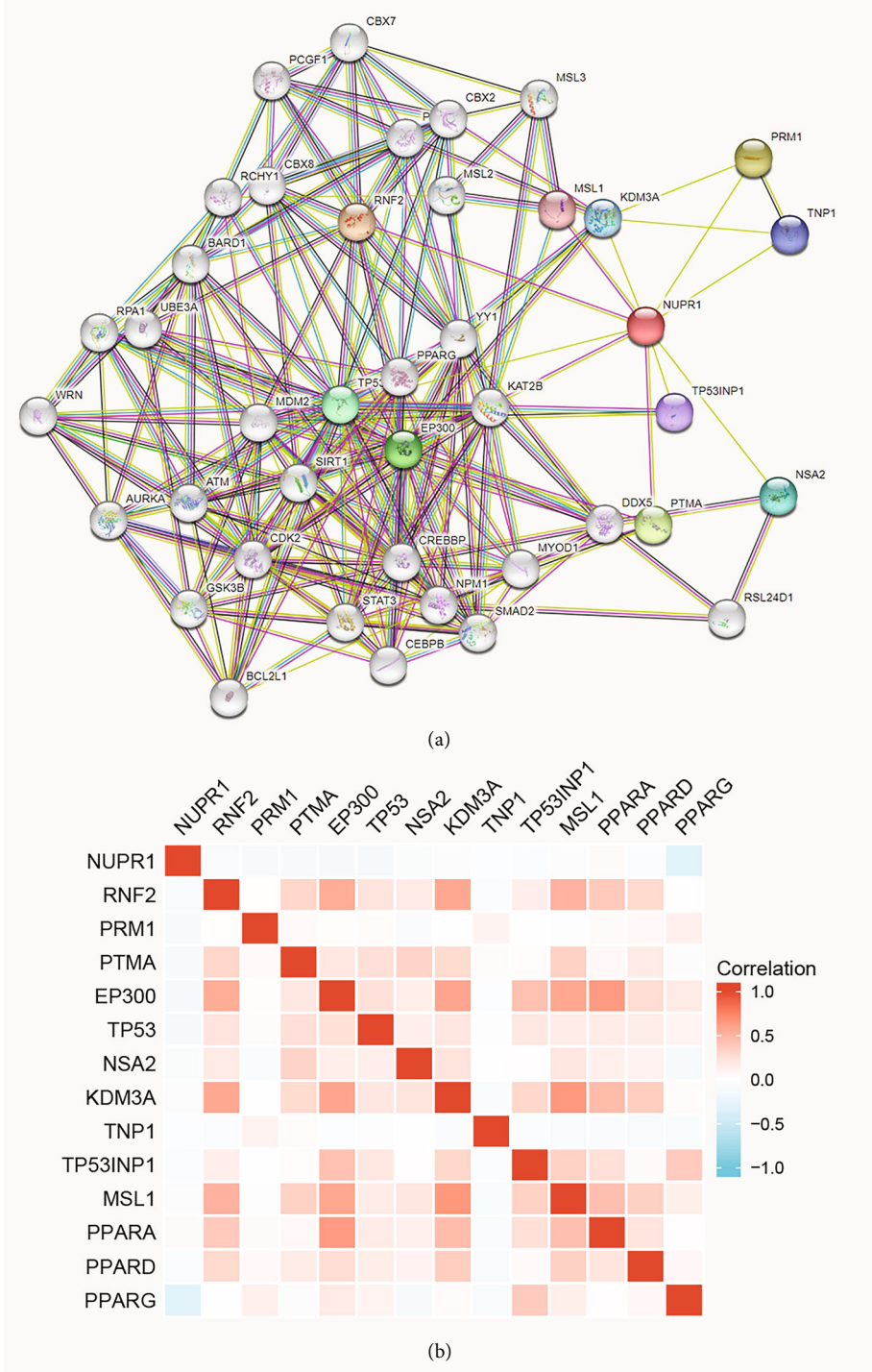

Figure 6: The crosstalk of *Nuclear protein 1* investigated by bioinformatic tools. The STRING database indicated that more than 30 proteins were involved in the correlation with *Nuclear protein 1* (a). PPARG was also the associated gene with *Nuclear protein 1* (b).

bioinformatic analysis to investigate the association between *Nuclear protein 1* expression and PPAR signaling pathway-related genes, including PPARA, PPARD, and PPARG. The expression of *Nuclear protein 1* was negatively correlated with PPARG ($R = -0.290$, $P < 0.001$, Figure 9(c)), but not with PPARA ($R = 0.047$, $P = 0.344$, Figure 9(a)) and PPARD ($R = -0.055$, $P = 0.260$, Figure 9(b)). Prognosis nomogram chart shows that low PPARG expression is an independent risk factor for the prognosis of BTCC (Figure 10). We further assessed the expression of PPARG in different stage of bladder cancer patients. The expression of PPARG was augmented in patients with early stage bladder cancer (Figure 11(a)). Patients with lower PPARG expression had shorter overall survival time than those with

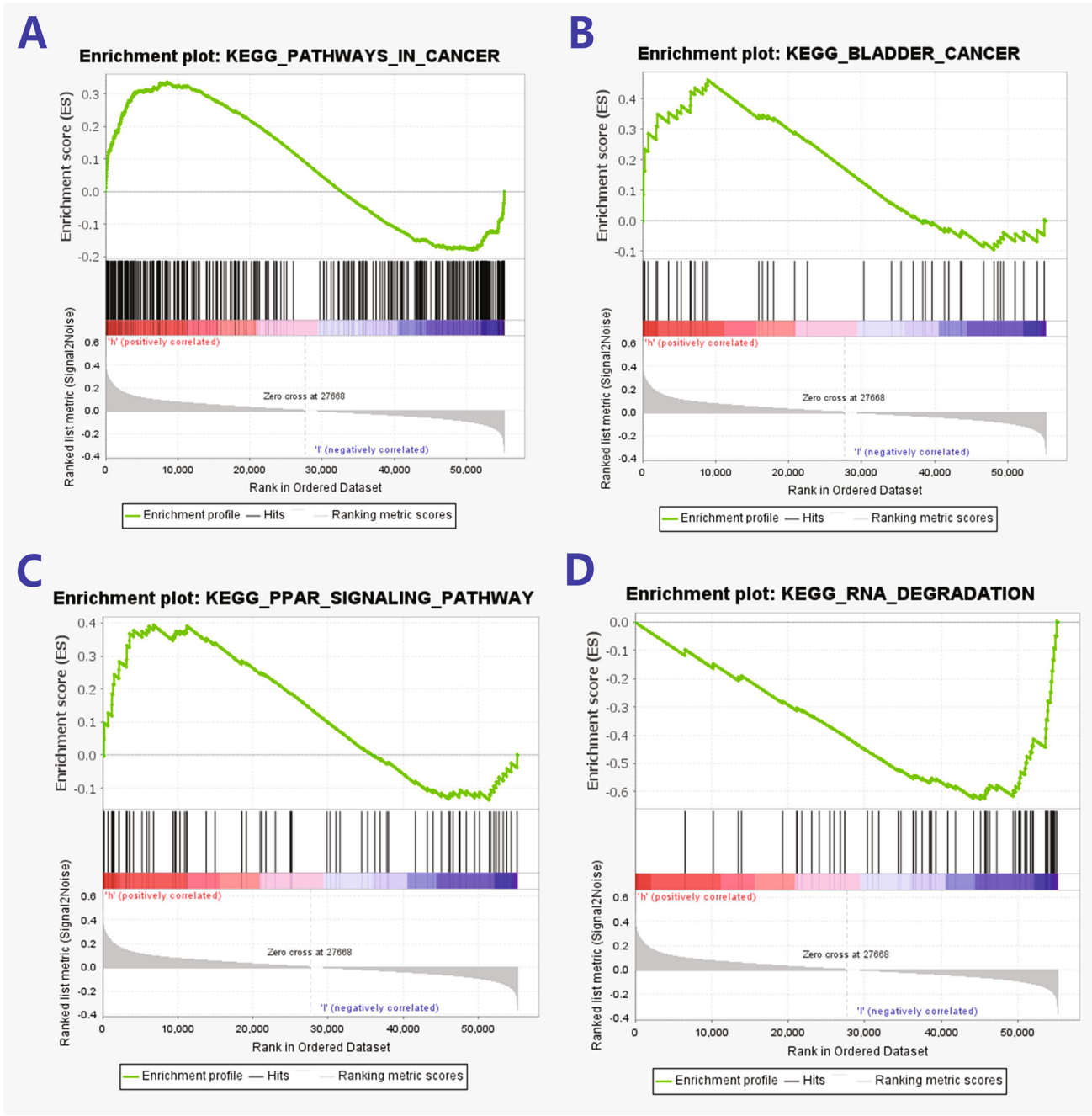

Figure 7: *Nuclear protein 1* is associated with PPAR signaling pathway by Gene Set Enrichment Analysis (GSEA). Results from the GSEA revealed that the signaling pathways in cancer (a) were associated with the expression of *Nuclear protein 1*, especially for BTCC (b). The PPAR (c) signaling pathway and RNA degradation (d) were correlated with a high expression of *Nuclear protein 1*.

higher expression ($P < 0.05$, Figure 11(b)). No significant difference was revealed for disease-free survival time ($P > 0.05$, Figure 11(c)).

4. Discussion

Malignant tumors are still the major diseases that threaten and shorten human life span. Scientists are trying to understand the causes and pathogenesis of cancer, but the results are still not satisfactory [21–24]. Previous retrospective studies have found that different molecular subtypes of BTCC patients show different responses to targeted therapy and different prognoses [25]. The discovery of new genes related to predicting the prognosis of BTCC can provide guidance for the immune microenvironment, lifetime, and chemotherapy responses of patients with BTCC [26]. In this study, we evaluated the expression of *Nuclear protein 1* in the tissues of patients with BTCC from the online database and those enrolled at our center. At the same time, lentivirus-mediated siRNA method was adopted to silence the expression of *Nuclear protein 1* in human BTCC cell lines. We further explored the effect of *Nuclear protein 1* on the biological

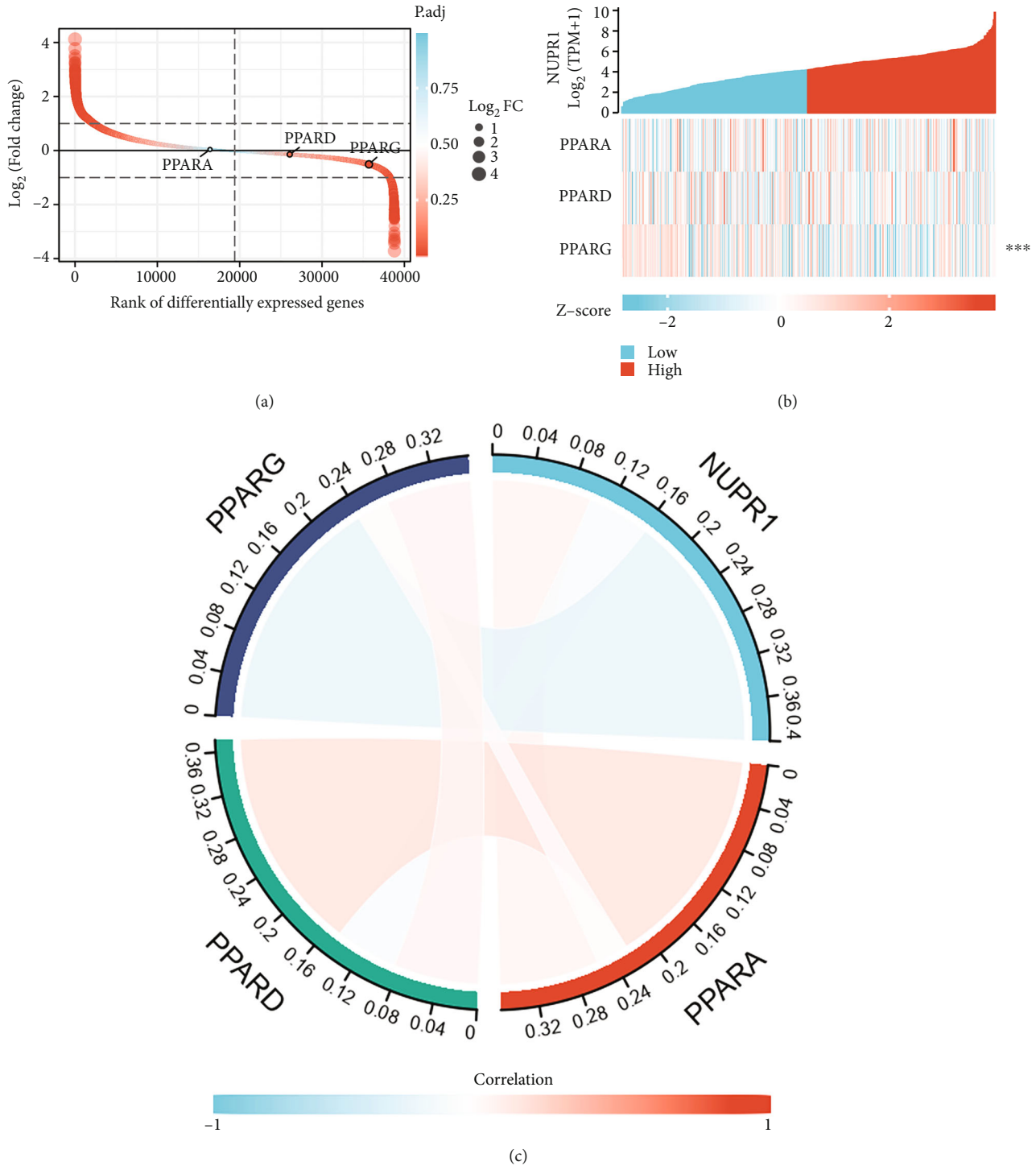

Figure 8: Rank of differentially expressed genes associated with *Nuclear protein 1*. The R language was used to analyze the correlation between *Nuclear protein 1* and PPARA, PPARD, and PPARG (a). *Nuclear protein 1* was significantly correlated with PPARG (b). The correlation chord diagram of *Nuclear protein 1*, PPARG, PPARA, and PPARD was shown in (c).

behavior of BTCC by functional experiments. We anticipate that our findings will offer a new guidance strategy for the early diagnosis and drug therapy of BTCC through investigating the biological function of *Nuclear protein 1* in BTCC.

Biomarkers associated with inflammation and immune activation may help to assess the risk of BTCC. Despite the lack of specificity at present, it would be helpful to predict the routine clinical and pathological prognosis of BTCC in the future. These biomarkers are also expected to improve the outcomes of patients with BTCC. Studies of prognostic models for BTCC patients have shown that many predictive models are promising to improve treatment decisions for BTCC patients. Although many models have not been confirmed in the BTCC patient cohort, some studies have tested

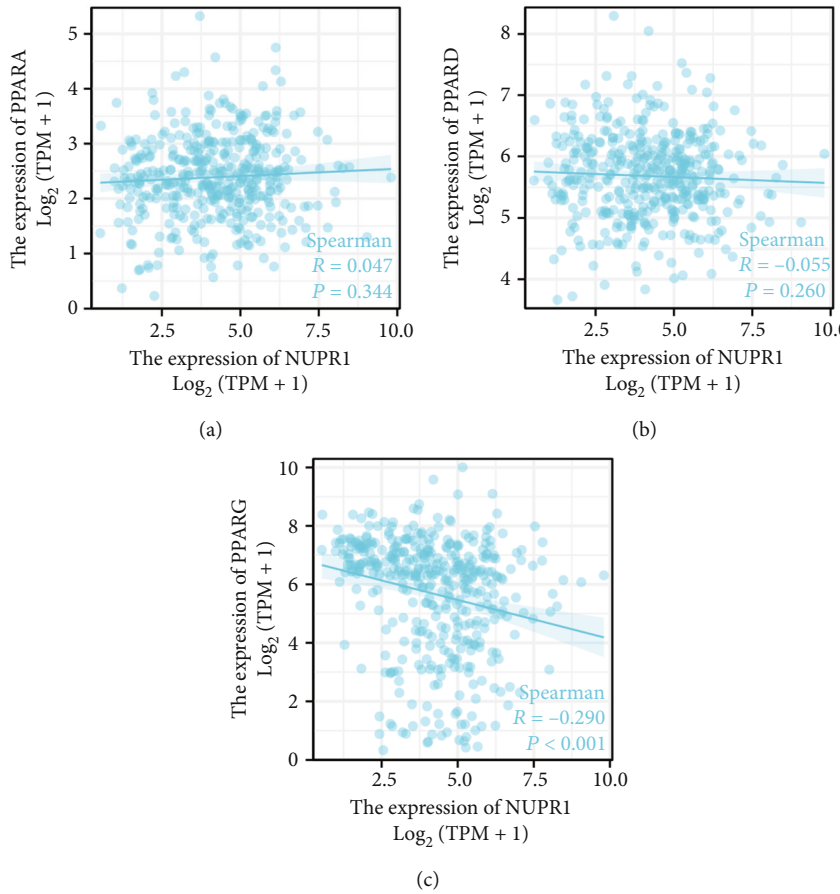

Figure 9: The correlation between *Nuclear protein 1* and PPARA, PPARD, PPARG. Bioinformatic analysis revealed that the expression of *Nuclear protein 1* was negatively correlated with PPARG ($R = -0.290$, $P < 0.001$, (c)), but not with PPARA ($R = 0.047$, $P = 0.344$, (a)) and PPARD ($R = -0.055$, $P = 0.260$, (b)).

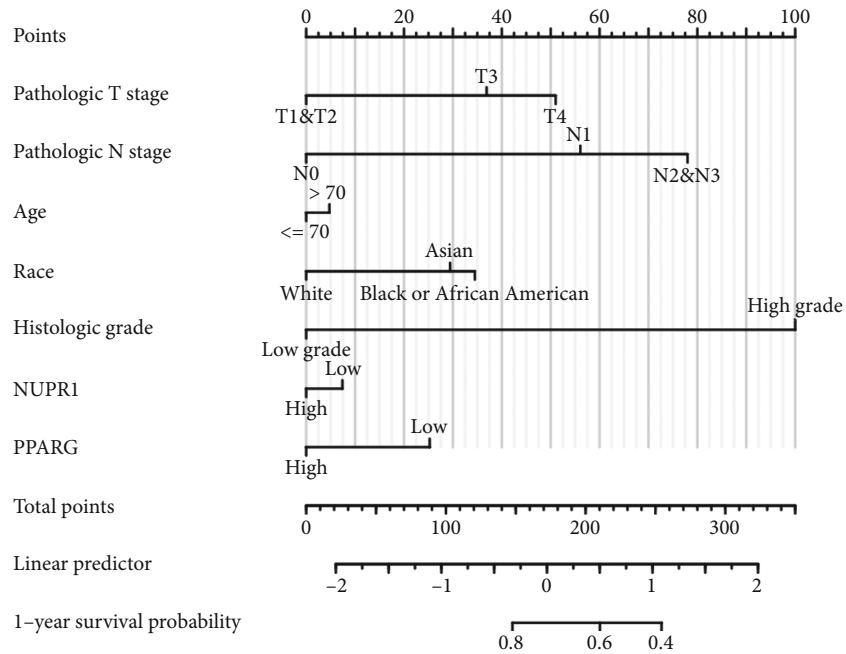

Figure 10: Prognosis nomogram chart of PPARG and *Nuclear protein 1* in BTCC. Prognosis nomogram chart shows that low PPARG expression is an independent risk factor for the prognosis of BTCC.

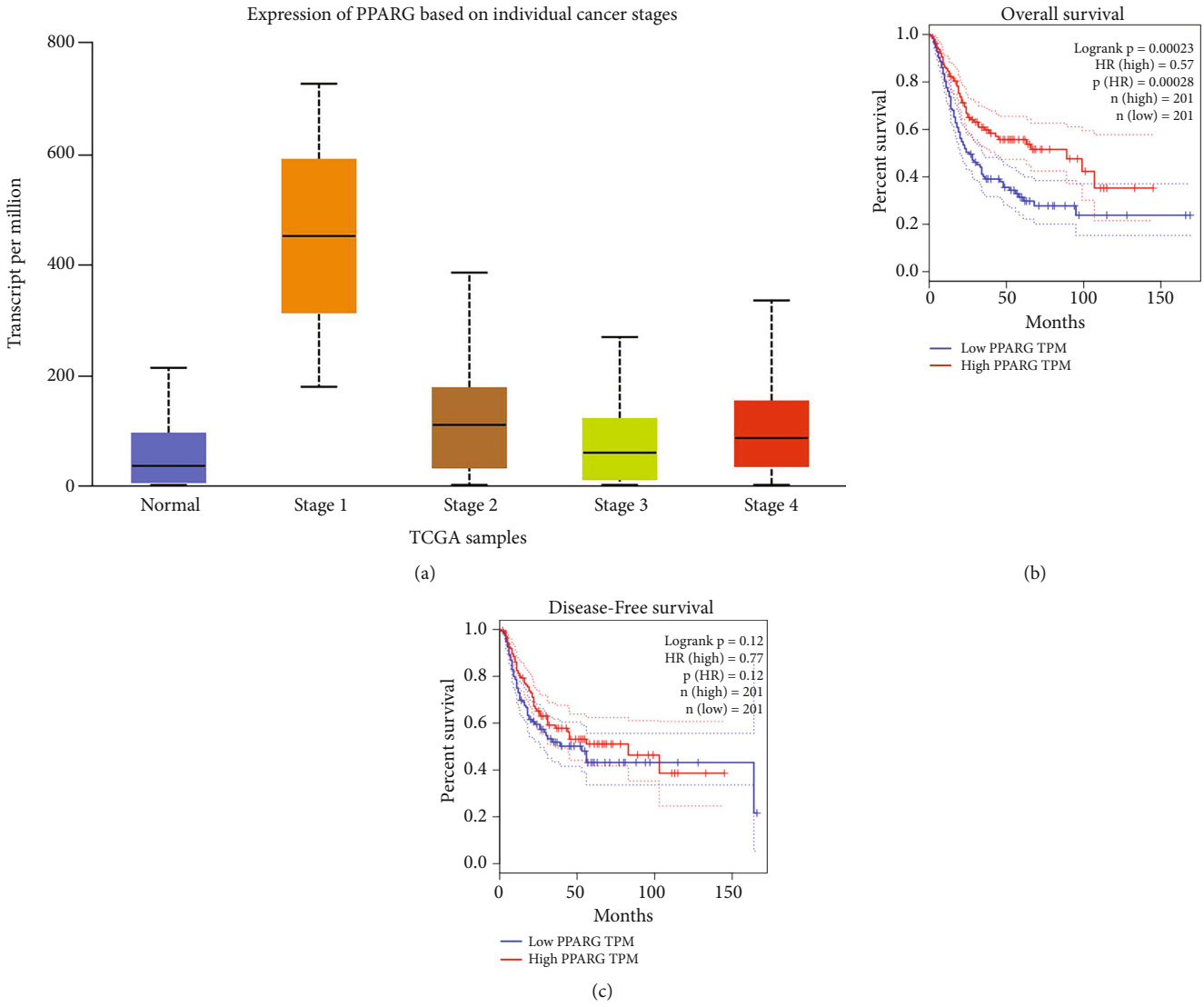

Figure 11: Expression of PPARG in different stage of bladder cancer patients. The expression of PPARG was augmented in patients with early stage bladder cancer (a). Expression of PPARG was diminished in patients with more advanced bladder cancer. Patients with lower PPARG expression had shorter overall survival time than those with higher expression ($P < 0.05$, (b)). No significant difference was revealed for disease-free survival time ($P > 0.05$, (c)).

the clinical utility of these models and improved the ability to make clinical decisions. The role of inflammation in BTCC has recently been demonstrated, providing insight into the clinical significance of inflammation in preventing the development and progression of BTCC [27–29]. Because BTCC is associated with inflammation, *Nuclear protein 1*, which plays an important role in acute inflammation, may also be associated with the development of BTCC. Hence, it is necessary to investigate the underlying mechanism of these inflammatory factors in malignant tumors to explore the molecular mechanism of drug resistance in cancer cells and provide strategies for the development of effective targets for tumor therapy [30, 31]. The *Nuclear protein 1* participates in numerous malignancy-related processes, including regulation of the cell proliferation, apoptosis, ferroptosis, auto-lysosomal efflux, drug resistance, tumor metastasis, and autophagic-associated cell death [32–38]. Nevertheless, the molecular mechanism of *Nuclear protein 1* in carcinomas has not been clarified. *Nuclear protein 1* dysregulation has been reported in several malignancies, including breast, pancreatic, lung, prostate, and colorectal cancer, as well as glioma [39–44].

To explore the biological function of *Nuclear protein 1* in BTCC, we first used an online database to assess the expression of *Nuclear protein 1*, which was then verified by clinical samples from our centers. We found that *Nuclear protein 1* in high-grade BTCC was augmented in low-grade BTCC. Moreover, *Nuclear protein 1* was positively associated with BTCC stage. Compared with Caucasian patients with BTCC, the *Nuclear protein 1* expression was attenuated in Asian patients. No difference was observed in the expression of *Nuclear protein 1* in patients with different ages. In *Nuclear protein 1* interference group, key proteins in apoptosis (BCL-2), cell cycle (cyclin-D1, CDK2), and

epithelial–mesenchymal transformation (vimentin, N-cadherin) were all diminished. Furthermore, we carried out the Affymetrix microarray to explore the relative regulatory molecules and signaling pathways associated with *Nuclear protein 1* in BTCC. Based on the results, lipopolysaccharide was the upstream regulatory factor of *Nuclear protein 1* in BTCC. The results of the present study were in line with those of a previous study conducted by Vasseur et al. [45]. *In vivo* and *in vitro* experiments on the pancreas have confirmed that the mRNA expression of *Nuclear protein 1* can be induced by lipopolysaccharides [46]. Results from *Nuclear protein 1*-knockout in mice showed that *Nuclear protein 1* deficiency hinders normal tissue response to lipopolysaccharides [45]. Prognosis nomogram chart shows that low PPARG expression is an independent risk factor for the prognosis of BTCC. Results from TCGA samples revealed that the expression of PPARG was augmented in patients with early stage bladder cancer and was attenuated in those with more advanced bladder cancer, which is in line with the result from prognosis nomogram chart. Although our previous studies revealed that *Nuclear protein 1* acts as an oncogene in bladder cancer, and the carcinogenic role may be achieved through EMT [47], the crosstalk of *Nuclear protein 1* and PPARG in bladder cancer has not been fully elucidated. Previous literature has shown that PPARG, as a nuclear receptor, is attenuated in basic bladder cancer with muscle invasive, but overexpressed in non-muscle invasive luminal bladder cancer [48]. Additionally, evidence from *in vivo* studies showed the PPARG dependency of bladder urothelial carcinoma and PPARG promotes bladder cancer progression through Sonic Hedgehog signaling-related cellular autonomic mechanisms [49]. In the current study, we found that the PPAR signaling pathway and RNA degradation were correlated with a high expression of *Nuclear protein 1*. Bioinformatic analysis revealed that the expression of *Nuclear protein 1* was negatively correlated with PPARG, but not with PPARA and PPARD. The expression of PPARG was augmented in patients with early stage bladder cancer. Patients with lower PPARG expression had shorter overall survival time than those with higher expression. There are some limitations that need to be mentioned. First, we found that lipopolysaccharide is the upstream regulatory factor of *Nuclear protein 1*; however, the specific regulatory mechanisms of lipopolysaccharides and *Nuclear protein 1* in BTCC tissues were warranted to be further elucidated by more functional experiments. Second, it is reasonable to assess the *Nuclear protein 1* expression in BTCC patients before and after chemotherapy. Nevertheless, due to lack of patients' authorization, we are unable to deal with it at this time. Third, further experiments are needed to confirm the molecular mechanism of *Nuclear protein 1* and PPARG in BTCC in more details.

5. Conclusion

The results of the current study indicate that *Nuclear protein 1* is positively associated with the malignancy degree of BTCC. Compared with Caucasian patients with BTCC, the *Nuclear protein 1* expression is attenuated in Asian patients. The Affymetrix microarray showed that lipopolysaccharide is the upstream regulatory factor of *Nuclear protein 1* in BTCC. The expression of *Nuclear protein 1* is associated with PPAR pathways, and *Nuclear protein 1* expression is negatively correlated with PPARG.

Data Availability

The original data of the study can be acquired from the corresponding authors when they got a rational request.

Ethical Approval

The present study was approved by Changzhou Second People's Hospital's Ethics Committee.

Conflicts of Interest

The authors declare that they have no conflicts of interest.

Authors' Contributions

L.Z. (Lifeng Zhang) and L.Z. (Li Zuo) were involved in the study design. L.Z. (Li Zhang), S.G., and X.S. performed the data analyses and functional experiments. Y.C. and S.W. participated in the statistical analyses. L.Z. (Lifeng Zhang), X.S., and S.G. drafted the manuscript. L.Z. (Lifeng Zhang) and C.L. were involved in the revision of the manuscript. L.Z. (Lifeng Zhang), C.L., and L.Z. (Li Zuo) provided funding support. All of the authors have approved the submitted version. Chao Lu, Shenglin Gao, and Li Zhang contributed equally to this work.

Acknowledgments

The current study was granted by Top Talent of Changzhou "The 14th Five-Year Plan" High-Level Health Talents Training Project (No. 2022CZBJ057), Project of Jiangsu Province 333 High-Level Talent, Changzhou Innovation Team (Project No. XK201803), Grants from Young Talent of Changzhou Health Commission (Project No. CZQM2020065), Changzhou 11th Batch of Science and Technology Plan (CE20215034). We would like to thank Dr. Yuanyuan Mi and Dr. Chunjian Qi for their assistance to the paper.

Supplementary Materials

Supplementary Materials. Supplemental Table 1. Baseline data sheet of enrolled bladder transitional cell carcinoma patients in TCGA database.

Supplementary Materials. Supplemental Table 2. Logistic regression model was used to analyze the Odds Ratio (OR) of different characteristics.

References

[1] R. L. Siegel, K. D. Miller, H. E. Fuchs, and A. Jemal, "Cancer statistics, 2022," *CA: A Cancer Journal for Clinicians*, vol. 72, no. 1, pp. 7–33, 2022.

[2] M. L. Kwan, B. Garren, M. E. Nielsen, and L. Tang, "Lifestyle and nutritional modifiable factors in the prevention and

treatment of bladder cancer," *Urologic Oncology*, vol. 37, no. 6, pp. 380–386, 2019.

[3] A. Richters, K. K. H. Aben, and L. A. L. M. Kiemeney, "The global burden of urinary bladder cancer: an update," *World Journal of Urology*, vol. 38, no. 8, pp. 1895–1904, 2020.

[4] K. Ng, A. Stenzl, A. Sharma, and N. Vasdev, "Urinary biomarkers in bladder cancer: a review of the current landscape and future directions," *Urologic Oncology*, vol. 39, no. 1, pp. 41–51, 2021.

[5] J. L. Iovanna, "Expression of the stress-associated protein p8 is a requisite for tumor development," *International Journal of Gastrointestinal Cancer*, vol. 31, no. 1–3, pp. 89–98, 2002.

[6] G. V. Mallo, F. Fiedler, E. L. Calvo et al., "Cloning and expression of the rat p8 cDNA, a new gene activated in pancreas during the acute phase of pancreatitis, pancreatic development, and regeneration, and which promotes cellular growth," *The Journal of Biological Chemistry*, vol. 272, no. 51, pp. 32360–32369, 1997.

[7] S. Goruppi and J. L. Iovanna, "Stress-inducible protein p8 is involved in several physiological and pathological processes," *The Journal of Biological Chemistry*, vol. 285, no. 3, pp. 1577–1581, 2010.

[8] S. Vasseur, G. V. Mallo, A. Garcia-Montero et al., "Structural and functional characterization of the mouse p8 gene: promotion of transcription by the CAAT-enhancer binding protein α (C/EBPα) and C/EBPβ trans-acting factors involves a C/EBP cis-acting element and other regions of the promoter," *The Biochemical Journal*, vol. 343, no. 2, pp. 377–383, 1999.

[9] S. P. Georgescu, M. J. Aronovitz, J. L. Iovanna, R. D. Patten, J. M. Kyriakis, and S. Goruppi, "Decreased metalloprotease 9 induction, cardiac fibrosis, and higher autophagy after pressure overload in mice lacking the transcriptional regulator p8," *American Journal of Physiology. Cell Physiology*, vol. 301, no. 5, pp. C1046–C1056, 2011.

[10] S. Goruppi, J. V. Bonventre, and J. M. Kyriakis, "Signaling pathways and late-onset gene induction associated with renal mesangial cell hypertrophy," *The EMBO Journal*, vol. 21, no. 20, pp. 5427–5436, 2002.

[11] S. Weis, T. C. Schlaich, F. Dehghani et al., "p8 deficiency causes siderosis in spleens and lymphocyte apoptosis in acute pancreatitis," *Pancreas*, vol. 43, no. 8, pp. 1277–1285, 2014.

[12] A. Murphy and M. Costa, "Nuclear protein 1 imparts oncogenic potential and chemotherapeutic resistance in cancer," *Cancer Letters*, vol. 494, pp. 132–141, 2020.

[13] T. A. Martin, A. X. Li, A. J. Sanders et al., "NUPR1 and its potential role in cancer and pathological conditions (review)," *International Journal of Oncology*, vol. 58, no. 5, p. 21, 2021.

[14] P. Santofimia-Castaño, W. Lan, J. Bintz et al., "Inactivation of NUPR1 promotes cell death by coupling ER-stress responses with necrosis," *Scientific Reports*, vol. 8, no. 1, p. 16999, 2018.

[15] C. Malicet, N. Lesavre, S. Vasseur, and J. L. Iovanna, "p8 inhibits the growth of human pancreatic cancer cells and its expression is induced through pathways involved in growth inhibition and repressed by factors promoting cell growth," *Molecular Cancer*, vol. 2, no. 1, p. 37, 2003.

[16] M. J. Sandi, T. Hamidi, C. Malicet et al., "p8 expression controls pancreatic cancer cell migration, invasion, adhesion, and tumorigenesis," *Journal of Cellular Physiology*, vol. 226, no. 12, pp. 3442–3451, 2011.

[17] D. W. Clark, A. Mitra, R. A. Fillmore et al., "NUPR1 interacts with p53, transcriptionally regulates p21 and rescues breast epithelial cells from doxorubicin-induced genotoxic stress," *Current Cancer Drug Targets*, vol. 8, no. 5, pp. 421–430, 2008.

[18] L. Wang, J. Sun, Y. Yin et al., "Transcriptional coregualtor NUPR1 maintains tamoxifen resistance in breast cancer cells," *Cell Death and Disease*, vol. 12, no. 2, p. 149, 2021.

[19] W. G. Jiang, G. Davies, T. A. Martin, H. Kynaston, M. D. Mason, and O. Fodstad, "Com-1/p8 acts as a putative tumour suppressor in prostate cancer," *International Journal of Molecular Medicine*, vol. 18, no. 5, pp. 981–986, 2006.

[20] A. Subramanian, P. Tamayo, V. K. Mootha et al., "Gene set enrichment analysis: a knowledge-based approach for interpreting genome-wide expression profiles," *Proceedings of the National Academy of Sciences of the United States of America*, vol. 102, no. 43, pp. 15545–15550, 2005.

[21] Y. Y. Mi, Y. Z. Chen, J. Chen, L. F. Zhang, L. Zuo, and J. G. Zou, "Updated analysis of vitamin D receptor gene FokI polymorphism and prostate cancer susceptibility," *Archives of Medical Science*, vol. 13, no. 6, pp. 1449–1458, 2017.

[22] L. F. Zhang, K. W. Ren, L. Zuo et al., "VEGF gene rs3025039C/T and rs833052C/a variants are associated with bladder cancer risk in Asian descendants," *Journal of Cellular Biochemistry*, vol. 120, no. 6, pp. 10402–10412, 2019.

[23] L. F. Zhang, L. J. Zhu, W. Zhang et al., "MMP-8 C-799 T, Lys460Thr, and Lys87Glu variants are not related to risk of cancer," *BMC Medical Genetics*, vol. 20, no. 1, p. 162, 2019.

[24] T. Peng, L. Zhang, L. Zhu, and Y. Y. Mi, "MSMB gene rs10993994 polymorphism increases the risk of prostate cancer," *Oncotarget*, vol. 8, no. 17, pp. 28494–28501, 2017.

[25] D. J. McConkey and W. Choi, "Molecular subtypes of bladder cancer," *Current Oncology Reports*, vol. 20, no. 10, p. 77, 2018.

[26] K. Zhu, L. Xiaoqiang, W. Deng, G. Wang, and B. Fu, "Identification of a novel signature based on unfolded protein response-related gene for predicting prognosis in bladder cancer," *Human Genomics*, vol. 15, no. 1, p. 73, 2021.

[27] R. Nabavizadeh, K. Bobrek, and V. A. Master, "Risk stratification for bladder cancer: biomarkers of inflammation and immune activation," *Urologic Oncology*, vol. 38, no. 9, pp. 706–712, 2020.

[28] A. Masson-Lecomte, M. Rava, F. X. Real, A. Hartmann, Y. Allory, and N. Malats, "Inflammatory biomarkers and bladder cancer prognosis: a systematic review," *European Urology*, vol. 66, no. 6, pp. 1078–1091, 2014.

[29] L. A. Kluth, P. C. Black, B. H. Bochner et al., "Prognostic and prediction tools in bladder cancer: a comprehensive review of the literature," *European Urology*, vol. 68, no. 2, pp. 238–253, 2015.

[30] G. Gakis, "The role of inflammation in bladder cancer," *Advances in Experimental Medicine and Biology*, vol. 816, pp. 183–196, 2014.

[31] H. Y. Pan, Y. Y. Mi, K. Xu et al., "Association of C-reactive protein (CRP) rs1205 and rs2808630 variants and risk of cancer," *Journal of Cellular Physiology*, vol. 235, no. 11, pp. 8571–8584, 2020.

[32] J. Li, S. Ren, Y. Liu et al., "Knockdown of NUPR1 inhibits the proliferation of glioblastoma cells via ERK1/2, p38 MAPK and caspase-3," *Journal of Neuro-Oncology*, vol. 132, no. 1, pp. 15–26, 2017.

[33] L. Shan, C. Hao, Z. Jun, and C. Qinghe, "Histone methyltransferase Dot1L inhibits pancreatic cancer cell apoptosis by promoting NUPR1 expression," *The Journal of International Medical Research*, vol. 50, no. 3, p. 3000605221088431, 2022.

[34] J. Liu, X. Song, F. Kuang et al., "NUPR1 is a critical repressor of ferroptosis," *Nature Communications*, vol. 12, no. 1, p. 647, 2021.

[35] Y. Mu, X. Yan, D. Li et al., "NUPR1 maintains autolysosomal efflux by activating SNAP25 transcription in cancer cells," *Autophagy*, vol. 14, no. 4, pp. 654–670, 2018.

[36] L. Jiang, W. Wang, Z. Li, Y. Zhao, and Z. Qin, "NUPR1 participates in YAP-mediate gastric cancer malignancy and drug resistance via AKT and p21 activation," *The Journal of Pharmacy and Pharmacology*, vol. 73, no. 6, pp. 740–748, 2021.

[37] T. Fan, X. Wang, S. Zhang et al., "NUPR1 promotes the proliferation and metastasis of oral squamous cell carcinoma cells by activating TFE3-dependent autophagy," *Signal Transduction and Targeted Therapy*, vol. 7, no. 1, p. 130, 2022.

[38] T. Hamidi, C. E. Cano, D. Grasso et al., "Nupr1-aurora kinase a pathway provides protection against metabolic stress-mediated autophagic-associated cell death," *Clinical Cancer Research*, vol. 18, no. 19, pp. 5234–5246, 2012.

[39] H. Xiao, J. Long, X. Chen, and M. D. Tan, "NUPR1 promotes the proliferation and migration of breast cancer cells by activating TFE3 transcription to induce autophagy," *Experimental Cell Research*, vol. 418, no. 1, p. 113234, 2022.

[40] C. E. Cano, T. Hamidi, M. N. Garcia et al., "Genetic inactivation of Nupr1 acts as a dominant suppressor event in a two-hit model of pancreatic carcinogenesis," *Gut*, vol. 63, no. 6, pp. 984–995, 2014.

[41] Y. J. Kim, S. E. Hong, S. K. Jang et al., "Knockdown of NUPR1 enhances the sensitivity of non-small-cell lung cancer cells to metformin by AKT inhibition," *Anticancer Research*, vol. 42, no. 7, pp. 3475–3481, 2022.

[42] P. M. Schnepp, G. Shelley, J. Dai et al., "Single-cell transcriptomics analysis identifies nuclear protein 1 as a regulator of docetaxel resistance in prostate cancer cells," *Molecular Cancer Research*, vol. 18, no. 9, pp. 1290–1301, 2020.

[43] X. Li, T. A. Martin, and W. G. Jiang, "COM-1/p8 acts as a tumour growth enhancer in colorectal cancer cell lines," *Anticancer Research*, vol. 32, no. 4, pp. 1229–1237, 2012.

[44] J. Li, Z. G. Lian, Y. H. Xu et al., "Downregulation of nuclear protein-1 induces cell cycle arrest in G0/G1 phase in glioma cells in vivo and in vitro via P27," *Neoplasma*, vol. 67, no. 4, pp. 843–850, 2020.

[45] S. Vasseur, A. Hoffmeister, A. Garcia-Montero et al., "Mice with targeted disruption of p8 gene show increased sensitivity to lipopolysaccharide and DNA microarray analysis of livers reveals an aberrant gene expression response," *BMC Gastroenterology*, vol. 3, no. 1, p. 25, 2003.

[46] Y. F. Jiang, M. I. Vaccaro, F. Fiedler, E. L. Calvo, and J. L. Iovanna, "Lipopolysaccharides induce p8 mRNA expression in vivo and in vitro," *Biochemical and Biophysical Research Communications*, vol. 260, no. 3, pp. 686–690, 1999.

[47] L. Zhang, S. Gao, X. Shi et al., "NUPR1 imparts oncogenic potential in bladder cancer," *Cancer Medicine*, vol. 12, no. 6, pp. 7149–7163, 2023.

[48] T. Tate, T. Xiang, S. E. Wobker et al., "Pparg signaling controls bladder cancer subtype and immune exclusion," *Nature Communications*, vol. 12, no. 1, p. 6160, 2021.

[49] D. J. Sanchez, R. Missiaen, N. Skuli, D. J. Steger, and M. C. Simon, "Cell-intrinsic tumorigenic functions of PPARγ in bladder urothelial carcinoma," *Molecular Cancer Research*, vol. 19, no. 4, pp. 598–611, 2021.